5-24-2017 12:00 AM

The Role of OATP-Mediated Statin Transport in Pancreatic Beta Cell Function

Michelle S. Kim
The University of Western Ontario

Supervisor
Dr. Ute Schwarz
The University of Western Ontario

Graduate Program in Physiology and Pharmacology
A thesis submitted in partial fulfillment of the requirements for the degree in Master of Science

Abstract

Cholesterol-lowering statins, or the 3-hydroxy-3-methyl-glutaryl-coenzyme A (HMG-CoA) reductase inhibitors, are one of the leading treatments for hypercholesterolemia and are recognized for their ability to prevent cardiovascular events. Though safe and effective for most, statin therapy has recently been associated with new-onset diabetes, with risk varying depending on potency and dose. Additionally, *in vitro* data suggest statin-mediated alterations in insulin secretion; however, the exact mechanism is currently unknown. Statins are known substrates of various membrane transporters belonging to the organic anion-transporting polypeptides (OATPs), on which they rely heavily for hepatic uptake and therapeutic efficacy. We have recently reported expression of OATP1B3 in healthy human pancreas, localized to insulin-secreting β cells in the islets of Langerhans. Given the evidence for statin-induced diabetes and potential expression of statin-transporting OATPs in the pancreas, we hypothesize that expression and activity of OATP transporters in pancreatic β cells regulate statin entry and contribute to statin-induced impairment of insulin secretion through disruption of mitochondrial function and ATP-dependent signalling. We demonstrated gene and protein expression of OATP1B3 and OATP2B1 in human adult islets, with differential distribution to α and β cells, respectively. Quantitative analysis showed variable co-localization of OATP1B3 with endocrine cells in relation to age. Our *in vitro* findings support a role of OATPs in mediating statin-induced impairment of insulin secretion and β cell function via mitochondrial dysfunction. Overall, our results suggest a link between pancreatic OATP expression and statin-induced effects on glucose-stimulated insulin secretion and provide novel insights into a currently unexplored mechanism.

Keywords

Organic anion-transporting polypeptides, islets of Langerhans, endocrine pancreas, statins, insulin secretion, incident diabetes, transport proteins, adenoviral overexpression, mitochondrial dysfunction

Co-Authorship Statement

Specific Aim 1:

A part of Sections 2 and 3 associated with Specific Aim 1 has been published in *Histochemistry and Cell Biology*:

Kim M, Deacon P, Tirona RG, Kim RB, Pin CL, Meyer zu Schwabedissen HE, Wang R, and Schwarz UI (2017). Characterization of OATP1B3 and OATP2B1 transporter expression in the islet of the adult human pancreas. *Histochemistry and Cell Biology*, doi:10.1007/s00418-017-1580-6.

UIS, RGT and RW designed the experiments. MK, PD, and UIS conducted the experiments and analyzed the data. RGT, RBK, CLP and RW provided human samples that were used for analysis in experiments. MK and UIS wrote the manuscript. All authors provided feedback on the manuscript and approved the final version.

Specific Aim 2:

Michelle S Kim designed, conducted, and analyzed all experiments and data with assistance from Dr. Ute Schwarz and Dr. Rennian Wang.

Acknowledgments

First and foremost, I would like to thank my supervisor, Dr. Ute Schwarz, for taking me on as her Master's student. Ute, thank you for your patience and for always being available to provide me with assistance. I am grateful for the countless hours you devoted to meeting with me and helping me troubleshoot unfamiliar and finicky experiments. Your input and advice were invaluable in my growth as a scientist. Thank you for your continuous encouragement through the many ups and downs of my project.

I would also like to thank the members of my advisory committee, Dr. Qingping Feng, Dr. Chris Pin, and Dr. Rennian Wang, for their valuable insight and direction throughout the course of my project.

Dr. Richard Kim and Dr. Rommel Tirona, I am privileged to have been a member of the Personalized Medicine lab and to have had the opportunity to learn from your vast expertise and research experience. I truly appreciate your guidance and support over the past few years.

To all past and present members of the Personalized Medicine lab, Dr. Crystal Engelage, Dr. Wendy Teft, Sara Mansell-Gallien, Cameron Ross, Dr. Sarah Woolsey, Heidi Yinyin Liao, Ahmed Almousa, Dr. Aze Wilson, Adrienne Borrie, Markus Gulilat, Perri Deacon, and Catherine Zhu, thank you for making long days in lab more bearable. Lunchtime with all of you was always the highlight of my day, whether we were having hilarious and silly conversations, playing board games, or struggling to finish an "easy" crossword. Thank you all for your friendship and encouragement.

Lisa Choi and Mandy Li, thank you for being the best roommates I could have ever asked for. I am so grateful to have lived with friends and classmates that fully understood the struggles and stresses that I faced, and I can't express how much of a blessing it was to be able to knock on your doors at whatever hour to ask for advice or just to talk.

To my fellow grad students and close friends Nicole Edwards, Melissa Fenech, Cheynne McLean, Catherine Nevin, and Laura Russell, thank you for the countless memories (softball, half-marathon, Wine Wednesdays, etc.) and for being my dates to so many events over the past few years.

Lastly, I would like to thank my family and friends for always being there for me. To my siblings, Ashley, Ingrid, and Scott, and my brother-in-law, Mark, thank you so much for being an endless source of support and advice, and helping me maintain my sanity by (constantly) bugging me to take study breaks and play games with you guys. To my loving parents, Andrew and Nicki, thank you for being so supportive and encouraging no matter what the circumstance. Your unconditional love, patience, and understanding have helped me through the toughest points of my academic career and I know that I would not be where I am today without you.

Table of Contents

List of Tables

List of Figures

List of Appendices

List of Supplementary Figures

List of Supplementary Tables

List of Abbreviations

ABC	Avidin-Biotin Complex
ABC Transporter	Adenosine Triphosphate-Binding Cassette Transporter
ACh	Acetycholine
Ad-LacZ	LacZ Adenovirus
Ad-OATP2B1	Human OATP2B1 Adenovirus
AEC	3-Amino-9-Ethylcarbazole
ANOVA	Analysis of Variance
AP	Alkaline Phosphatase
ATP	Adenosine Triphosphate
AUC	Area Under the Curve
BCA	Bicinchoninic Acid
BCRP	Breast Cancer Resistance Protein
BSA	Bovine Serum Albumin
cDNA	Complementary Deoxyribonucleic Acid
Ca^{2+}	Calcium Ion
CoQ_{10}	Coenzyme Q_{10}/Ubiquinone
C_T	Threshold Cycle
CYP3A4	Cytochrome P450 3A4
DAPI	4’,6-Diamidino-2-Phenylindole
DMSO	Dimethyl Sulfoxide
DNA	Deoxyribonucleic Acid
EDTA	Ethylenediaminetetraacetic Acid
ELISA	Enzyme-Linked Immunosorbent Assay
ER	Endoplasmic Reticulum

FBS	Fetal Bovine Serum
GAPDH	Glyceraldehyde 3-Phosphate Dehydrogenase
GLP	Glucagon-Like Peptide
GLUT	Glucose Transporter Protein
GSIS	Glucose-Stimulated Insulin Secretion
GTP	Guanosine Triphosphate
HBSS	Hank's Balanced Salt Solution
HDL	High-Density Lipoprotein
HEPES	4-(2-Hydroxyethyl)-1-Piperazineethanesulfonic Acid
HG	High Glucose Stimulation
HMG-CoA	3-Hydroxy-3-Methyl-Glutaryl-Coenzyme A
HMGCR	HMG-CoA Reductase Gene
HNFa	Hepatocyte Nuclear Factor-4 Alpha
IC_{50}	Half Maximal Inhibitory Concentration
IgG	Immunoglobulin G
IHC	Immunohistochemistry
IF	Immunofluorescence
K^+	Potassium Ion
K_m	Michaelis Constant, Concentration Producing Half Maximal Velocity
KO	Knockout
KRH	Krebs-Ringer HEPES Buffer
LDL	Low-Density Lipoprotein
LG	Low Glucose Stimulation
logD	Distribution Coefficient
MDR	Multidrug Resistance Gene
MOI	Multiplicity of Infection

mRNA	Messenger Ribonucleic Acid
MM Analysis	Morphometric Analysis
MRP	Multidrug Resistance Protein
MTT	3-(4,5-Dimethylthiazol-2-yl)-2,5-Diphenyltetrazolium Bromide
Na^+	Sodium Ion
OAT	Organic Anion Transporter
OATP	Organic Anion-Transporting Polypeptide
P-gp	P-glycoprotein
p-p38 MAPK	Phosphorylated p38 Mitogen-Activated Protein Kinase
PBS	Phosphate Buffered Saline
PBS-T	Phosphate Buffered Saline-Tween
PDAC	Pancreatic Ductal Adenocarcinoma
qRT-PCR	Quantitative Real-Time Polymerase Chain Reaction
RNA	Ribonucleic Acid
ROI	Region of Interest
RPMI 1640	Roswell Park Memorial Institute 1640 Medium
rs	Reference SNP Cluster ID
RT	Room Temperature
SD	Standard Deviation
SG	Secretory Granule
SI	Stimulation Index
SLC/SLCO	Solute Carrier Gene
SNP	Single-Nucleotide Polymorphism
V	Volts
VG	Voltage-Gated
WT	Wild-Type

1 Introduction

1.1 Significance of Study

Statins are widely prescribed due to their therapeutic efficacy and ability to prevent cardiovascular events (Vaughan et al. 2013). They exert their cholesterol-lowering effects through inhibition of 3-hydroxy-3-methyl-glutaryl-coenzyme A (HMG-CoA) reductase, resulting in the upregulation of low-density lipoprotein cholesterol (LDL-C) receptors (Skarlovnik et al. 2014; Vaughan et al. 2000). Statin therapy is generally safe and effective; however, it has been associated with some undesirable side effects including new-onset diabetes (Navarese et al. 2013; Preiss et al. 2011). The growing clinical evidence supporting statin-induced incident diabetes has prompted the United States Food and Drug Administration and Health Canada to approve safety label changes on nearly all statins to reflect the small but significant increased risk (Sattar and Taskinen 2012; Health Canada 2013). Statin treatment has been associated with alterations in insulin secretion *in vitro*; however, some findings are conflicting and various mechanisms have been proposed (Zhou et al. 2014; Abe et al. 2010; Salunkhe et al. 2016; Yada et al. 1999; Yaluri et al. 2015; Zhao and Zhao 2015).

Statins are known substrates of the organic anion-transporting polypeptides (OATPs) (Konig et al. 2006), a family of membrane-bound uptake transporters found in many organs including the liver, kidney, and intestine (Hagenbuch and Stieger 2013). We have recently reported expression of the statin carrier OATP1B3 in healthy pancreas, localized to the beta (β) cells of the islets of Langerhans (Meyer Zu Schwabedissen et al. 2014). Given that OATP1B3 mediates statin transport, the recent discovery of pancreatic OATP expression taken together with evidence of statin-induced impaired insulin secretion point to a potential link in a currently unexplored mechanism.

1.2 Organic Anion-Transporting Polypeptides

Transport proteins expressed on the cell surface are essential in facilitating the transmembrane movement of various molecules. Many crucial signalling factors, nutrients, and therapeutic drugs cannot readily diffuse across the lipid bilayer and thus require pathways by which they can enter the cell. Of equal importance is the clearance of various substances from the cell which may also require transport proteins (Hagenbuch

and Stieger 2013; Iusuf et al. 2012a). The solute carrier gene (*SLC*) superfamily contains genes coding for more than 300 of these transport proteins divided into 55 different families (He et al. 2009). Each *SLC* family is made up of proteins that share at least 40% of their amino acid sequence identity and proteins can be further classified into subfamilies in which they have at least 60% shared amino acid sequence identity with other members (Hagenbuch and Stieger 2013).

1.2.1 OATP Structure and Mechanism of Transport

The organic anion-transporting polypeptides (human OATPs, rodent Oatps) are encoded by six *SLCO* gene families in humans (*Slco* in rodents) and have been recognized for their importance in the cellular uptake of many endogenous substrates as well as xenobiotics. Accordingly, OATPs are classified into six families (OATP1, OATP2, OATP3, OATP4, OATP5, OATP6) and various subfamilies (OATP1A, OATP1B, OATP1C, etc.) (Hagenbuch and Stieger 2013). To date, at least 11 human OATPs have been identified, including OATP1A2, OATP1B1, OATP1B3, OATP1C1, OATP2A1, OATP2B1, OATP3A1, OATP4A1, OATP4C1, OATP5A1, and OATP6A1 (Cheng et al. 2005; Glaeser et al. 2010). Due to genetic divergence and gene duplication within the *SLCO* family, rodent Oatps do not correspond exactly to their human OATP orthologues; the rodent Oatp1a subfamily currently comprises of 5 proteins (Oatp1a1, rat Oatp1a3, Oatp1a4, Oatp1a5, Oatp1a6) corresponding to the single human OATP1A2 (Cheng et al. 2005), while there exists a lone rodent orthologue (Oatp1b2) for human OATP1B1 and OATP1B3 (Meyer Zu Schwabedissen et al. 2009; Zaher et al. 2008).

Based on structural modelling, OATPs are believed to contain 12 transmembrane domains with multiple glycosylation sites on the second and fifth extracellular loops. The fifth extracellular loop is large and contains several conserved cysteine residues, some of which may be involved in transport activity (Glaeser et al. 2010; Roth et al. 2012; Hagenbuch and Stieger 2013).

The transport mechanisms of OATPs have not been fully characterized and remain somewhat controversial. OATPs are regarded as ATP- and sodium-independent uptake transporters, and studies suggest transport occurs through electroneutral exchange, with

anionic substrates exchanged for intracellular bicarbonate, glutathione, or glutathione conjugates; however, most of these studies have been conducted only with some rodent Oatps and the findings do not appear to be consistent for all OATPs (Ho and Kim 2005; Roth et al. 2012; Hagenbuch and Stieger 2013). There is evidence that uptake activity of OATPs can be affected by extracellular pH; OATP1B3 transport activity of cholecystokinin-8 and OATP2B1 uptake activity of rosuvastatin have shown to be stimulated with decreasing pH (Schwarz et al. 2011; Knauer et al. 2013). The driving force for OATP substrate transport is not yet known, but the coupled exchange of anion substrates for intracellular molecules may indicate dependence on substrate concentration gradients (Briz et al. 2006; Hagenbuch and Meier 2004).

1.2.2 Tissue Distribution

OATP expression has been primarily detected in polarized epithelial cells of many tissues throughout the body, mediating uptake of substrates from portal circulation or across luminal membranes (Hagenbuch and Stieger 2013; Ho and Kim 2005). The OATP1A/1B and OATP2B subfamilies have been thoroughly studied and very well characterized compared to the other OATP families.

1.2.2.1 OATP1A/Oatp1a Subfamily

OATP1A2, the lone human member of the *OATP1A* subfamily, exhibits the most abundant mRNA expression in the brain but has also been detected in kidney, liver, placenta, lung, testes, and prostate. OATP1A2 protein expression has been detected in the blood-brain barrier, distal nephron, bile duct, and ciliary body (Hagenbuch and Meier 2003; Hagenbuch and Stieger 2013). With respect to the rodent Oatp1a subfamily members, *Oatp1a1* and *Oatp1a4* are both highly expressed in mouse and rat liver, and *Oatp1a1* at a comparable level in mouse kidney. *Oatp1a5* is also expressed in liver but at relatively low levels (Hou et al. 2014; Cheng et al. 2005). *Oatp1a6* appears to be predominantly expressed in kidney in both mouse and rat, with some mRNA expression detected in mouse liver (Cheng et al. 2005; Choudhuri et al. 2003). A recent study has demonstrated mRNA and protein expression of *Oatp1a* subfamily members in mouse and rat pancreas (Abe et al. 2010). This study demonstrated gene expression of *Oatp1a1*,

Oatp1a4, and *Oatp1a5* in rat whole pancreas and showed localization of these proteins to the islets of Langerhans. The same study also examined the pancreata of db/db mice, a model for diabetic dyslipidemia, and showed mRNA expression of *Oatp1a4* and *Oatp1a5* in pancreas and immunostaining for Oatp1a5 protein in mouse islets (Abe et al. 2010).

1.2.2.2 OATP1B/Oatp1b Subfamily

The members of the OATP1B/Oatp1b subfamily (human OATP1B1 and OATP1B3, rodent Oatp1b2) are considered liver-specific transporters. While both carriers are highly expressed in human liver under physiological conditions, extrahepatic expression of OATP1B3 has previously been shown in various cancers (Thakkar et al. 2013b; Obaidat et al. 2012). In pancreas, increased expression of OATP1B3 has been observed in various disease states such as chronic pancreatitis and pancreatic ductal adenocarcinoma (PDAC) (Hays et al. 2013; Thakkar et al. 2013b; Pressler et al. 2011). In addition to the expected high expression in liver, Cheng *et al.* reported low but detectable mRNA expression of *Oatp1b2* in stomach (Cheng et al. 2005). Furthermore, Oatp1b2 protein was found to be abundant in rat ciliary body epithelium (Gao et al. 2005). Little is known regarding OATP expression in the normal human pancreas, specifically in the islets of Langerhans; however, we recently reported the presence of OATP1B3 in human adult islets with likely distribution in β cells (Meyer Zu Schwabedissen et al. 2014).

1.2.2.3 OATP2B/Oatp2b Subfamily

OATP2B1 and Oatp2b1 make up the human and rodent members, respectively, of the OATP2B subfamily. In contrast to members of the OATP1B family, human OATP2B1 is present in many tissues throughout the body, with the greatest abundance of mRNA detected in liver (Kullak-Ublick et al. 2001). Protein expression of OATP2B1 has also been confirmed in intestine, kidney, muscle, placenta, epidermis, mammary gland, heart, and brain (Roth et al. 2012; Hagenbuch and Meier 2004; Knauer et al. 2010). Similar tissue distribution is seen in mouse and rat with Oatp2b1 highly expressed in liver and detectable in many of the same tissues as human OATP2B1 (Choudhuri et al. 2003; Cheng et al. 2005; Hagenbuch and Meier 2004).

1.2.3 OATP Substrate Specificity and Function

Generally, OATP substrates are anionic and amphipathic with a molecular weight greater than 450 kilodaltons (kDa) (Hagenbuch and Meier 2004). OATPs are able to transport a diverse spectrum of endogenous molecules as well as xenobiotics (Hagenbuch and Meier 2003; Konig et al. 2006; Glaeser et al. 2010). More specifically, OATP1B1, OATP1B3, and OATP2B1 are now recognized as major players in several physiological processes and in drug disposition (Ho and Kim 2005). These transport proteins, along with their rodent orthologues, have shown overlapping substrate specificity including various substrates such as steroid conjugate estrone-3-sulfate, thyroid hormones, and cholesterol-lowering statins (Hagenbuch and Meier 2003; Ho and Kim 2005; Cheng et al. 2005; Choudhuri et al. 2003).

The role of OATPs in liver physiology has been well established. Expressed at the basolateral membrane of hepatocytes, OATP1B1 and OATP1B3 mediate uptake of endogenous substrates such as bile acids and bilirubin into the liver, and are therefore essential components of enterohepatic circulation of bile acids and bilirubin metabolism (Iusuf et al. 2012a). This is supported by studies in transporter-deficient animal models such as the *Oatp1a/1b*$^{-/-}$ cluster knockout mouse lacking five genes of the *Oatp1a* and *Oatp1b* subfamilies, that demonstrate considerably increased total plasma bilirubin levels compared to wild-type (WT) mice under physiological conditions (van de Steeg et al. 2010). In humans, the characteristic conjugated hyperbilirubinemia that presents in Rotor syndrome is associated with a complete deficiency of *OATP1B1* and *OATP1B3* genes (van de Steeg et al. 2012). In terms of the relevance of OATPs in drug disposition, *Oatp1a/1b*$^{-/-}$ mice demonstrated altered pharmacokinetics of the anticancer agent methotrexate and the antihistamine fexofenadine; plasma drug levels were substantially increased and hepatic accumulation of both drugs reduced compared to WT mice (van de Steeg et al. 2010). Furthermore, mice deficient in Oatp1b2 showed significantly reduced hepatic accumulation and elevated plasma concentrations of the antibiotic rifampicin compared to WT mice (Zaher et al. 2008). Taken together, these findings support the critical role of OATPs/Oatps in distribution and clearance of endogenous and xenobiotic compounds.

1.3 Endocrine Pancreas

The pancreas acts both as an exocrine and an endocrine gland. The exocrine pancreas makes up the majority of the organ at 95-99% of total pancreatic mass. Exocrine tissue is comprised mostly of acinar cells, which produce many enzymes required for digestion in the duodenum (Williams 2010; Dolensek et al. 2015; Stanger and Hebrok 2013). The endocrine pancreas constitutes only 1-5% of the total pancreatic volume, and is composed of the islets of Langerhans (Dolensek et al. 2015; Lazo de la Vega-Monroy and Fernandez-Mejia 2011).

1.3.1 Islets of Langerhans

The islets of Langerhans contain five different endocrine cell types, each of which secretes a unique hormone. Insulin-producing beta (β) cells are the predominant cell type as they constitute 50-70% of cells in human islets. Alpha (α) cells secrete glucagon and are the second most abundant, accounting for 20-40% of islet cells. Delta (δ) cells and PP cells produce somatostatin and pancreatic polypeptide, respectively, and are less abundant at less than 10% of islet cells. Epsilon (ε) cells are responsible for the production of ghrelin and make up less than 1% of cells (Lazo de la Vega-Monroy and Fernandez-Mejia 2011; Dolensek et al. 2015). The composition of islets is different in humans and in mice; in humans, the distribution of cell types is scattered while in mice, β cells are largely concentrated in the middle of the islet and α cells are seen around the periphery (Dolensek et al. 2015). Additionally, mice have a slightly higher proportion of β cells than humans at 60-80% of islet cell volume, while α cells make up 10-30% of islets (Lazo de la Vega-Monroy and Fernandez-Mejia 2011; Dolensek et al. 2015)

1.3.2 Regulation of Glucose Homeostasis

The endocrine cells of the islets of Langerhans play an important role in the tight regulation of glucose homeostasis, working in a complex yet organized fashion to detect and respond to changes in blood glucose levels. The β and α cells are arguably the most important islet cells in glucose homeostasis due to their prominence in the islet and the function of their secreted hormones (Quesada et al. 2008).

1.3.2.1 Beta Cells and Insulin

Of the islet cell types, β cells have been most comprehensively studied; thus, the insulin secretion pathway is relatively well understood. In states of elevated blood glucose, β cells respond by releasing insulin to reduce glucose levels throughout the body. Insulin counteracts elevated glucose by stimulating glucose uptake into tissues like adipose, muscle, and liver, and by promoting glucose storage in glycogen or fat (Quesada et al. 2008). Glucose enters the β cell through glucose transporters (GLUT1 in humans, GLUT2 in rodents) and is phosphorylated by glucokinase to form glucose-6-phosphate. This phosphorylation step has been recognized as being crucial in glucose-stimulated insulin secretion such that glucokinase is considered the glucose sensor for the β cell (Dolensek et al. 2015). Glucose-6-phosphate then continues through cellular respiration to produce ATP, which closes ATP-sensitive potassium (K^+) channels (K_{ATP}). Closure of K_{ATP} channels prevents K^+ ion efflux while sodium (Na^+) ions continue to enter the cell, disrupting the balance of charge and causing depolarization of the cell membrane. This membrane depolarization opens voltage-dependent T-type calcium (Ca^{2+}) and Na^+ channels, flooding the cell with more Na^+ and Ca^{2+} ions and causing further depolarization. L-type voltage-dependent calcium channels open, triggering action potentials that increase intracellular Ca^{2+} levels. The increase of intracellular Ca^{2+} levels stimulates the movement of insulin-containing granules to the plasma membrane, where they fuse and release insulin (Dolensek et al. 2015; Hiriart and Aguilar-Bryan 2008).

1.3.2.2 Alpha Cells and Glucagon

Alpha cells act opposite to β cells, secreting glucagon that acts to increase blood glucose levels. Glucagon primarily targets the liver and induces glycogenolysis and gluconeogenesis to release more glucose into the blood (Quesada et al. 2008). Like β cells, α cells respond to changes in extracellular glucose, and as such K_{ATP} channels are crucial in initiating the glucagon secretion process. In conditions of low glucose, K_{ATP} channels close to increase the membrane potential to a voltage where the T-type Ca^{2+} channels open. The opening of T-type channels further depolarizes the membrane and activates Na^+ and N-type Ca^{2+} channels that produce regenerative action potentials.

Glucagon secretion is induced by the influx of Ca^{2+} caused by opening of N-type channels (Quesada et al. 2008).

1.3.3 Risk Factors for Type II Diabetes

Type II diabetes is characterized by impaired insulin secretion brought on by a progressive decrease in β cell mass and function, and insulin insensitivity (Butler et al. 2003). Many risk factors associated with the development of type II diabetes have been identified, including family history of type II diabetes, race, obesity, hypertension, elevated blood glucose, and dyslipidemia (Xu et al. 2010; Roy et al. 2016). Some of these risk factors may contribute directly to β cell pathophysiology; persistently high levels of glucose and fatty acids can cause endoplasmic reticulum (ER) stress and subsequent dysfunction in the β cell (Volchuk and Ron 2010).

1.4 HMG-CoA Reductase Inhibitors

The HMG-CoA reductase inhibitors, or statins, represent one of the leading treatments for the management of hypercholesterolemia. In the United States, an estimated 100 million prescriptions are filled annually for about 25 million patients (Vaughan et al. 2013). They are generally safe and have been proven to be very effective in managing cholesterol levels and reducing the likelihood of cardiovascular events (Thompson et al. 2003).

1.4.1 Mechanism of Action

Statins act by competitively inhibiting HMG-CoA reductase, the rate-limiting enzyme in the cholesterol synthesis pathway, and by upregulating expression of LDL-C receptors, thereby promoting cholesterol uptake into tissues and lowering plasma LDL levels (Burg and Espenshade 2011; Marcoff and Thompson 2007; Vaughan et al. 2000). Inhibition of HMG-CoA reductase prevents the formation of mevalonate, which is a crucial step in the production of cholesterol. By blocking the mevalonate pathway of *de novo* cholesterol synthesis, statins effectively reduce elevated levels of LDL-C (Thompson et al. 2003). Statins slightly differ in their extent of HMG-CoA reductase inhibition, also referred to as potency. Atorvastatin, rosuvastatin, and simvastatin (IC_{50} values in nM: 8.2, 5.4, 11.2, respectively) are considered the most potent statins, while pravastatin (IC_{50}: 44.1 nM) is

labelled as a low-potency statin (Carter et al. 2013; Chan et al. 2015; Hargreaves et al. 2005).

1.4.2 Statin Pharmacokinetics

Cholesterol-lowering largely differ in their physicochemical characteristics such as lipophilicity, as illustrated by differing logD values (distribution coefficient) (**Table 1.1**) (Ho et al. 2006; Shitara and Sugiyama 2006). Lipophilic statins such as atorvastatin, simvastatin, or lovastatin, are characterized by higher logD values and more readily diffuse across membranes, often resulting in higher tissue distribution (Bonsu et al. 2013; Shitara et al. 2003). On the other hand, less lipophilic statins such as rosuvastatin and pravastatin are thought to require active transport systems to efficiently enter the cell (Shitara and Sugiyama 2006). As amphipathic molecules, statins are ionizable and thus their membrane permeability further varies with pH (Iusuf et al. 2012b; Shitara and Sugiyama 2006; Knauer et al. 2013).

1.4.2.1 OATPs and Statin Pharmacokinetics

Most statins require OATP transport for their uptake into liver, the main target tissue, and subsequent clearance from the body, despite considerable differences in their lipophilicity (Ho and Kim 2005; Shitara and Sugiyama 2006) An overview of physicochemical characteristics and OATP/Oatp substrate specificity for different statins is provided in **Table 1.1**.

Implications of OATP transport in statin pharmacokinetics were explored after first observations that, although not considerably metabolized in humans, statin plasma concentrations showed great interindividual variability (Neuvonen et al. 1998). Several single-nucleotide polymorphisms (SNPs) in genes encoding OATPs, mainly *OATP1B1*, have been identified that may contribute to changes in systemic exposure of statins. Perhaps the best-known of these SNPs is *OATP1B1* 521T>C, which is associated with decreased OATP1B1 protein function; reduced transport activity due to impaired cell surface trafficking was demonstrated *in vitro* (Tirona et al. 2001) and clinical data in individuals with this polymorphism show a marked increase in statin plasma levels and significantly reduced effects on cholesterol synthesis inhibition (Niemi et al. 2004; Niemi

et al. 2005; DeGorter et al. 2013). Importantly, a genome-wide association study found a strong association of the *OATP1B1* 521T>C polymorphism with statin-induced myopathy (muscle pain or weakness) in patients on high dose simvastatin treatment (Link et al. 2008). Despite many SNPs having been identified in OATP1A2, OATP1B3, and OATP2B1, their implications on statin transport and potential clinical outcomes are less clear. Functional validation studies performed *in vitro* for various SNPs in *OATP1B3* (*OATP1B3* 699G>A, 1559A>C, 1679T>C) indicated impaired rosuvastatin transport activity of the variant allele compared to wild-type (Schwarz et al. 2011). Various polymorphisms have also been described in *OATP1A2,* and while not specifically tested for statin transport, a few have shown altered transport activity for other drug substrates *in vitro* (Lee et al. 2005). Very few polymorphisms have been identified in OATP2B1; however, one study was able to demonstrate reduced transport activity for *OATP2B1* 43C>T and 601G>A (Stieger and Meier 2011).

In addition to genetic factors contributing to statin pharmacokinetics, interactions of OATPs with other drugs can result in changes in statin disposition in the body. Cyclosporine is an immunosuppressant commonly administered concomitantly with statins in patients who develop hypercholesterolemia following transplantation (Shitara et al. 2003). Though largely recognized as an inhibitor of the drug-metabolizing enzyme cytochrome P450 3A4 (CYP3A4), cyclosporine also inhibits OATP1B1 and OATP1B3 and has been associated with increased statin plasma concentrations (Simonson et al. 2004; Shitara et al. 2003; Karlgren et al. 2012). The antibiotic rifampicin, when administered acutely, has also shown inhibitory effects on OATP1B1 and OATP1B3, whereas chronic administration leads to strong induction of CYP3A4 and other enzymes (Anderson et al. 2013; Reitman et al. 2011). Therefore, *in vitro* statin transport activity of OATP1B1 and OATP1B3 is inhibited by co-treatment with rifampicin, and clinical data show increased statin plasma concentration following concomitant administration with rifampicin (Karlgren et al. 2012). Another antibiotic, clarithromycin, significantly increased patients' systemic exposure of pravastatin, simvastatin, and atorvastatin when co-administered (Jacobson 2004). In a separate *in vitro* study, clarithromycin inhibited uptake activity of OATP1B1 and OATP1B3; however, these two findings have not been investigated and validated together (Karlgren et al. 2012).

Table 1.1. OATP/Oatp substrate specificity and physicochemical characteristics of statins.

Species	Protein	Statin (K_m value in µM)	Statin LogD (pH 7 or *7.4*)	Reference
Human	OATP1A2	Pitavastatin (3)	1.5	Fujino et al. (2005)
		Rosuvastatin (3)	*-0.25 – -0.50*	Ho et al. (2006)
	OATP1B1	Atorvastatin (10)	1.53	Lau et al. (2006)
		Cerivastatin (4)	2.32	Shitara et al. (2003)
		Fluvastatin (1.4-3.5)	1.75	Kopplow et al. (2005); Noe et al. (2007)
		Pitavastatin (3)	1.5	Fujino et al. (2005); Hirano et al. (2004)
		Pravastatin (14-35)	-0.47	Hsiang et al. (1999); Nakai et al. (2001)
		Rosuvastatin (4-7.3)	*-0.25 – -0.50*	Ho et al. (2006)
		Simvastatin acid (NR)	4.4	Pasanen et al. (2006)
	OATP1B3	Atorvastatin (NR)	1.53	Schwarz et al. (2011)
		Fluvastatin (7)	1.75	Kopplow et al. (2005)
		Rosuvastatin (9.8)	*-0.25 – -0.50*	Ho et al. (2006)
		Pitavastatin (3.25)	1.5	Hirano et al. (2004)
	OATP2B1	Atorvastatin (0.2)	1.53	Kalliokoski and Niemi (2009)
		Fluvastatin (0.7)	1.75	Kopplow et al. (2005); Noe et al. (2007)
		Pitavastatin (1.17)	1.5	Hirano et al. (2006)
		Pravastatin (2.25)	-0.47	Nozawa et al. (2004)
		Rosuvastatin (2.4)	*-0.25 – -0.50*	Ho et al. (2006)
Rat	Oatp1a1	Pravastatin (30)	-0.47	Hsiang et al. (1999)
		Rosuvastatin (NR)	*-0.25 – -0.50*	Ho et al. (2006)
	Oatp1a4	Atorvastatin (22.2)	1.53	Lau et al. (2006)
		Pravastatin (38)	-0.47	Tokui et al. (1999)
		Rosuvastatin (NR)	*-0.25 – -0.50*	Ho et al. (2006)
	Oatp1a5	Pitavastatin (2.4)	1.5	Shirasaka et al. (2011)
		Pravastatin (NR)	-0.47	Shirasaka et al. (2010)
		Rosuvastatin (NR)	*-0.25 – -0.50*	Ho et al. (2006)
	Oatp1b2	Atorvastatin (7.12)	1.53	Lau et al. (2006)
		Rosuvastatin (NR)	*-0.25 – -0.50*	Ho et al. (2006)
	Oatp2b1	Pitavastatin (NR)	1.5	Shirasaka et al. (2011)
		Pravastatin (NR)	-0.47	Shirasaka et al. (2010)

Adapted from Konig et al. (2006), Shitara and Sugiyama (2006), and Roth et al. (2012);
K_m – Michaelis constant, logD – distribution coefficient; NR – not reported

1.4.2.2 Other Carriers and Statin Pharmacokinetics

Though statin pharmacokinetics are greatly influenced by many OATPs, it is important to recognize other key transport proteins involved in the disposition of statins. There is a crucial interplay between uptake transporters and efflux transporters resulting in absorption, systemic distribution, and excretion of statins (Knauer et al. 2010).

The organic anion transporter (OAT) family is another important group of uptake transporters belonging to the *SLC* superfamily. Like OATPs, OATs are present in many human tissues and demonstrate a wide and diverse substrate specificity. Abundantly expressed in the kidneys, they are largely recognized for mediating active transport of substrates from blood to urine across renal proximal tubule cells (VanWert et al. 2010; Roth et al. 2012). Most human OATs, including OAT1 and OAT3, have shown transport activity for statins; the latter having been detected in liver and thus more relevant in statin pharmacokinetics (VanWert et al. 2010). There is limited knowledge of OAT3-associated drug-drug interactions and polymorphisms affecting statin pharmacokinetics; however, an *in vitro* study has demonstrated a dose-dependent inhibition of OAT1 and OAT3 transport with fluvastatin and simvastatin up to 120 μM (Takeda et al. 2004).

The ATP-binding cassette (ABC) efflux transporters have been well established as key players in statin disposition. In particular, breast cancer resistance protein (BCRP), multidrug resistance-associated protein 2 (MRP2), and P-glycoprotein (P-gp) are thought to be important in mediating statin clearance from tissues. Each of these ATP-dependent efflux transporters has shown uptake activity of various statins, including common substrate specificity for pitavastatin, pravastatin, and rosuvastatin (Hirano et al. 2005; Huang et al. 2006; Kitamura et al. 2008). Like with the OATPs, statin pharmacokinetics were shown to be affected by various common impaired-function polymorphisms or drug-drug interactions involving *BCRP*, *MRP2*, and *P-gp*. A clinical study in healthy volunteers found that individuals expressing the *BCRP* 421C>A polymorphism had a significantly increased area under the curve (AUC) for rosuvastatin plasma concentration (Zhang et al. 2006). The *MRP2* 1446C>G SNP has been associated with significantly reduced pravastatin plasma concentration AUC in heterozygous individuals (Niemi et al. 2006). Concomitant administration of simvastatin acid with antiretroviral drugs ritonavir

or saquinavir was reported to cause a 30-fold increase in simavastatin acid AUC due to dual inhibition of OATP1B1 and P-gp (Neuvonen et al. 2008).

Thus, in addition to OATPs, OAT uptake transporters and ABC efflux transporters are also important in the distribution and elimination of statins from the body.

1.4.3 Statin-Induced Muscle Toxicity

Though statins are among the most effective treatments for hypercholesterolemia, they have been associated with the development of skeletal muscle side effects. These can range from mild muscle pain or weakness to life-threatening rhabdomyolysis (Marcoff and Thompson 2007). Though rhabdomyolysis is very rare, up to 15% of patients on statin therapy experience some form of muscle side effect (myopathy) that can cause treatment cessation (Vaughan et al. 2013; Marcoff and Thompson 2007). Among other potential culprits, a role of depleted CoQ_{10} in statin-induced muscle toxicity has been proposed but is still controversial as studies have shown conflicting findings regarding the effectiveness of CoQ_{10} supplementation in improving muscle symptoms (Vaughan et al. 2013; Marcoff and Thompson 2007).

1.4.4 Statin-Induced Incident Diabetes

In addition to muscle toxicity, statin therapy has also recently been associated with an increased risk for new-onset diabetes. While the clinical relevance of this correlation is still debated, there is a growing body of literature supporting potential diabetogenic effects of statins that may relate to altered insulin sensitivity and/or secretion.

1.4.4.1 Clinical Evidence

Several meta-analyses of major clinical statin trials have provided evidence for statin-induced incident diabetes. A meta-analysis by Sattar *et al.* included nearly all large randomized placebo-controlled statin trials up until 2010 involving atorvastatin, rosuvastatin, pravastatin, simvastatin, and lovastatin treatment, consisting of over 90,000 patients (Sattar et al. 2010). Though the rate of new-onset diabetes over the mean follow-up of 4 years varied from trial to trial, the combined data from these thirteen trials showed an additional 174 cases of new-onset diabetes in previously nondiabetic patients

treated with statins compared to placebo control, representing a 9% increased risk of developing incident diabetes with statin treatment (Sattar et al. 2010). Preiss *et al.* analyzed five different randomized clinical trials including more than 30,000 non-diabetic patients prescribed atorvastatin or simvastatin who were followed up for an average of approximately 5 years (Preiss et al. 2011). They reported that 8.4% of participants developed diabetes during the follow-up period (Preiss et al. 2011). Another group studied three randomized atorvastatin trials (two of which overlap with the study by Preiss *et al.*) with an average follow up of 5 years and reported an up to 34% increased risk of developing new-onset diabetes with atorvastatin treatment (Waters et al. 2011). A more recent population-based cohort study in almost 9000 non-diabetic men evaluated changes in insulin sensitivity and insulin secretion with statin therapy over 6 years (Cederberg et al. 2015). After adjusting for several confounding factors including age and body mass index (BMI), statin therapy was associated with a 46% increased risk for new-onset diabetes (Cederberg et al. 2015).

1.4.4.2 Risk Factors for Statin-Induced Incident Diabetes

Several clinical risk factors have been described to contribute to statin-induced new-onset diabetes, such as lower overall high-density lipoprotein (HDL) cholesterol, and higher blood pressure, BMI, fasting glucose, and triglycerides (Waters et al. 2011; Cederberg et al. 2015). In addition, two SNPs in the HMG-CoA reductase (*HMGCR*) gene (rs17238484 and rs12916) have been identified as predictors of new-onset diabetes in a genome-wide association study (Swerdlow et al. 2015). These SNPs demonstrated strong associations with lower circulating LDL cholesterol, and gene expression data demonstrated reduced hepatic expression of *HMGCR* associated with the variant T allele of rs12916 (Swerdlow et al. 2015), suggesting a potential relevance of the extent of HMG-CoA reductase inhibition, or potency of statins, in incident diabetes. This is further supported by experimental and clinical data comparing high-potency statins (atorvastatin, rosuvastatin) to moderate-potency (simvasatatin) and low-potency statins (fluvastatin, lovastatin, pravastatin) (Carter et al. 2013). Pravastatin, a low-potency hydrophilic statin, has shown minimal effects on insulin secretion and calcium signalling *in vitro* compared to more potent lipophilic statins such as atorvastatin and simvastatin (Ishikawa et al.

2006; Yada et al. 1999). Clinical data have demonstrated neutral or even protective effects of pravastatin when evaluating the risk for new-onset diabetes; atorvastatin, rosuvastatin, and simvastatin treatment has been associated with a significantly greater risk for incident diabetes compared to pravastatin treatment (Carter et al. 2013; Sattar et al. 2010). Atorvastatin therapy has also been associated with higher rates of new-onset diabetes compared to simvastatin therapy (Waters et al. 2011). Furthermore, there may also be a dose-dependent effect of statins. The above noted meta-analysis of five statin trials involving over 30,000 patients found that, of 2749 patients that developed diabetes, 149 more developed incident diabetes (odds ratio 1.12) on intensive-dose statin therapy than moderate-dose statin therapy (Preiss et al. 2011). Moreover, high dose atorvastatin therapy was associated with a slight increase in new-onset diabetes compared to low-dose atorvastatin therapy (Waters et al. 2011). Simvastatin and atorvastatin treatment were found to increase risk of incident diabetes and reduce insulin secretion in a dose-dependent manner (Carter et al. 2013). Taken together, the risk of incident diabetes with statin therapy appears to vary with type of statin, potency, and dose.

1.4.4.3 Proposed Mechanisms for Statin-Induced Alterations in Insulin Secretion

Based on the available experimental and clinical evidence, statins are thought to either impair insulin sensitivity or insulin secretion (Cederberg et al. 2015), the latter of which being the focus of this project. While the exact molecular mechanisms for statin-induced impairment of insulin secretion are currently unknown, multiple mechanisms have been proposed, most of which suggest disruptions in signalling that prevent secretion of insulin from β cells. Various *in vitro* studies have been conducted to elucidate potential mechanisms of statin effects on insulin secretion; an overview of their findings is provided in **Table 1.2**.

Table 1.2. Overview of *in vitro* studies with statin-induced altered insulin secretion.

Cell Type Used	Statin(s) Tested (Time)	Effect on Insulin Secretion	Proposed Mechanism	Reference
Rat islets	Simvastatin (30 min) Pravastatin (30 min)	0.3 µg/mL: ↓ with HG 100 µg/mL: no effect	Inhibition of L-type Ca^{2+} channels impairs responsiveness to glucose	Yada et al. (1999)
Mouse islets	Atorvastatin (24 hr) Simvastatin (24 hr) Pravastatin (24 hr)	100 nM, 1 µM, 10 µM: no effect 100 nM, 1 µM, 10 µM: no effect 100 nM, 1 µM, 10 µM: no effect	No effect on insulin secretion in *ex vivo* islet studies	Ishikawa et al. (2006)
MIN6 (Mouse)	Lovastatin (24 hr)	10 µM: ↑ with LG, ↑ with HG, ↓ insulin content, increased SG size	Increase in basal and stimulated insulin suggests disruption of insulin secretion; effect reversed with mevalonate and squalene treatment; depleted cholesterol may weaken SG membranes	Tsuchiya et al. (2010)
INS-1e (Rat) Mouse islets	Pravastatin (48 hr) Pravastatin (48 hr)	30 µM: ↑ with HG 30 µM: ↑ with HG	Reduction of β cell cholesterol by statins prevents toxic lipid accumulation and promotes insulin secretion	Abe et al. (2010)
MIN6 (Mouse)	Simvastatin (48 hr)	2 µM: ↓ with LG, 5 µM: ↓ with LG 10 µM: ↓ with LG, ↓ with HG	Upregulation of potassium channel Kir6.2, suppression of VG Ca^{2+} channel and GLUT2 prevent membrane depolarization and Ca^{2+} influx	Zhou et al. (2014)

MIN6 (Mouse)	Simvastatin (30 min) Pravastatin (30 min)	14.3 μM: ↓ with LG, ↓ with HG 26.3 μM: ↑ with HG	Reduced insulin secretion mediated by alternative pathways (ACh, GLP, lipid-sensing receptors); inhibition of VG Ca^{2+} channels	Yaluri et al. (2015)
Human islet β cells	Atorvastatin (24 hr) Pitavastatin (24 hr) Pravastatin (24 hr) Rosuvastatin (24 hr)	100 nM: ↓ SI 100 nM: ↓ SI 10 nM: ↓ SI 100 nM: ↓ SI 100 nM: ↓ SI	Dose-dependent effects for all statins; altered expression of GLUT-2 (reduced with atorvastatin and pravastatin, increased with rosuvastatin and pitavastatin); β cell apoptosis induced by upregulation of p-p38 MAPK	Zhao and Zhao (2015)
INS-1 832/13 (Rat)	Rosuvastatin (48 hr)	200 nM: ↓ with HG 2 μM: ↑ with LG, ↓ with HG 20 μM: ↑ with LG, ↓ with HG	Reduced Ca^{2+} currents through VG Ca^{2+} channels prevent exocytosis of insulin granules; treatment with mevalonate but not squalene reversed effect	Salunkhe et al. (2016)

LG: low glucose stimulation (represents basal insulin secretion); HG: high glucose stimulation (represents glucose-induced insulin secretion); SI: stimulation index (high glucose insulin secretion/low glucose insulin secretion); VG: voltage-gated; GLUT2: glucose transporter 2; ACh: acetylcholine; GLP: glucagon-like peptide; p-p38 MAPK: phosphorylated p38 mitogen-activated protein kinase

Dose-dependent statin-induced alterations in gene expression of ion channels and glucose transporters have been reported *in vitro* that may contribute to statin-mediated effects on insulin secretion, as both are important in maintaining proper electrophysiology and voltage-dependent signalling in the β cell (Zhou et al. 2014; Zhao and Zhao 2015). Some statins (rosuvastatin, simvastatin) have been shown to affect ion channel activity via inhibition of channels or ion flow disturbance (Salunkhe et al. 2016; Yada et al. 1999). Function of the β cell may also be affected by statins in a dose-dependent manner, as exemplified by reduced insulin secretion and induction of apoptosis in β cell models following statin treatment (Zhou et al. 2014; Ishikawa et al. 2006; Zhao and Zhao 2015).

Insulin secretion from β cells may be influenced in opposite ways by statin-mediated changes in intracellular cholesterol levels. Reduction of β cell cholesterol by statins may improve insulin secretion by mitigating lipotoxicity associated with intracellular lipid accumulation; indeed, pravastatin treatment has been associated with increased insulin secretion (Abe et al. 2010; Yaluri et al. 2015). Conversely, decreased intracellular cholesterol may impair insulin secretion by disrupting insulin secretory granules (Tsuchiya et al. 2010). Secretory granule membranes contain high levels of endogenous cholesterol which can be depleted with statin treatment, resulting in compromised membrane integrity and leakage of insulin within the β cell (Tsuchiya et al. 2010).

Lastly, inhibition of the mevalonate pathway (**Figure 1.1**) has been proposed as a mechanism for statin-induced changes in insulin secretion (Salunkhe et al. 2016; Tsuchiya et al. 2010). Inhibition of HMG-CoA reductase by statins can also prevent production of other intermediate compounds such as farnesyl pyrophosphate (Salunkhe et al. 2016). Farnesyl pyrophosphate is an important intermediate not only in cholesterol synthesis but also in synthesis of CoQ_{10} and prenylated proteins (Marcoff and Thompson 2007; Goldstein and Brown 1990). CoQ_{10} is an essential component of the electron transport chain and critical in proper mitochondrial function and in ATP production, the latter of which is required to initiate glucose-stimulated insulin secretion (Vaughan et al. 2013; Lazo de la Vega-Monroy and Fernandez-Mejia 2011). Prenylated proteins include guanosine triphosphate (GTP)-binding proteins (also known as GTPases) such as Rac and Rab, which are both reported to be involved in glucose-stimulated insulin secretion

(Kowluru and Veluthakal 2005). A schematic of currently proposed mechanisms for statin-induced alterations in insulin secretion is shown in **Figure 1.2**.

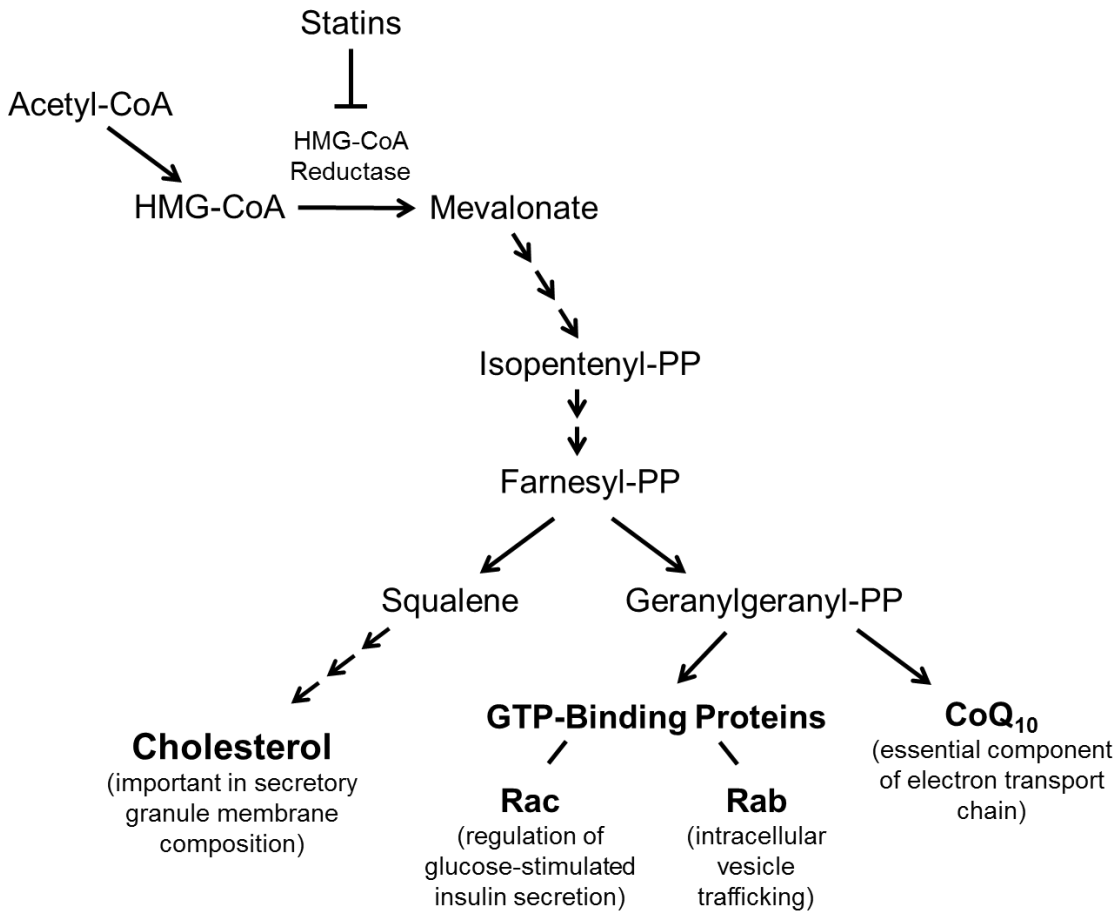

Figure 1.1. Mevalonate pathway and relevance for beta cell function. Inhibition of this pathway by statins reduces cholesterol synthesis and prevents the production of intermediates essential in insulin secretion. Adapted from Goldstein and Brown (1990), Kowluru and Veluthakal (2005), and Salunkhe et al. (2016).

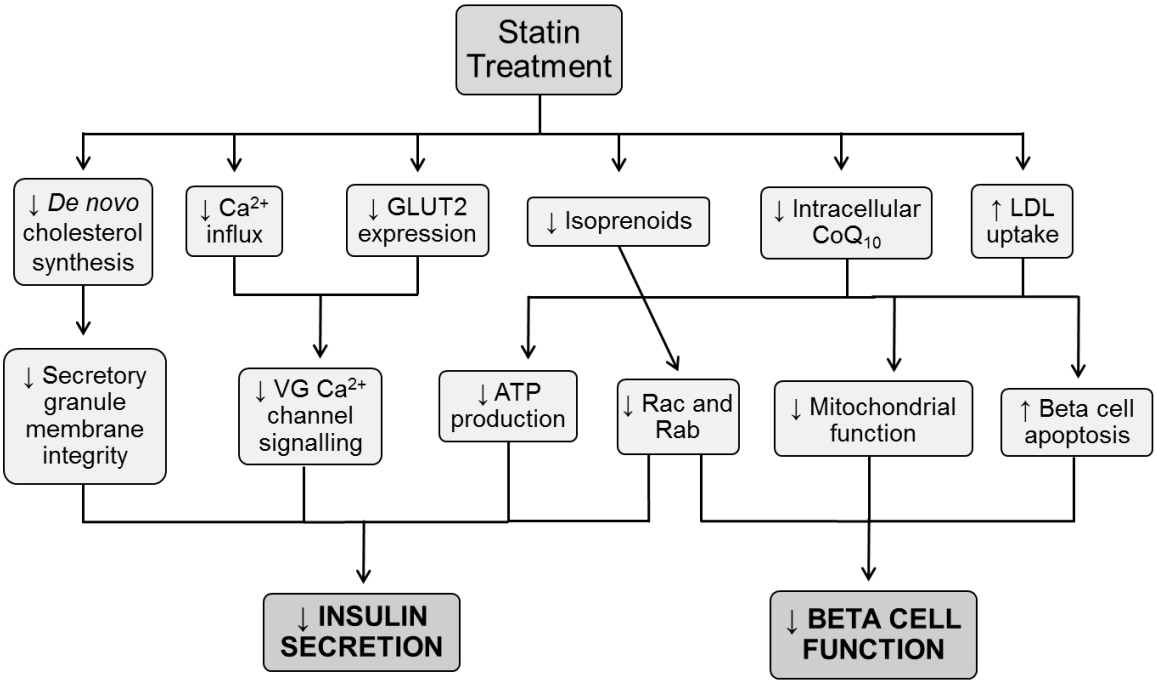

Figure 1.2. Hypothesized mechanisms of statin effects on β cells. Several different pathways have been proposed for statin-mediated effects on insulin secretion and β cell function. Adapted from Chan et al. (2015) and Tsuchiya et al. (2010).

1.5 Rationale, Hypothesis, and Specific Aims

1.5.1 Rationale

OATPs have been most extensively studied in excretory organs such as the liver, kidney, and intestine, as well as at blood-tissue barriers including the brain and placenta. In pancreas, increased expression of OATP1B3 has been observed in chronic pancreatitis and pancreatic ductal adenocarcinoma (PDAC) (Hays et al. 2013; Pressler et al. 2011; Thakkar et al. 2013b). Little is known about OATP expression in the normal pancreas, specifically in the islets of Langerhans where they may be involved in islet function. We recently reported the presence of OATP1B3 in human adult islets with likely distribution in β cells (Meyer Zu Schwabedissen et al. 2014). We observed that transient overexpression of OATP1B3 enhanced the insulinotropic effect of the sulfonylurea glibenclamide, a substrate of OATP1B3, in the mouse β cell line MIN6 (Meyer Zu Schwabedissen et al. 2014).

Meta-analyses of recent clinical trials indicate an up to 34% increased risk of new-onset diabetes associated with statin therapy (Waters et al. 2011), with risk varying with statin type, potency, and dose (Bonsu et al. 2013; Ishikawa et al. 2006; Yada et al. 1999; Preiss et al. 2011). Based on limited experimental and clinical evidence, statins are thought to either affect insulin sensitivity or insulin secretion (Cederberg et al. 2015). While the exact mechanisms in stain-induced impairment of insulin secretion have not been elucidated, the role of CoQ_{10} in modulating islet β cell function offers an intriguing link. Inhibition of HMG-CoA reductase lowers cholesterol but also synthesis of CoQ_{10}, the latter required as an electron carrier during mitochondrial oxidative phosphorylation to generate ATP. β cell depletion of CoQ_{10} by statins may diminish ATP, preventing closure of ATP-sensitive K^+ channels and membrane depolarization, resulting in reduced insulin release; additionally, mitochondrial dysfunction may also be a consequence. While statins have been shown to inhibit glucose-induced insulin secretion (Salunkhe et al. 2016; Zhou et al. 2014; Zhao and Zhao 2015), suppress CoQ_{10} synthesis (Marcoff and Thompson 2007), and production of ATP (Zhou et al. 2014), a role for OATP-mediated statin transport in this mechanism has not been explored.

1.5.2 Hypothesis

We hypothesize that expression and activity of OATP transporters in pancreatic β cells regulate statin entry and contribute to statin-induced impairment of insulin secretion through disruption of mitochondrial function and ATP-dependent signalling.

1.5.3 Specific Aims

The aims of this project are:

1) To characterize the presence and interindividual variation of OATP1B3 and other key statin carriers in human adult pancreatic islets as well as their co-localization with α and β cells to gain first insights to specific endocrine roles

2) To elucidate the role of statin transport in β cell function using a murine β cell model with altered OATP expression

2 Materials and Methods[1]

[1]Specific Aim 1 reproduced (adapted) from: Kim M, Deacon P, Tirona RG, Kim RB, Pin CL, Meyer zu Schwabedissen HE, Wang R, and Schwarz UI (2017). Characterization of OATP1B3 and OATP2B1 transporter expression in the islet of the adult human pancreas. *Histochemistry and Cell Biology*, doi:10.1007/s00418-017-1580-6, with permission of Springer © Springer-Verlag Berlin Heidelberg 2017.

2.1 Specific Aim 1: Characterization of statin carrier expression and OATP subcellular localization in human pancreatic islets

2.1.1 Histologic sections of pancreata, isolated islets and other tissues

Normal human adult hepatic RNA (N=1) and pancreatic RNA (N=1) were purchased from Biochain (Newark, California, USA) or RNA extracted from a liver tissue sample (N=1) obtained through the Liver Tissue Cell Distribution System (Minneapolis, Minnesota; funded by NIH Contract #N01-DK-7-0004/HHSN267200700004C) and from a pancreas tissue sample (N=1; gift by Dr. V. McAllister) with approval by the Health Science Research Ethics Board (HSREB) at the University of Western Ontario (protocol HSREB-2597). Isolated human adult islets from 4 different individuals (approximately 5000 islet equivalents per subject received) were provided by the Juvenile Diabetes Research Foundation Centre for Islet Cell Replacement at the McGill University Health Centre, and RNA extracted for analysis as previously described (Krishnamurthy et al. 2011).

Formalin fixed paraffin-embedded tissue sections of normal pancreata were purchased (N=3; Biochain) or obtained as previously reported (N=7) (Krishnamurthy et al. 2011). Diseased pancreatic tissues including tumour-adjacent pancreas (NP, sections from N=3 patients), chronic pancreatitis (INFP, N=3) and pancreatic ductal adenocarcinoma (PDAC, N=3) were obtained from the Pathology Archive (London Health Science Centre, Ontario, Canada) with approval from the HSREB at the University of Western Ontario (protocol HSREB-17012). All tissue sections and subject characteristics are summarized in **Table 2.1**.

Table 2.1. Subject characteristics of paraffin-embedded pancreatic tissue sections utilized for immunostaining.

Sample ID	*Age (years)*	*Sex*	*Histology*	*Source*	*Analyses*
B105098	76	Male	Normal	BioChain	IF/ MM analysis
B903130, B903132	77	Male	Normal	BioChain	IF/ MM analysis
B605108	71	Male	Normal	BioChain	IHC, IF/ MM analysis
AHP 1, AHP 3, AHP 4	39	Male	Normal	JDRF, McGill University	IF/ MM analysis
AHP 2	20	Unknown	Normal	JDRF, McGill University	IF/ MM analysis
05SH44	60	Female	Normal	JDRF, McGill University	IHC; IF/ MM analysis
05SH45	60	Female	Normal	JDRF, McGill University	IF/ MM analysis
05SH46	46	Male	Normal	JDRF, McGill University	IHC; IF/ MM analysis
05SH47	61	Male	Normal	JDRF, McGill University	IF/ MM analysis
05SH57	56	Male	Normal	JDRF, McGill University	IF/ MM analysis
09-30492 A3 [P1-NP]	Unknown	Unknown	Tumour-adjacent	Pathology archive, UWO	IHC
09-37568 B11 [P2-NP]	Unknown	Unknown	Tumour-adjacent	Pathology archive, UWO	IHC
93-11845 N [P3-NP]	Unknown	Unknown	Tumour-adjacent	Pathology archive, UWO	IHC

01-25068 A8 [P4-INFP]	Unknown	Unknown	Chronic inflammation	Pathology archive, UWO	IHC
94-3136 H [P5-INFP]	Unknown	Unknown	Chronic inflammation	Pathology archive, UWO	IHC
00-31340 B3 [P6-INFP]	Unknown	Unknown	Chronic inflammation	Pathology archive, UWO	IHC
10-941 C6 [P7-PDAP]	Unknown	Unknown	Adenocarcinoma	Pathology archive, UWO	IHC
06-5970 E4 [P8-PDAP]	Unknown	Unknown	Adenocarcinoma	Pathology archive, UWO	IHC
06-10423 H8 [P9-PDAP]	Unknown	Unknown	Adenocarcinoma	Pathology archive, UWO	IHC

JDRF, Juvenile Diabetes Research Foundation Centre for Islet Cell Replacement; UWO, University of Western Ontario; IHC, immunohistochemistry; IF, immunofluorescence; MM analysis, morphometric analysis

2.1.2 Gene expression analysis

Total RNA was reverse transcribed (2 μg) into cDNA using TaqMan® Reverse Transcription Reagents (Applied Biosystems, Carlsbad, CA). Relative mRNA expression of statin transporters *OATP1B3*, *OATP1B1*, *OATP1A2*, *OATP2B1*, *BCRP*, *MRP2*, and *P-gp* in human pancreas and islets was examined compared to liver or kidney, tissues with known expression, by quantitative real-time polymerase chain reaction (qRT-PCR) with SYBR® Green (ABI Prism 7700, Applied Biosystems) utilizing previously optimized primer sets (Glaeser et al. 2007; Prentice et al. 2014) (Primer sequences in **Table 2.2**). Due to reported lack of expression for *OATP1B1* and *OATP1B3*, kidney represents a negative control for these two genes. Reactions were performed in duplicate for human islet preparations, and in triplicate for all other tissues. Gene expression levels for each tissue were normalized to *18S* ribosomal RNA expression (TaqMan Assay Hs99999901_s1), and analyzed using the ΔC_T method ($\Delta C_T = C_{T,\ target} - C_{T,\ 18S}$) (Schmittgen and Livak 2008). Data are presented as the fold-difference in transporter gene expression in islets or other tissues compared to that of liver (i.e. mean $2^{-\Delta CT}$ for OATP1B3 in islets or other tissues/ mean $2^{-\Delta CT}$ for OATP1B3 in liver). All qRT-PCR consisted of an initial denaturation at 95°C for 20 seconds, followed by 40 cycles at 95°C for 1 second, 60°C for 20 seconds. RNAse-free water was used as the non-template control.

Table 2.2. Primers used for qRT-PCR analysis of human statin transporter expression.

Origin	*Gene*	*Forward (5'-3')*	*Reverse (5'-3')*	*Reference*
Human	*OATP1A2*	AAGACCAACGCAG GATCCAT	GAGTTTCACCCATT CCACGTACA	Glaeser et al. (2007)
	OATP1B1	TGAACACCGTTGG AATTGC	TCTCTATGAGATGT CACTGGAT	Glaeser et al. (2007)
	OATP1B3	GTCCAGTCATTGGC TTTGCA	CAACCCAACGAGA GTCCTTAGG	Glaeser et al. (2007)
	OATP2B1	CTTCATCTCGGAGC CATACC	GCTTGAGCAGTTGC CATTG	Glaeser et al. (2007)
	OAT3	CGATGTCCCAGCCA AGTTCA	AAGGGCACAAAGG TGAGAGC	Prentice et al. (2014)
	BCRP	TGGCTGTCATGGCT TCAGTA	GCCACGTGATTCTT CCACAA	Glaeser et al. (2007)
	MRP2	ATGCTTCCTGGGGA TAAT	TCAAAGGCACGGA TAACT	Glaeser et al. (2007)
	P-gp	GTCCCAGGAGCCC ATCCT	CCCGGCTGTTGTCT CCAT	Glaeser et al. (2007)

2.1.3 Immunostaining of human pancreatic tissue

Paraffin-embedded pancreatic tissue sections were stained for OATP1B3, OATP2B1, insulin and glucagon according to standard immunohistochemistry (IHC) or immunofluorescent (IF) protocols. Briefly, slides were deparaffinized, rehydrated, and subjected to antigen retrieval using Retrievit 8 (pH 8.0, BioGenex, Fremont, California), citrate buffer (0.01 M, pH 6.0), or EDTA buffer (0.01 M, pH 8), followed by blocking with 5% fetal bovine serum (FBS) in phosphate-buffered saline (PBS). Subsequently, sections were incubated at 4°C overnight with the following primary antibodies: rabbit polyclonal anti-OATP1B3 (dilution 1:150, custom-made) (Ho et al. 2006), rabbit polyclonal anti-OATP2B1 (1:50, custom-made) (Knauer et al. 2010), mouse monoclonal anti-insulin (1:1000; I2018, Sigma-Aldrich, St. Louis, Missouri, USA), and mouse monoclonal anti-glucagon (1:1000; G2654, Sigma-Aldrich). Sections were then incubated with the appropriately labeled secondary antibodies. For IHC, the avidin-biotin complex (ABC) method was used to detect rabbit or mouse primary antibodies via secondary biotinylated antibodies and streptavidin-horseradish peroxidase or alkaline phosphatase conjugates, respectively (Vectastain ABC kit rabbit IgG or ABC-AP kit mouse IgG, Vector Laboratories Inc., Burlingame, California, USA). Positive signals were visualized via the appropriate substrate/chromogen (AEC or Vector® Red, Vector Laboratories Inc.). Nuclei were counterstained using hematoxylin. For IF, slides were incubated with fluorescently labelled antibodies conjugated to Alexa Fluor® 488 or 633 (Thermo-Fisher Scientific, Waltham, Massachusetts, USA). Slides were counterstained to mark nuclei using mounting medium containing DAPI (VECTASHIELD, Vector Laboratories Inc.). Stained sections were viewed using a Nikon Eclipse 80i microscope (Nikon Instruments Inc., Melville, New York, USA) or by confocal microscopy (LSM 510 Meta laser scanning microscope, Carl Zeiss, Jena, Germany).

2.1.4 Quantitative imaging analysis of endocrine pancreatic morphology and colocalization

Quantitative imaging analysis has been performed on normal human pancreatic sections of 10 subjects (**Table 2.1**) after dual immunofluorescent staining for insulin or glucagon with OATP1B3. Relative α- and β-cell area as well as the percentage colocalization of OATP1B3 with α and β cells within islets were analyzed by sex and age using the NIS Elements Basic Research Microscope Imaging Software (Nikon Instruments Inc.).

To estimate α- and β-cell populations in all individuals, the relative β-cell area was calculated as the ratio of β-cell area to exocrine area (Butler et al. 2003). To measure these ratios, consecutive immunostained sections from each subject were examined. For each individual, a representative area of a section was randomly chosen at 4x objective magnification for subsequent imaging analysis. Subsequently, images of 20 islets per subject were captured at 20x objective magnification. Islets, defined as a grouping of at least 4 insulin or glucagon positive cells, were selected in a systematic fashion across each tissue section. Using the analysis software, the total tissue area of each image was first quantified. Thereafter, the areas stained for insulin and glucagon were quantified based on signal intensity after performing an *intensity threshold* on a binary layer, and a *region of interest* (ROI) automatically created around the thresholded area(s). The resulting *thresholded binary areas* for a specific fluorophore allowed the calculation of the relative β-cell or α-cell area to exocrine tissue area (total tissue area minus β-cell or α-cell area of the image), respectively, as well as β-cell to α-cell ratio. For each individual, mean relative β-cell and α-cell areas (in percent) and β-cell to α-cell ratio were calculated based on the results from 20 islets, and average data (± SD) for all individuals as well as by age and sex presented.

Subsequently, the percentage of OATP1B3 colocalized with α and β cells and variability by age and sex was determined on the above described images of normal pancreatic tissues (N=10, **Table 2.1**) assessing 20 islets per individual using the NIS imaging software. To determine colocalization with β cells, areas positive for OATP1B3, insulin as well as areas with overlapping staining for OATP1B3 and the endocrine marker, referred to as *Intersection Mean Binary Area*, were quantitatively assessed by performing

an *intensity threshold* and ROI on *multiple binary layers* including the two fluorophores as described earlier. Subsequently, colocalization with α cells was also assessed. The percentage of cells where OATP1B3 co-localized with either β or α cells was calculated as the ratio of the *Intersection Mean Binary Area* to insulin-positive binary area or glucagon-positive binary area, and reported in percent. Data were expressed as mean ± SD of islets, and differences among ages assessed by an unpaired Student's t test.

IF co-staining for OATP2B1 with endocrine markers was not feasible, therefore we visually explored co-expression of OATP2B1 with endocrine islet cells using IHC after serial staining for OATP2B1 followed by insulin or glucagon in a subset of normal tissue sections from selected 3 patients.

Furthermore, explorative analysis of variable OATP1B3 islet expression was performed in diseased pancreatic tissue sections (tumour adjacent, chronic inflammation, adenocarcinoma) of 9 different patients (**Table 2.1**) by immunostaining (IHC only).

2.2 Specific Aim 2: Elucidating the role of OATP-mediated statin transport in pancreatic islet cell function using a murine β cell model

2.2.1 Cell culture and maintenance

INS-1 cells were seeded in 75 cm^2 Falcon™ tissue culture treated flasks (Thermo-Fisher Scientific) with RPMI 1640 medium (Gibco 31800-022, Thermo-Fisher Scientific) supplemented with 10% FBS, 25 mM HEPES, 2 mM L-glutamine, 50 µM 2-mercaptoethanol, 23.8 mM sodium bicarbonate, and 1 mM sodium pyruvate. When confluent, cells were washed with Dulbecco's phosphate-buffered saline (Gibco 14040-182, Thermo-Fisher Scientific) and digested with 0.05% trypsin (Gibco 25300-054, Thermo-Fisher Scientific). Once all cells were detached, trypsin was deactivated by adding RPMI growth medium and resuspended cells transferred to a new flask with fresh growth medium at the desired ratio.

2.2.2 Gene expression analysis

RNA was extracted from INS-1 rat insulinoma β cell line with TRIzol® according to the manufacturer's instructions (Thermo-Fisher Scientific, Waltham, Massachusetts, USA). Gene expression analysis was performed in INS-1 (N=3) and rat liver (N=1, pool of 10 donors, B204116, BioChain) as described in **Section 2.1.2** using previously published primers (Hou et al. 2014) (Primer sequences in **Table 2.3**). Reactions were performed in triplicate for each sample. Gene expression levels for INS-1 and rat liver were normalized to *Gapdh* and analyzed using the ΔC_T method ($\Delta C_T = C_{T,\,target} - C_{T,\,18S}$) (Schmittgen and Livak 2008). Data are presented as described in **Section 2.1.2**, with the fold-difference in gene expression in INS-1 or other tissues compared to liver. All qRT-PCR consisted of an initial denaturation at 95°C for 20 seconds, followed by 40 cycles at 95°C for 1 second, 60°C for 20 seconds. RNAse-free water was used as the non-template control.

Table 2.3. Primers used for qRT-PCR analysis of rat statin uptake transporter expression.

Origin	*Gene*	*Forward (5'-3')*	*Reverse (5'-3')*	*Reference*
Rat	*Oatp1a1*	AGGTCGAGAATGACGGAGAA	ATTCCGGAGGAAGGGAAGTGT	Custom-designed
	Oatp1a4	CCTAGGCATAGGCATTTGGA	TCAACCAAAGCACAAAGCAG	Hou et al. (2014)
	Oatp1a5	GCAGGATGATGTGGATGGAACTAAC	GCATGTAAATCGGATTGCAGGAG	Hou et al. (2014)
	Oatp1b2	AACATGCTTCGTGGGATAGG	CATGGAAGTGTGCCCTTCTT	Hou et al. (2014)
	Gapdh	AACTTGGCATTGTGGAAGGG	GGATGCAGGGATGATGTTCT	Hou et al. (2014)

2.2.3 Adenoviral transduction

An adenoviral vector for human OATP2B1 was previously created using the ViraPower Adenoviral Expression System (Invitrogen) (Knauer et al. 2010) and used to confer transient overexpression of human OATP2B1 in INS-1 cells. A previously purified LacZ adenovirus (Yin 2014) was used as a negative control. Cells were plated in multiwell plates and adenovirus diluted in phenol red free RPMI medium was added the following day at the desired multiplicity of infection (MOI) as previously determined. After 24 hours, growth medium was changed and cells were allowed to grow for an additional 24 hours before the desired experiments were performed.

2.2.4 Rosuvastatin transport and uptake inhibition studies in INS-1 cells

INS-1 cells were plated in 12-well plates at a density of 2.0 x 10^5 cells/mL and incubated for 24 hours at 37°C and 5% CO_2. Following the 24-hour incubation, growth medium was replaced with pre-warmed Opti-MEM and cells were incubated for 30 minutes. To initiate transport, radiolabeled [^{3}H]-rosuvastatin (0.1 µM) was applied to cells for 30 minutes, then cells were washed with ice-cold PBS to arrest transport activity. Cells were lysed with 1% sodium dodecyl sulfate (SDS) and radioactivity of cell lysates subsequently assessed by liquid scintillation spectrometry to quantify intracellular accumulation of radiolabeled substrate.

To assess uptake inhibition, INS-1 cells were co-treated with [^{3}H]-rosuvastatin and known OATP inhibitors rifampicin (1000 µM) or indomethacin (100 µM) for 30 minutes and analyzed as described above.

Rosuvastatin transport studies were also performed in INS-1 cells following 48-hour adenoviral transduction with human OATP2B1 (Ad-OATP2B1) compared to INS-1 cells transduced with LacZ adenovirus control (Ad-LacZ).

2.2.5 ATP concentration assay

ATP concentration was measured using a CellTiter-Glo® Luminscent Viability Assay (Promega Corporation, Madison, Wisconson, USA). In brief, INS-1 cells were plated in 96-well plates at 2.5 x 10^5 cells/ml and incubated for 24 hours at 37°C and 5% CO_2, after

which growth medium was replaced with rosuvastatin, atorvastatin, or pravastatin (10, 1, 0.1, 0.01 μM) or DMSO control (0.01%) diluted in phenol red free growth medium for an additional 24 hours. To quantify ATP concentration, CellTiter-Glo® reagent was added to each well and cell lysis was induced by shaking for 2 minutes. Luminescence from each well was measured by a GloMax® 20/20 Luminometer (Promega). ATP concentration was also measured following 24-hour statin treatment in INS-1 cells transduced with Ad-OATP2B1 compared to Ad-LacZ control.

2.2.6 Glucose-stimulated insulin secretion

INS-1 cells were plated in 48-well plates at 1.0 x 10^5 cells/ml and incubated for 48 hours, with RPMI medium changed after 24 hours. RPMI medium was replaced with phenol red free RPMI containing rosuvastatin, atorvastatin, or pravastatin (10, 1, 0.1 μM) with or without rifampicin (100 μM) for 24 hours. Subsequently, glucose-stimulated insulin secretion (GSIS) was performed. First, growth medium was collected from each well and cells were washed with Krebs-Ringer HEPES (KRH) wash buffer. Low-glucose KRH buffer (2.2 mM glucose) stimulation for basal insulin secretion occurred as two consecutive 1-hour incubations, followed by a 1-hour incubation in high-glucose KRH buffer (22 mM); supernatant was collected every hour. Glucose concentrations and KRH buffers were adapted from previously published methods (Wang et al. 2004; Pedersen et al. 2007; Orecna et al. 2008). All collected supernatants were stored at -20°C for insulin quantification. For this study, samples from the second low-glucose stimulation and the high-glucose stimulation were used for analysis. Stimulation index (SI), calculated as insulin concentration following high-glucose stimulation divided by insulin concentration following low-glucose stimulation, was used as a normalized measure of insulin secretion.

GSIS was also performed in Ad-OATP2B1 INS-1 cells following 24-hour statin treatment with or without rifampicin and compared to INS-1 cells transduced with Ad-LacZ control.

2.2.7 Enzyme-linked immunosorbent assay

Insulin concentrations were quantified by enzyme-linked immunosorbent assay (ELISA) using an Ultra-Sensitive Rat Insulin ELISA Kit (Crystal Chem, Downers Grove, Illinois, USA). Samples were diluted ten-fold and incubated in a 96-well antibody-coated microplate for 2 hours at 4°C. Each well was washed five times with wash buffer and incubated with 100 uL anti-insulin enzyme conjugate for 30 minutes at RT. Wells were washed seven times and then incubated in the dark with 100 uL light-sensitive enzyme substrate solution. The reaction was stopped after 40 minutes with 100 uL enzyme reaction stop solution and absorbance values at 450 and 630 nm (A_{450} and A_{630}) were measured on a Multiskan Spectrum microplate spectrophotometer (Thermo-Fisher Scientific). Insulin concentrations (ng/mL) were calculated by subtracting A_{630} values from A_{450} values and interpolating from a rat insulin standard curve.

2.2.8 Immunofluorescent staining of cultured cells

INS-1 cells were seeded onto a 4-well lysine-coated CultureSlide (Thermo-Fisher Scientific) at a density of 5.0×10^5 cells/mL and transduced with OATP2B1 adenovirus at an MOI of 100 as previously described. Cells were fixed onto the slide with 4% paraformaldehyde (1:4 diluted from 16% formaldehyde, CAAA43368-9M, VWR International, Mississauga, Ontario), washed, and then blocked for 1 hour at RT with 5% FBS in PBS containing 0.01% TritonX-100 (Sigma-Aldrich). Slides were then incubated overnight at 4°C with a commercial anti-OATP2B1 antibody (1:200, H-189, Santa Cruz Biotechnology, Dallas, Texas, United States) diluted in 5% FBS in PBS. After an additional blocking step, slides were incubated with AlexaFluor® 488 (Thermo-Fisher Scientific) for 1 hour, washed thoroughly, and VECTASHIELD® Antifade Mounting Medium with DAPI (Vector Laboratories Inc.) was added to each section. Images were taken with a Nikon Eclipse 80i microscope (Nikon Instruments Inc.).

2.2.9 Evaluation of mitochondrial function

Caspase-9 activity was used as a measure of mitochondrial function and was evaluated with the Caspase 9 Assay Kit (Colorimetric) (Abcam Inc, Toronto, ON, Canada). INS-1 cells were plated at a density of 5.0×10^5 cells/mL in a 12-well plate and transduced with

either LacZ or OATP2B1 adenovirus the following day as previously described. Medium was then replaced with 0.1% DMSO, 1 µM rosuvastatin, or 10 µM rosuvastatin diluted in phenol red free RPMI medium on the fourth day. After a 24-hour incubation, cell lysates were collected in lysis buffer and incubated on ice for 10 minutes. Lysates were centrifuged at 10,000 x g for 1 minute to pellet cell debris. The supernatant was transferred to a fresh tube and protein was quantified using a BCA assay (see below). Following protein quantification, protein lysates were diluted to 2 µg/µL in lysis buffer and plated onto a 96-well plate. An equal volume of reaction buffer containing 10 mM DTT was added to each sample and then the reaction was initiated with 5 µL of LEHD-pNA substrate. The plate was incubated at 37°C for 2 hours and then absorbance was read at 405 nm on a Multiskan Spectrum microplate spectrophotometer (Thermo-Fisher Scientific). Caspase activity was expressed as fold-difference from DMSO.

2.2.10 Protein quantification

INS-1 cells were grown to 80-90% confluency in 12-well plates then lysed with chilled Pierce IP Lysis Buffer (Thermo-Fisher Scientific) supplemented with Protease Inhibitor Cocktail (P8340, Sigma-Aldrich). Cell lysates were transferred to microcentrifuge tubes and incubated on ice for 5 minutes, then centrifuged at 13,000 x g for 10 minutes at 4°C to pellet cell debris. The supernatant was transferred to a fresh tube and quantified using the Pierce BCA Protein Assay Kit (Thermo-Fisher Scientific). In brief, 25 µL of protein lysate and 200 µL of BCA Working Reagent were added per well of a 96-well microplate and incubated at 37°C for 30 minutes. The absorbance value of each well was read at 562 nm on a Multiskan Spectrum spectrophotometer and concentrations calculated from a BCA standard curve.

2.2.11 Western blot analysis

An XCell SureLock Mini-Cell electrophoresis system (Thermo-Fisher Scientific) was used to perform gel electrophoresis. Protein lysates were collected as previously described and loaded onto a NuPage 4-12% Bis-Tris Protein Gel (Thermo-Fisher Scientific). The XCell SureLock Mini-Cell was run at 150 volts (V) for 1 hour and 30 minutes and then proteins were transferred onto a nitrocellulose membrane in an XCell II

Blot Module (Thermo-Fisher Scientific) at 30 V for 1 hour and 30 minutes. The nitrocellulose membrane was washed in Phosphate Buffered Saline-Tween (PBS-T, 0.1% Tween-20) and incubated in blocking buffer (5% milk and 1% bovine serum albumin in PBS-T) for 1 hour at RT. The membrane was then incubated overnight at 4°C with an anti-OATP2B1 antibody diluted in PBS-T with 0.1% BSA (1:200, H-189, rabbit, Santa Cruz Biotechnology, Dallas, Texas, USA). Following the incubation with primary antibody, the membrane was washed with PBS-T and an HRP-conjugated secondary antibody was added (1:20,000, 172-1019, goat anti-rabbit, Bio-Rad, Hercules, California, USA) for 1 hour at RT. To visualize protein, 2 mL of Amersham ECL Western Blotting Detection Reagent (GE Healthcare Life Sciences, Mississauga, Ontario, Canada) was added to the membrane for 1 minute and then the membrane was exposed on an ImageQuant LAS 500 imager (GE Healthcare Life Sciences).

2.3 Statistical analyses

All statistical analyses were performed using GraphPad Prism 5 (GraphPad Software Inc., La Jolla, CA, USA). Unpaired Student's t test, Mann-Whitney U test, Kruskal-Wallis test followed by Dunn's Multiple Comparison test, and two-way ANOVA followed by Bonferonni post-hoc analysis were performed as appropriate after testing for normal distribution of the data. Results were considered statistically significant at $P<0.05$.

3 Results[1]

[1]Specific Aim 1 reproduced (adapted) from: Kim M, Deacon P, Tirona RG, Kim RB, Pin CL, Meyer zu Schwabedissen HE, Wang R, and Schwarz UI (2017). Characterization of OATP1B3 and OATP2B1 transporter expression in the islet of the adult human pancreas. *Histochemistry and Cell Biology*, doi:10.1007/s00418-017-1580-6, with permission of Springer © Springer-Verlag Berlin Heidelberg 2017.

3.1 Specific Aim 1: Characterization of statin carrier expression and OATP subcellular localization in human pancreatic islets

3.1.1 Statin transporter gene expression in human pancreatic islets

Based on our previous report (Meyer Zu Schwabedissen et al. 2014), we assessed relative mRNA expression of *OATP1B3* as well as other important members of the *OATP1* and *OATP2* families in normal adult pancreatic islets compared to liver, kidney and pancreas (**Figure 3.1**).

In human islets, marked mRNA expression of uptake transporters *OATP1B3* (C_T: 29.3 ± 2.09), *OATP2B1* (C_T: 25.6), and *OATP1A2* (C_T: 28.4 ± 0.54) was detected. Compared to human liver, a tissue recognized for its abundant expression of *OATP1B3* and *OATP2B1*, expression in islets was 13.5-fold lower for *OATP1B3*, and 7.3-fold higher for *OATP2B1*. Interestingly, *OATP1A2* islet expression was 49-fold higher than liver, and 64-fold higher than kidney, the latter tissue also known to express *OATP1A2*. Human islets showed abundant mRNA expression of statin efflux transporters *BCRP* and *P-gp* (mean C_T values: 20.3, 24.6); expression was 320- and 24.3-fold greater than liver, respectively (**Figure 3.2**). We detected very low levels of uptake transporters *OATP1B1* and *OAT3* and efflux transporter *MRP2* in islets (mean C_T values: 34.7, 34.7, and 33.4, respectively) and no *OATP1B1* or *OATP1B3* mRNA in kidney (negative control).

To evaluate differential expression in endocrine to exocrine pancreas, we compared islet expression of uptake and efflux transporters to human pancreas. On average, islet expression of uptake transporters *OATP2B1*, *OATP1B3*, and *OATP1A2* was 54.0-, 5.1-, and 199-fold higher, respectively, than that observed in total pancreatic tissue. Efflux transporters *P-gp* and *BCRP* were detected in islets at levels 2091- and 204-fold greater than pancreas.

Figure 3.1. Statin uptake transporter expression in human tissues. Relative mRNA expression of *OATP2B1*, *OATP1B3, OATP1A2*, *OATP1B1*, and *OAT3* normalized to *18S* ribosomal RNA. Results are represented as mean fold-difference of mRNA expression compared to liver. *OATP2B1*, *OATP1B3*, and *OATP1A2* were detected in adult human islets. Each data point represents one individual and mean ± SEM for each organ is shown.

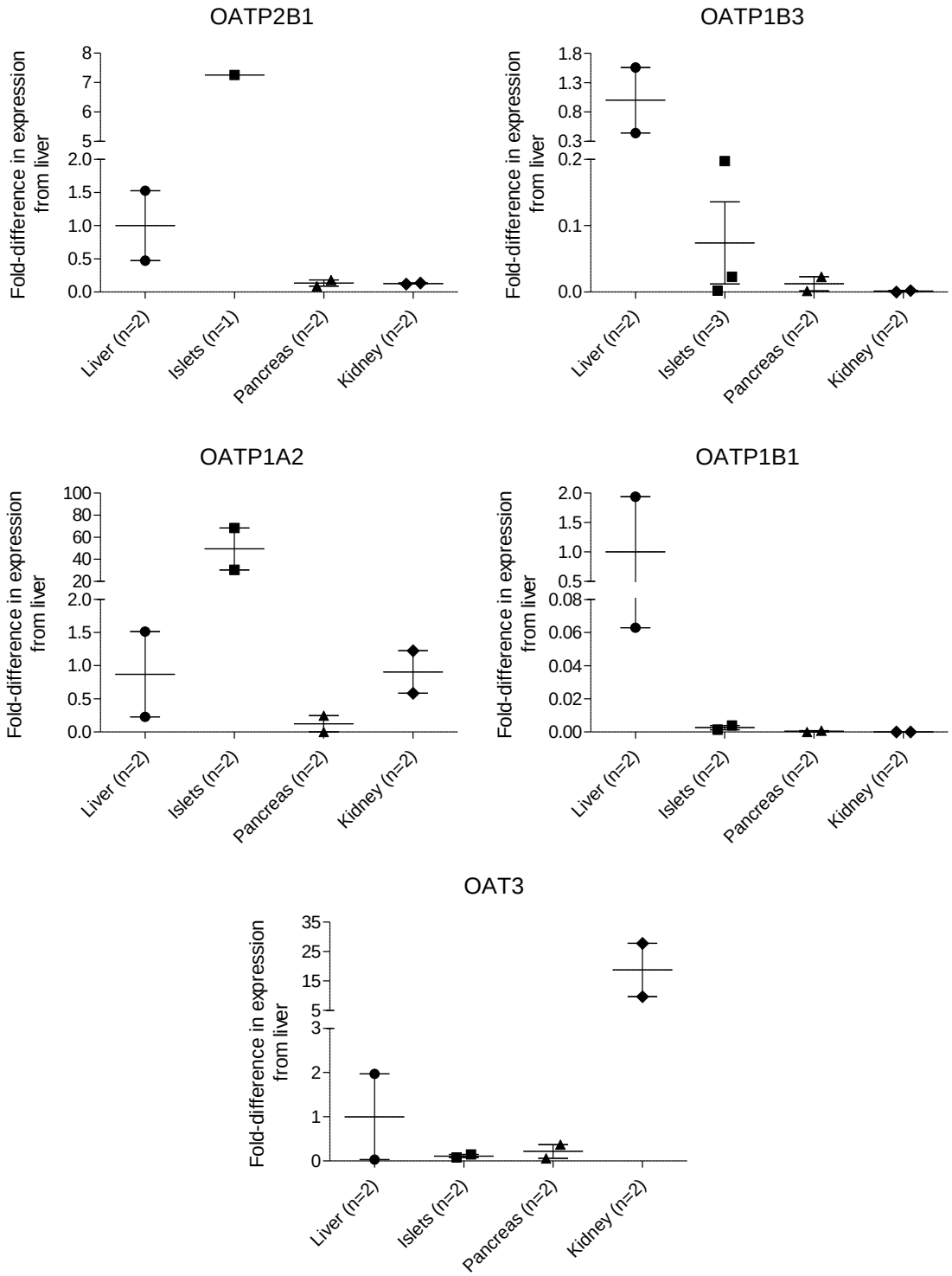

Figure 3.1. Statin uptake transporter gene expression in human tissues.

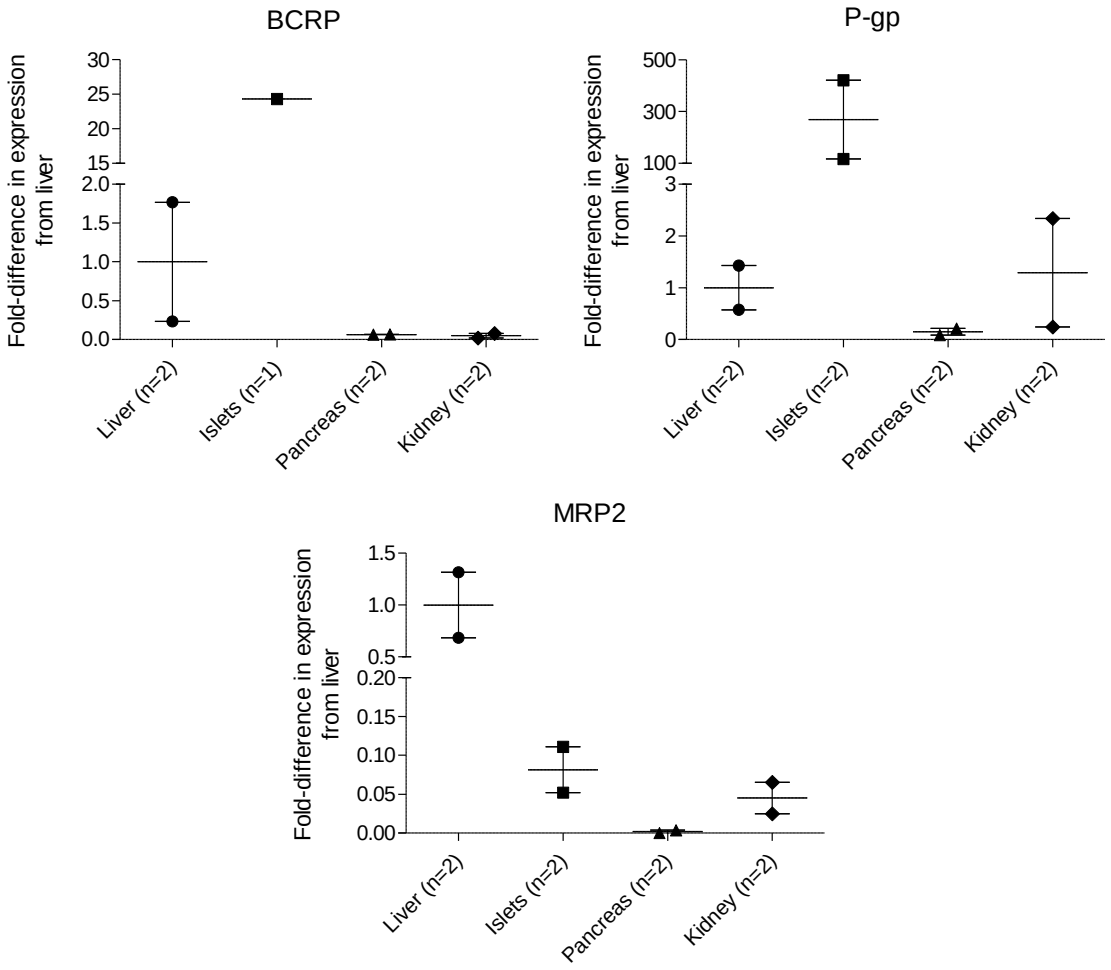

Figure 3.2. Statin efflux transporter expression in human tissues. Relative mRNA expression of *BCRP*, *P-gp*, and *MRP2* normalized to *18S* ribosomal RNA. Results are represented as mean fold-difference of mRNA expression compared to liver. High levels of *BCRP* and *P-gp* were detected in human islets. Each data point represents one individual and mean ± SEM for each organ is shown.

3.1.2 Characterization of OATP1B3 protein expression and distribution in normal adult islets

After demonstrating marked gene expression of *OATP1B3* in human islets, we next assessed its expression and distribution within the islet by co-staining with the endocrine markers insulin or glucagon in sections of normal pancreatic tissue. Dual immunofluorescent staining (**Figures 3.3, 3.4**) confirmed OATP1B3 islet expression and showed that within islets, OATP1B3 was primarily detected in glucagon-positive (α) cells, and in only a few insulin-positive (β) cells. Using confocal microscopy, staining was largely observed within the endocrine cells (**Figure 3.3B**).

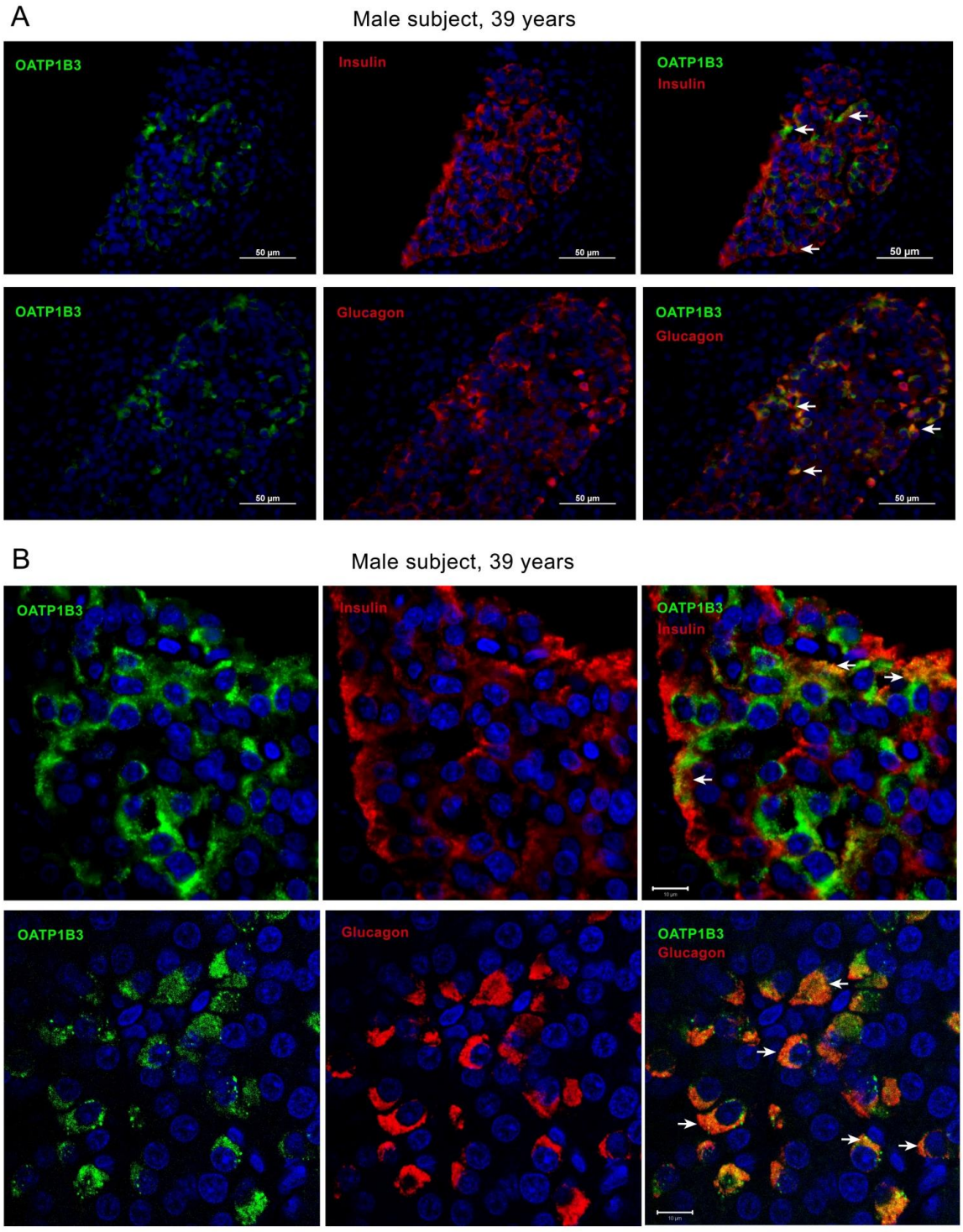

Figure 3.3. Representative images of OATP1B3 co-localization with α and β cells in adult pancreatic islets. Using immunofluorescent staining, pancreas sections of a 39-year old male subject were double-stained for OATP1B3 [green] with insulin [red] or glucagon [red] and DAPI [blue]. Separate and merged images are shown (**A**, 40x objective; **B**, 100x objective). Scale bars in 50 or 10 µm. White arrows indicate co-localization.

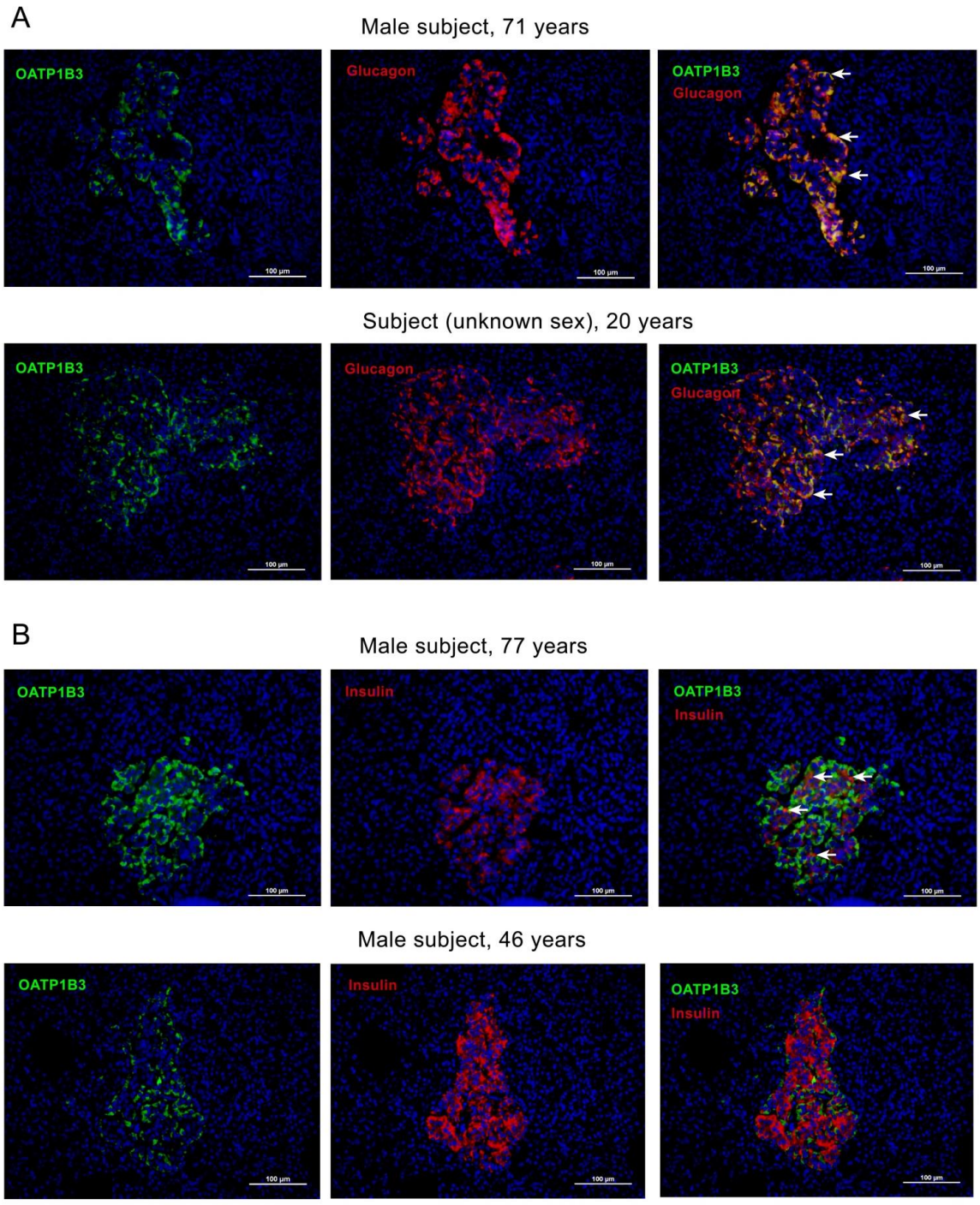

Figure 3.4. Representative images of OATP1B3 co-localization with α and β cells by age in a series of adult individuals. Using immunofluorescent staining, pancreatic tissue sections were stained for OATP1B3 [green] with glucagon [red] **(A)** or insulin [red] **(B)** and DAPI [blue]. Separate and merged images are shown (20x objective). Scale bar in 100 µm. White arrows indicate co-localization.

We further quantitatively explored variability in co-expression and the effect of age and sex on the presence of OATP1B3 in these endocrine cell types in normal pancreatic tissue sections of 10 subjects (**Figure 3.6**). We first evaluated relative α and β cell area and relative β to α cell ratio in studied normal pancreatic tissue sections (**Figure 3.5**). Relative α and β cell area (%) was 4.4 ± 1.2% and 4.6 ± 2.5%, respectively, and the β to α cell area ratio was 1.35 ± 1.08 (min, max; 0.44, 3.92), indicating no difference of endocrine cell populations between the studied age groups (**Figure 3.5**). We observed overall variable expression of OATP1B3 with both endocrine cell types (**Figure 3.6**). Among all subjects, 10.7 ± 8.3% (mean ± SD) of insulin-positive cells also showed staining for OATP1B3 compared to 40.4 ± 25.1% of glucagon-positive cells. Stratified by age, 2- to 3-fold higher percentage of OATP1B3 co-localized with endocrine cells was observed in older individuals (≥60 years) compared to those <60 years. The age cutoff of 60 years is commonly used in studies assessing type II diabetes risk in older individuals; furthermore, type II diabetes prevalence is thought to peak at 60-74 years of age (Kirkman et al. 2012; De Tata 2014). Age-related differences reached statistical significance for OATP1B3 co-localized with β cells (<60 years: 4.5 ± 2.0% and ≥60 years: 14.9 ± 8.4%; p=0.0449), but were not significant for OATP1B3 co-localized with α cells (<60 years: 22.2 ± 7.6% and ≥ 60 years: 52.6 ± 25.7%; p=0.054); representative IF images are shown in **Figure 3.4**. We were not able to assess sex-related differences due to the limited sample size (2 females due to unknown sex of one subject).

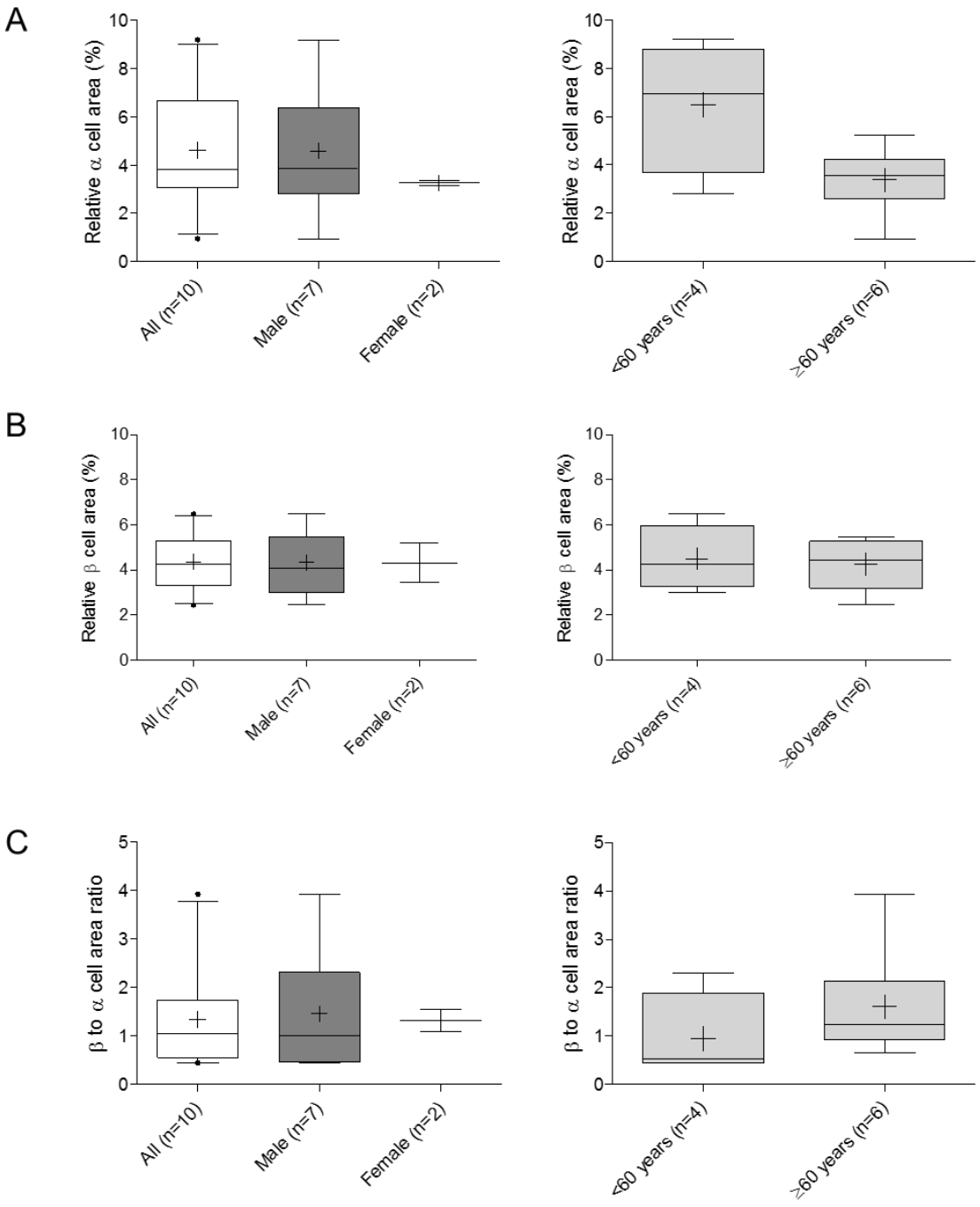

Figure 3.5. Quantitative analysis of endocrine cell area in healthy human pancreatic tissue sections from 10 individuals. (A) Relative α-cell area expressed as percentage of surrounding exocrine tissue area. **(B)** Relative β-cell area expressed as percentage of surrounding exocrine tissue area. **(C)** Ratio of β-cell area to α-cell area. No significant age-related difference was detected for endocrine cell area or endocrine cell area ratio. Results shown as mean ± SD. Statistical analyses performed using an unpaired Student's t test.

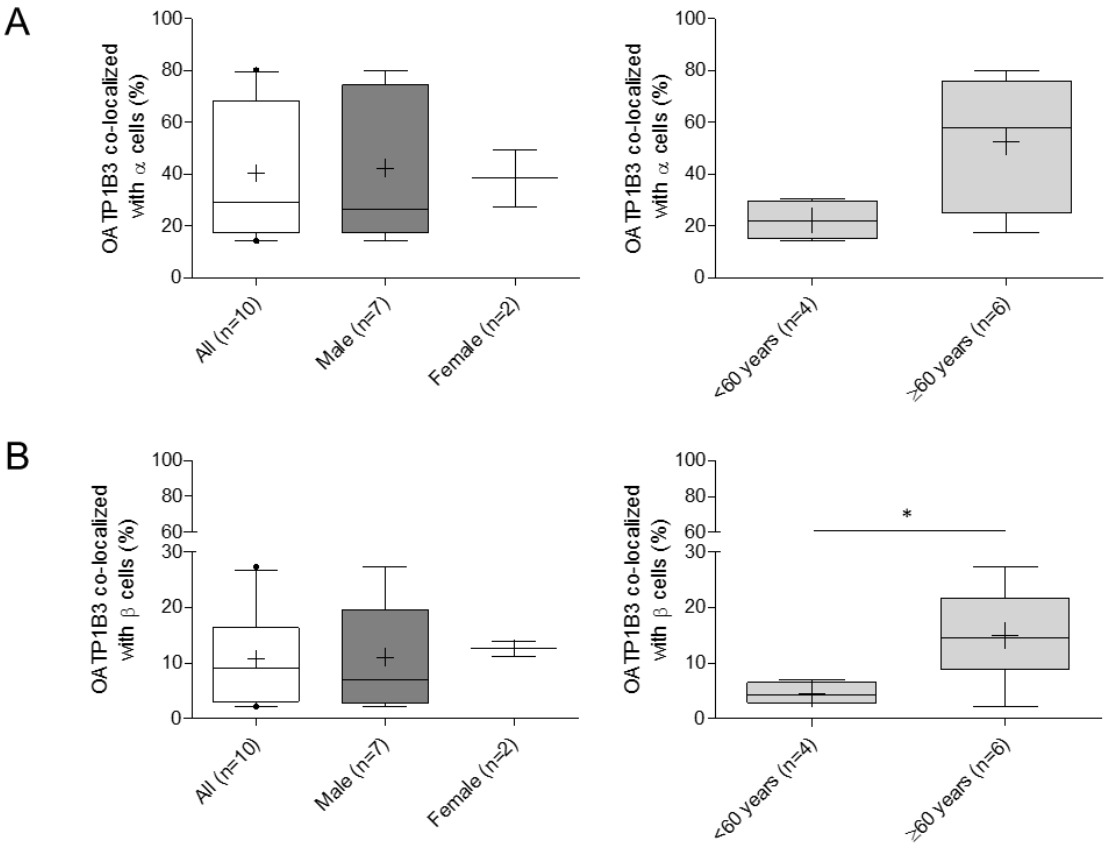

Figure 3.6. Quantitative analysis of OATP1B3 co-localization in normal human pancreatic tissue sections from 10 individuals. (A) Co-localization of OATP1B3 with α cells, expressed as percentage of α cell area. **(B)** Co-localization of OATP1B3 with β cells, expressed as percentage of β cell area. Statistical significance was reached for age-related differences, with individuals older than 60 years of age having greater co-localization (p=0.0449). Results shown as mean ± SD. Statistical analyses performed using an unpaired Student's t test.

3.1.3 Characterization of OATP2B1 protein expression and distribution in normal adult islets

OATP2B1 mRNA expression was also abundant in islets, exceeding that of liver. In contrast to OATP1B3, OATP2B1 was primarily detected in insulin-positive (β) cells, and only to a more limited extent in glucagon-positive (α) cells (**Figure 3.7**) using serial immunocytochemistry staining of OATP2B1 and endocrine markers in normal pancreatic tissues from 3 different individuals.

Figure 3.7. Immunohistochemical staining of OATP2B1 in human pancreatic tissue sections from 3 individuals. For each individual, consecutive pancreatic sections were stained for OATP2B1 (brown staining - AEC), insulin (purple - Vector® Red), glucagon (purple) alone (**A,** top 2 rows), or co-stained for OATP2B1 with insulin or glucagon (**A**, bottom row; **B**; **C**), resulting in two visible chromogens per section (brown and purple). Images were taken at 10x or 40x objective. No primary antibody was used for control **(A)**. Scale bar in 100 µm (10x objective) or 50 µm (40x objective). Black arrows indicate areas of co-localization.

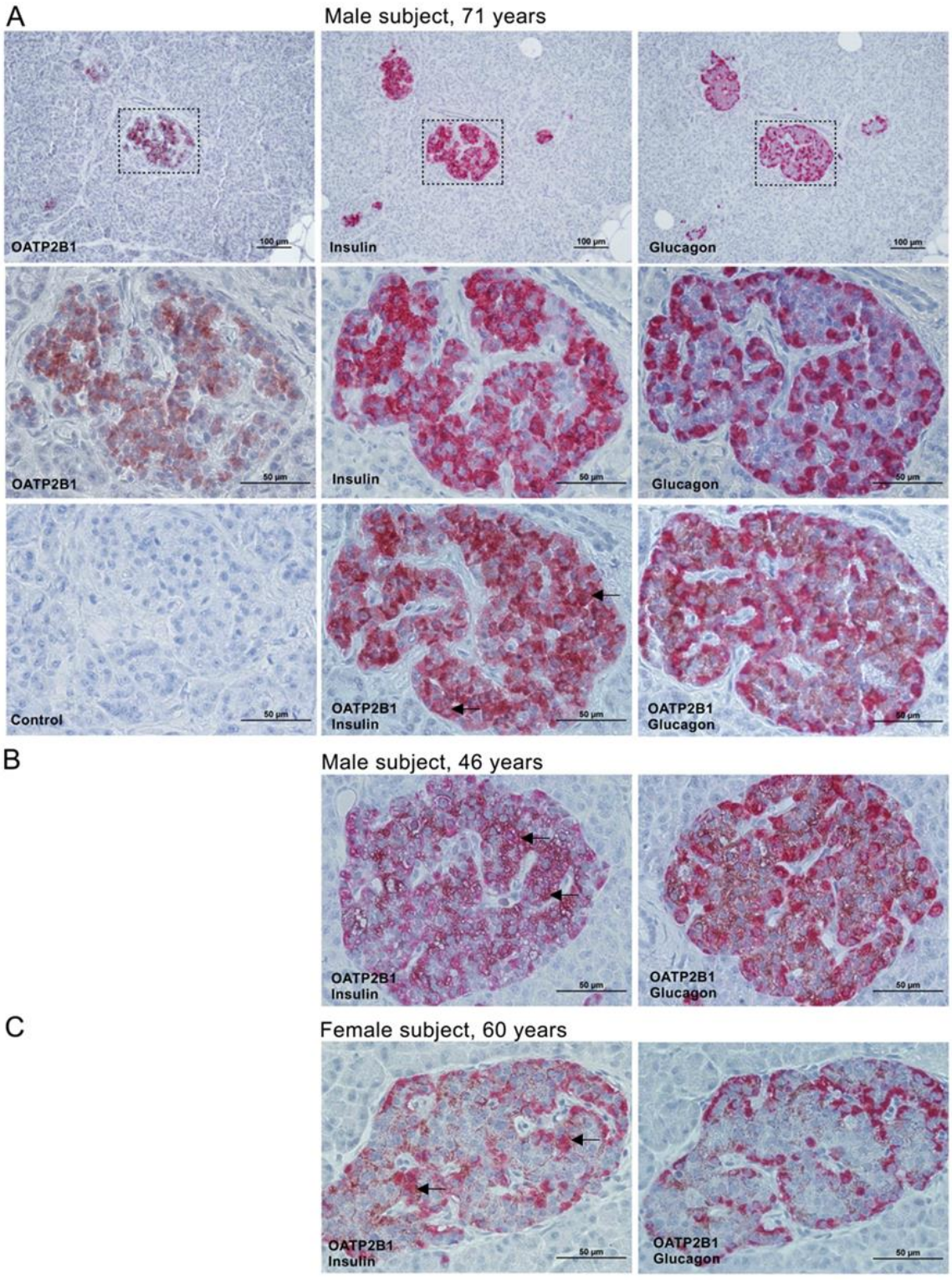

Figure 3.7. Immunohistochemical staining of OATP2B1 in human pancreatic tissue sections from 3 individuals.

3.1.4 Characterization of OATP1B3 expression in islets of the diseased pancreas

We further evaluated by immunocytochemistry, if pancreatic disease affects OATP1B3 islet expression, and observed more intense OATP1B3 staining in islets from patients with chronic pancreatitis as well as PDAC compared to tumour-adjacent normal pancreatic tissues (**Figure 3.8**).

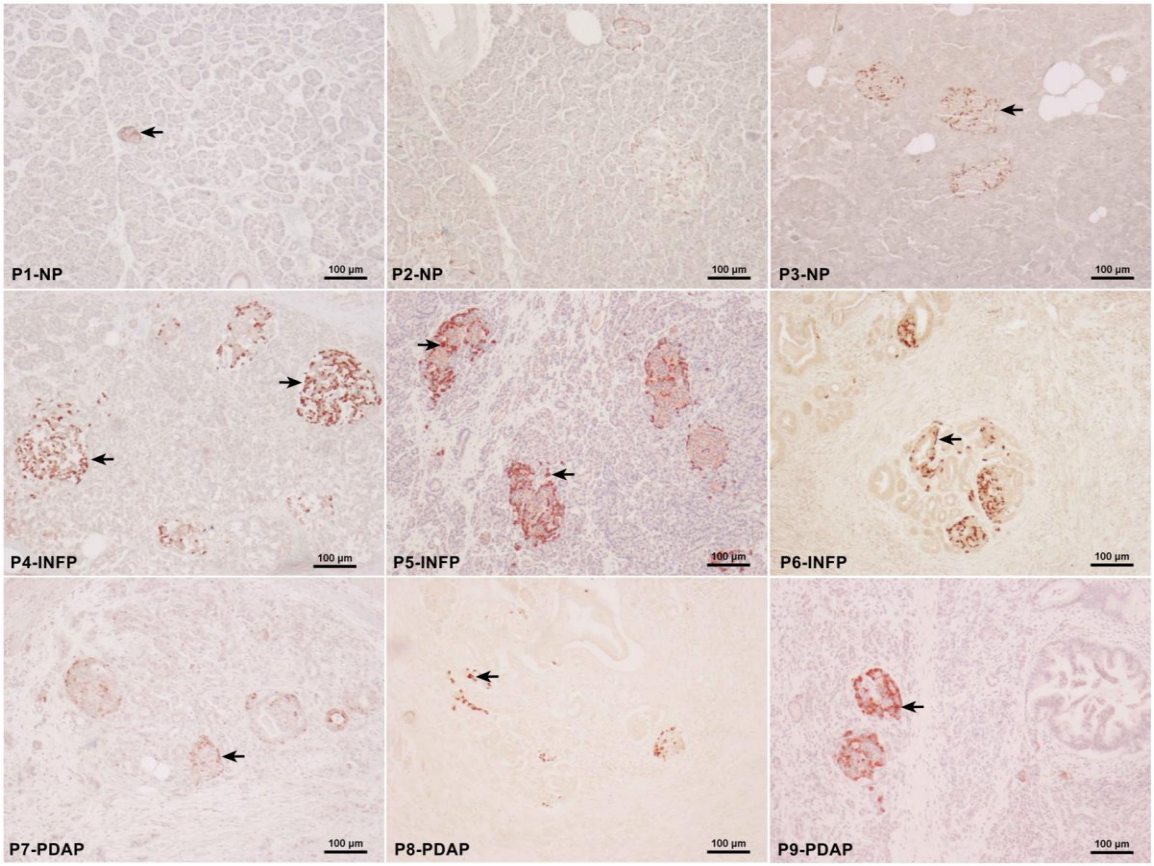

Figure 3.8. Immunocytochemical detection of OATP1B3 in paraffin-embedded human diseased pancreatic tissue sections. Immunohistochemical staining of OATP1B3 in human pancreatic tissue sections from 9 patients with chronic pancreatitis (INFP; P4-P6) and pancreatic ductal adenocarcinoma (PDAP; P6-P9) compared to normal tumour-adjacent pancreatic tissue. Images suggest highly variable OATP1B3 expression among diseased pancreatic tissues (staining observed: INFP>PDAP>NP), largely restricted to islets. Representative images were taken at low power (Objective, scale bar; 10x, 100 µm). Black arrows indicate OATP1B3 detection in islets.

3.2 Specific Aim 2: Elucidating the role of OATP-mediated statin transport in pancreatic islet cell function using a murine β cell model

3.2.1 Statin transporter gene expression analysis in INS-1 cells

Gene expression analysis of rat *Oatp* isoforms, many capable of statin transport (Ho et al. 2006), was performed in the rat β cell model INS-1 and compared to rat liver. We detected abundant expression of *Oatp1a5* in INS-1, whereas other *Oatp* isoforms were expressed at very low levels (*Oatp1a1, Oatp1a4*) or likely lacking (*Oatp1b2*) (**Figure 3.9**).

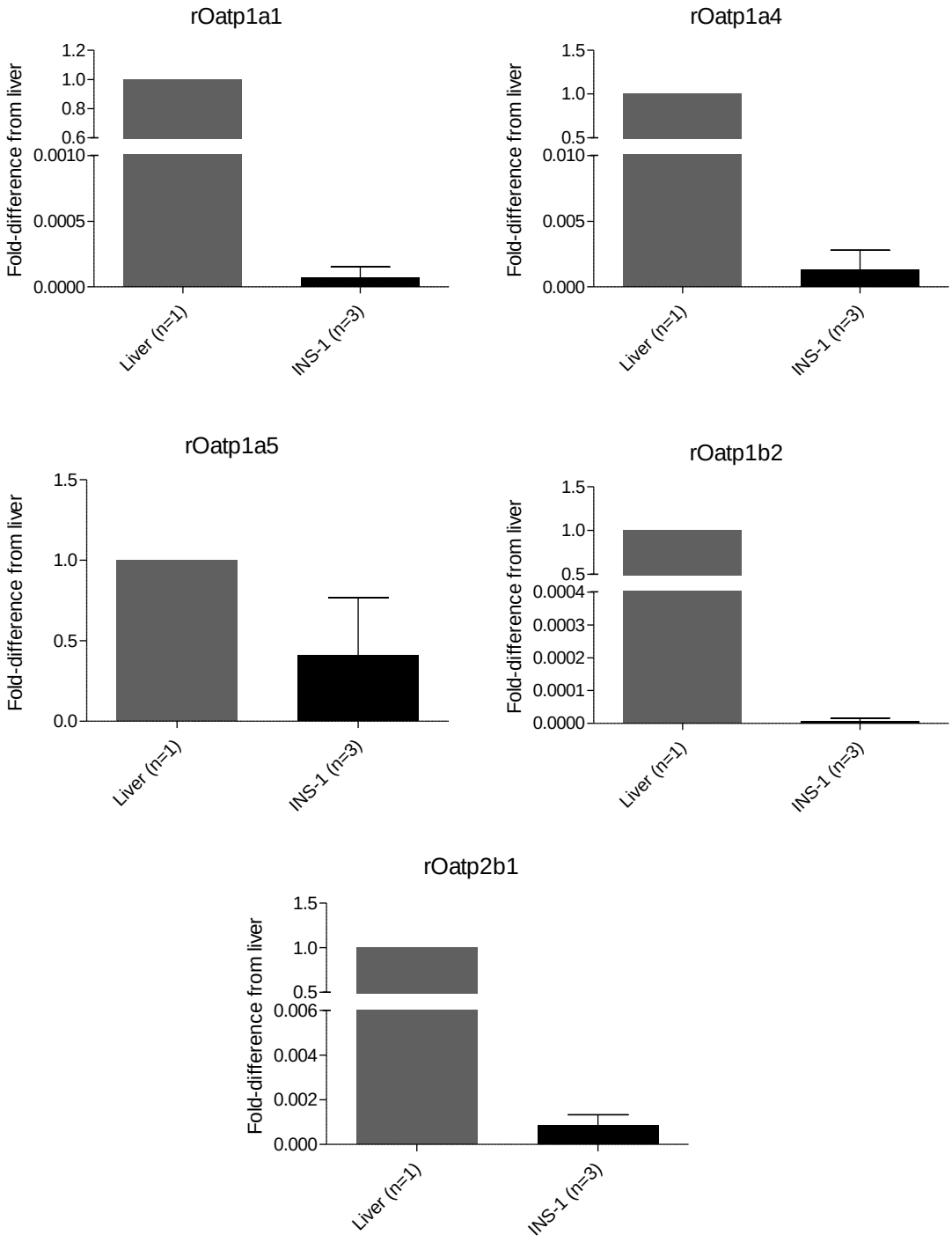

Figure 3.9. Statin uptake transporter gene expression in INS-1. Relative mRNA expression of statin uptake transporters in INS-1 normalized to rat *Gapdh*. Results are expressed as fold-difference of INS-1 mRNA expression compared to liver. Expression of *Oatp1a5* was detected in INS-1 cells while little to no expression of other *Oatps* was seen. Results are shown as mean ± SD.

3.2.2 Inhibition of rosuvastatin uptake in INS-1 cells by OATP inhibitors

The INS-1 rat insulinoma cell line was selected as a β cell model due to its ability to secrete insulin in response to glucose (Pedersen et al. 2007). Due to the abundant expression of the statin carrier *Oatp1a5*, we next evaluated the uptake activity of rosuvastatin in this beta cell line. To assess statin uptake activity, transport experiments with [^{3}H]-rosuvastatin were performed over 30 minutes as described. Dependence of statin uptake on rat Oatps was evaluated by co-incubation of INS-1 with rosuvastatin and two known OATP inhibitors, rifampicin or indomethacin. Uptake of [^{3}H]-rosuvastatin in INS-1 cells was demonstrated and intracellular accumulation was significantly reduced ($P<0.01$) when [^{3}H]-rosuvastatin was coadministered with rifampicin (1000 μM) or indomethacin (100 μM) (34.3% and 41.9% of control, respectively) (**Figure 3.10**). Statistical analyses performed using Kruskal-Wallis test with Dunn's Multiple Comparison Test.

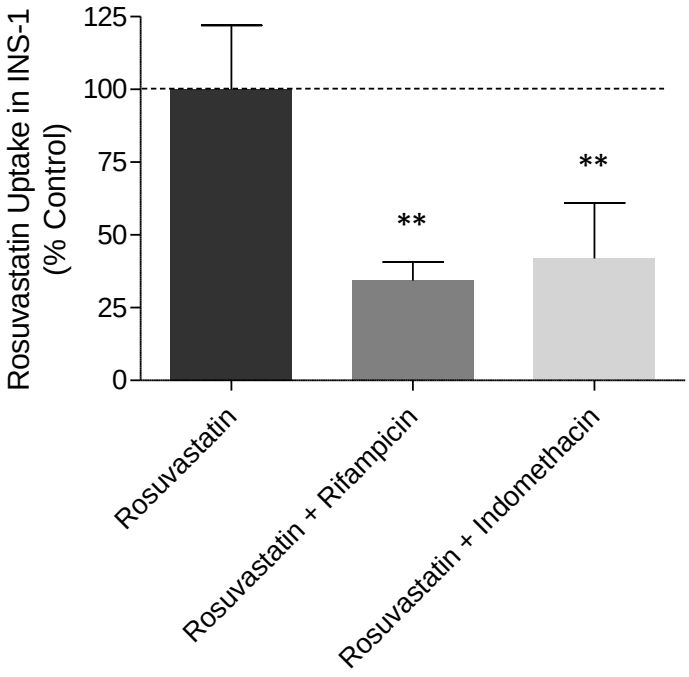

Figure 3.10. Intracellular accumulation of [^{3}H]-rosuvastatin in INS-1 cells. Coadministration of known OATP inhibitors rifampicin (1000 µM) and indomethacin (100 µM) significantly reduced [^{3}H]-rosuvastatin uptake at 30 minutes (**, P<0.01), as determined by Kruskal-Wallis test with Dunn's Multiple Comparison Test. Results are shown as mean ± SD, n=3.

3.2.3 ATP concentration in INS-1 cells following statin treatment

INS-1 intracellular ATP concentration was evaluated following a 24-hour treatment with rosuvastatin, atorvastatin, and pravastatin at concentrations ranging from 0.01-10 µM, since statin-induced reductions in ATP production have been previously reported (Zhou et al. 2014; Knauer et al. 2010). Compared to DMSO control, cell viability was only significant reduced when treated with 10 µM of rosuvastatin and atorvastatin ($P<0.05$ and $P<0.001$, respectively), but not pravastatin (**Figure 3.11**). Despite statistical significance, rosuvastatin and atorvastatin treatment at 10 µM only slightly reduced INS-1 ATP concentration to about 89.7% and 82.5% of DMSO control, respectively.

Results for this experiment consist of a total of 6 mean values per treatment from three separate experimental days (n=3). Statistical analyses performed using two-way ANOVA followed by Bonferroni post-hoc test.

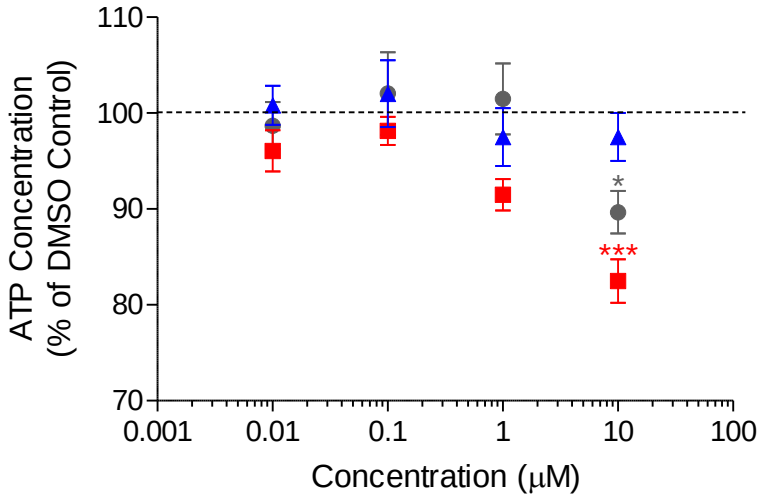

Figure 3.11. ATP concentration in INS-1 cells following 24-hour statin treatment.ATP concentration as percentage of DMSO control in INS-1 cells following 24-hour treatment with rosuvastatin (●), atorvastatin (■), or pravastatin (▲), as determined by a luminescent assay. Significant reduction of ATP concentration was observed in INS-1 cells after 10 μM rosuvastatin (*, $P<0.05$) and atorvastatin (***, $P<0.001$) compared to DMSO control (100%), as determined by two-way ANOVA followed by Bonferroni post-hoc test. Results shown as mean ± SD, n=3.

3.2.4 Glucose-stimulated insulin secretion following statin treatment in INS-1 cells

After ruling out biologically relevant changes in cell viability among the assessed concentration range of statins, glucose-stimulated insulin secretion (GSIS) was next evaluated in statin-treated INS-1 cells after 24-hour incubation with rosuvastatin, atorvastatin, and pravastatin at 0.1, 1, and 10 μM. Rosuvastatin significantly impaired high glucose-stimulated insulin secretion compared to DMSO control at a concentration of 10 μM ($P<0.05$), which is further reflected in a significant reduction in stimulation index (SI) ($P<0.01$) (**Figure 3.12**). Dose-dependent reductions of high glucose-stimulated insulin secretion and SI were observed for rosuvastatin; a significant difference was detected between insulin secretion at 0.1 μM and 10 μM rosuvastatin. Atorvastatin treatment at 1 μM significantly decreased SI compared to control ($P<0.05$). No significant changes in insulin secretion were detected with pravastatin treatment at all concentrations. Statistical analysis was not performed for 10 μM atorvastatin treatment due to small sample size with data from only two experimental days.

Results for this experiment, except atorvastatin at 10 μM consist of a total of 8 mean values per treatment from three separate experimental days (n=3). Statistical analyses performed using two-way ANOVA followed by Bonferroni post-hoc test.

Figure 3.12. Glucose-stimulated insulin secretion (GSIS) in statin-treated INS-1 cells. Insulin secretion for low glucose (LG) and high glucose (HG) conditions represented as percentage of DMSO control. Significant reductions in HG-stimulated insulin secretion and stimulation index for rosuvastatin (10 µM) and atorvastatin (1 µM) compared to DMSO control. Dose-dependent effects were seen with rosuvastatin treatment. Results are shown as mean ± SD, n=3 (with the exception of atorvastatin 10 µM, n=2). Statistical analysis performed by two-way ANOVA followed by Bonferroni post-hoc test (*, $P<0.05$; **, $P<0.01$). Test results for atorvastatin at 10 µM are not presented due to small sample size.

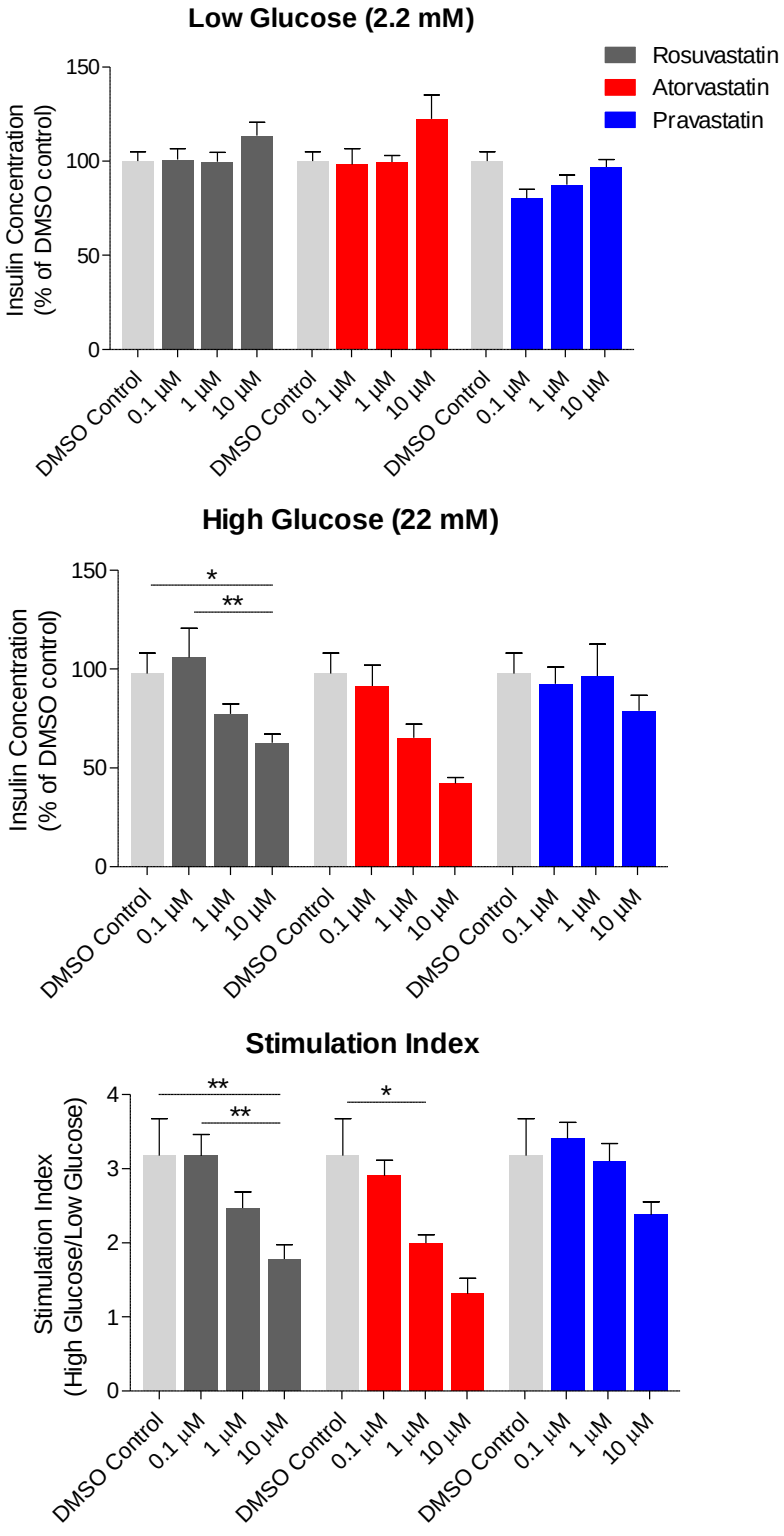

Figure 3.12. Glucose-stimulated insulin secretion (GSIS) in statin-treated INS-1 cells.

The GSIS experiment was repeated in INS-1 cells co-incubated with statins at 1 and 10 µM and the known Oatp inhibitor rifampicin in order to evaluate if unspecific inhibition of intracellular statin accumulation would rescue impaired insulin secretion. A significant overall effect of the inhibitor on SI was detected for rosuvastatin treatment (P=0.0259); however, no significant differences were observed after pairwise comparison for any of the assessed outcomes after 24-hour treatment of INS-1 cells with rosuvastatin, atorvastatin, and pravastatin at 1 and 10 µM with or without rifampicin (**Figure 3.13**).

Results for this experiment consist of a total of 6 mean values per treatment from three separate experimental days (n=3). Statistical analyses performed using two-way ANOVA followed by Bonferroni post-hoc test.

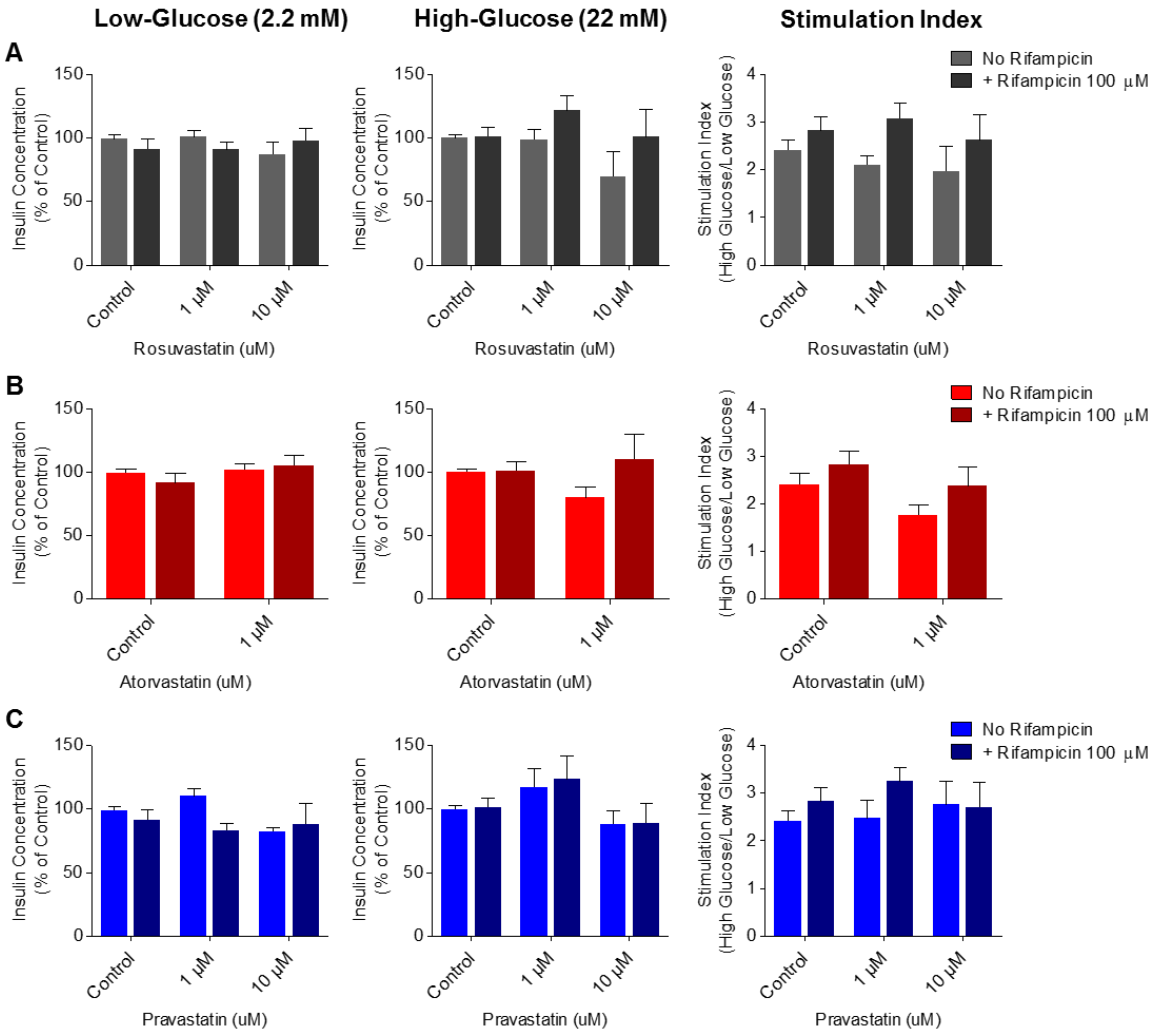

Figure 3.13. Insulin secretion in INS-1 cells treated with statins and rifampicin. GSIS was assessed in INS-1 cells after 24-hour treatment with **(A)** rosuvastatin, **(B)** atorvastatin, and **(C)** pravastatin with or without Oatp inhibitor rifampicin (100 µM). No significant difference in insulin secretion was observed in INS-1 cells treated with statins compared to INS-1 cells treated with statins and rifampicin, as determined by two-way ANOVA followed by Bonferroni post-hoc test. Results for low-glucose (2.2 mM) and high-glucose (22 mM) stimulation expressed as percentage of DMSO control. All results are shown as mean ± SD, n=3.

3.2.5 Validation of Ad-OATP2B1 INS-1 cells as an OATP overexpression model

To directly assess the role of OATP2B1 statin transport on insulin secretion, we transduced INS-1 cells with human OATP2B1 adenovirus (Ad-OATP2B1) as a β cell model with OATP overexpression which was compared to LacZ adenovirus control (Ad-LacZ) in subsequent *in vitro* studies. To confirm OATP2B1 protein expression in Ad-OATP2B1 INS-1 cells, Western blot analysis and immunofluorescent staining were applied. When probing for OATP2B1 on a Western blot, protein lysates from OATP2B1-transduced INS-1 cells (MOI 100) showed the appropriate bands at the expected size of 75 kDa (Hanggi et al. 2006), while intensity increased with protein concentration (**Figure 3.14**). INS-1 cells transduced with LacZ adenovirus did not show any OATP2B1 expression (**Figure 3.14**). Immunofluorescent staining for OATP2B1 confirmed predominant membrane expression of OATP2B1 protein in Ad-OATP2B1 INS-1 cells, whereas no staining was detected in control Ad-LacZ INS-1 (**Figure 3.14**).

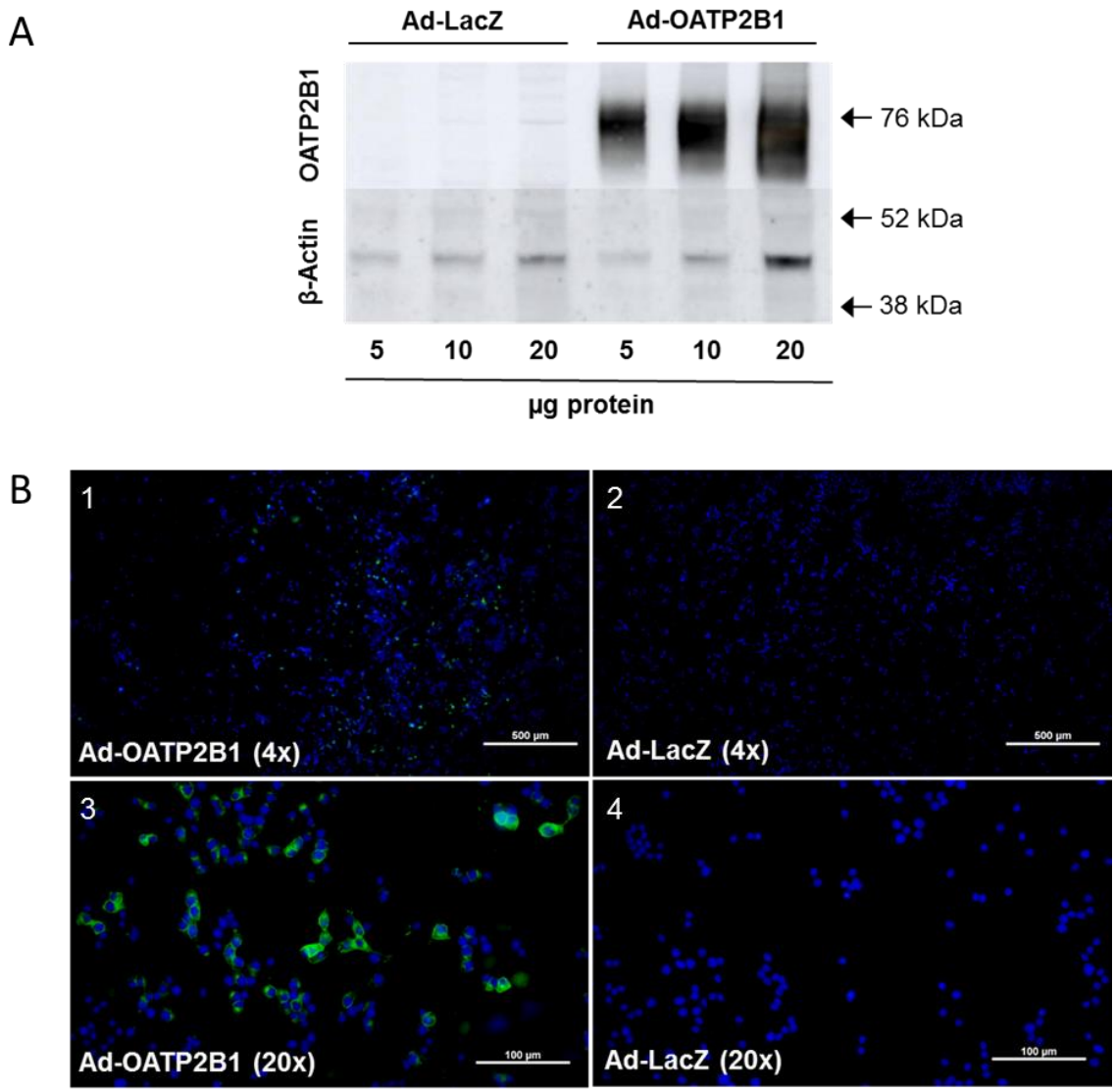

Figure 3.14. Overexpression of human OATP2B1 adenovirus in INS-1 cells. (A) Western blot showing expression of OATP2B1 adenovirus (Ad-OATP2B1) in INS-1 cells following transduction. **(B)** Immunofluorescent staining for OATP2B1 in INS-1 cells transduced with Ad-OATP2B1 4x **(1)** and 20x **(3)** magnification. LacZ control **(2,4)** showed no staining for OATP2B1 (4x and 20x magnification). Scale bars in 500 µM (4x) and 100 µM (20x).

3.2.6 Statin transport activity of INS-1 cells transduced with OATP2B1 adenovirus

Rosuvastatin transport activity was assessed using [^{3}H]-rosuvastatin as described previously to functionally validate INS-1 cells 24 hours after transduction with Ad-OATP2B1. Rosuvastatin uptake in INS-1 cells increased in a dose-dependent manner when transduced with Ad-OATP2B1 compared to Ad-LacZ control at increasing MOIs (**Figure 3.15**). An MOI of 100 resulted in a 1.54-fold greater intracellular accumulation of [^{3}H]-rosuvastatin in Ad-OATP2B1 INS-1 cells compared to LacZ, and was chosen for subsequent experiments as a β cell model with OATP2B1 overexpression.

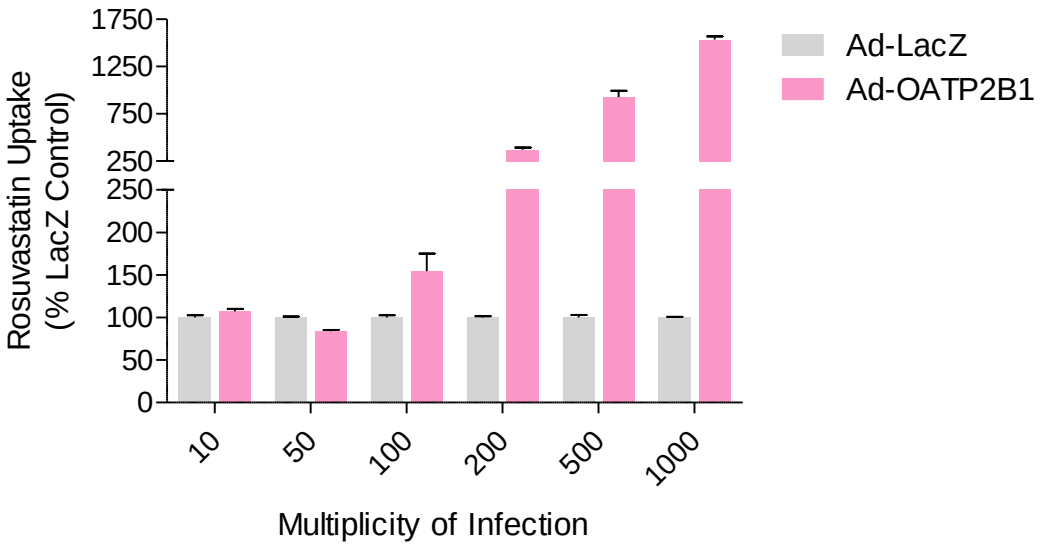

Figure 3.15. Intracellular accumulation of [^{3}H]-rosuvastatin in transduced INS-1 cells. Uptake of [^{3}H]-rosuvastatin shown as percentage of LacZ control. INS-1 cells expressing OATP2B1 showed an increase in rosuvastatin uptake. Results are shown as mean ± SD, n=2. Statistical analysis has not been performed.

3.2.7 ATP concentration in OATP2B1-overexpressing INS-1 cells after statin treatment

We then assessed ATP concentration using a luminescent assay as described previously. ATP concentration was measured in Ad-OATP2B1 versus Ad-LacZ INS-1 cells 48 hours after transduction (MOI 100) following 24-hour statin treatment with rosuvastatin, atorvastatin, or pravastatin at 1 µM and 10 µM. Our results showed no significant difference between INS-1 cells transduced with LacZ control or OATP2B1 adenovirus (**Figure 3.16**).

Results for this experiment consist of a total of 9 mean values per treatment from three separate experimental days (n=3). Statistical analyses performed using two-way ANOVA followed by Bonferroni post-hoc test.

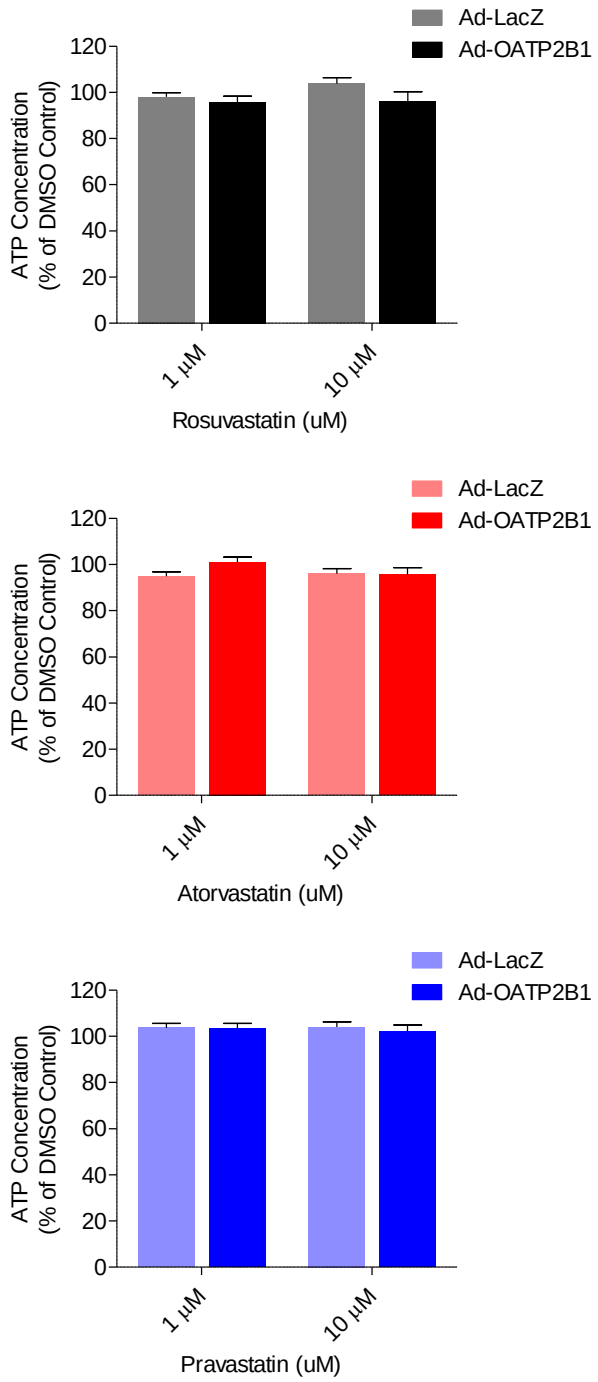

Figure 3.16. ATP concentration in INS-1 following adenoviral transduction and statin treatment. ATP concentration shown as percentage of DMSO control. No significant change in ATP concentration was observed following 24-hour statin treatment in Ad-OATP2B1 INS-1 cells compared to Ad-LacZ control. Results shown as mean ± SD, n=3. Statistical analysis performed by two-way ANOVA followed by Bonferroni post-hoc test.

3.2.8 Glucose-stimulated insulin secretion in Ad-OATP2B1 INS-1 cells treated with statins

In order to evaluate direct effects of OATP2B1-mediated statin transport on insulin secretion, GSIS was performed in INS-1 cells transduced with Ad-OATP2B1 compared to Ad-LacZ. High glucose-stimulated insulin secretion was significantly impaired in Ad-OATP2B1 INS-1 cells compared to Ad-LacZ INS-1 cells when treated with 1 µM and 10 µM rosuvastatin (0.31-fold reduction, $P<0.001$; 0.29-fold reduction, $P<0.01$, respectively) (**Figure 3.17A**). Ad-OATP2B1 INS-1 cells treated with 1 µM pravastatin showed a 0.40-fold reduction in high glucose-stimulated insulin secretion compared to Ad-LacZ INS-1 cells ($P<0.001$), and a 0.41-fold reduction when treated with 10 µM pravastatin ($P<0.001$) (**Figure 3.17C**). No significant difference was detected between Ad-OATP2B1 INS-1 cells compared to Ad-LacZ cells treated with atorvastatin (1 µM) for any of the assessed outcomes. Statistical analysis was not performed for 10 µM atorvastatin due to the small sample size of two experimental days.

Additionally, a significant increase in high glucose-stimulated insulin secretion was observed in Ad-LacZ INS-1 cells after pravastatin treatment at 1 µM compared to DMSO control ($P<0.001$, not shown on graph). Although this is not an OATP-mediated effect, this increase in insulin secretion with pravastatin treatment should be noted as it supports observations in literature (Abe et al. 2010).

Results for this experiment, except for atorvastatin 10 µM, consist of a total of 6 mean values per treatment from three separate experimental days (n=3). Statistical analyses performed using two-way ANOVA followed by Bonferroni post-hoc test.

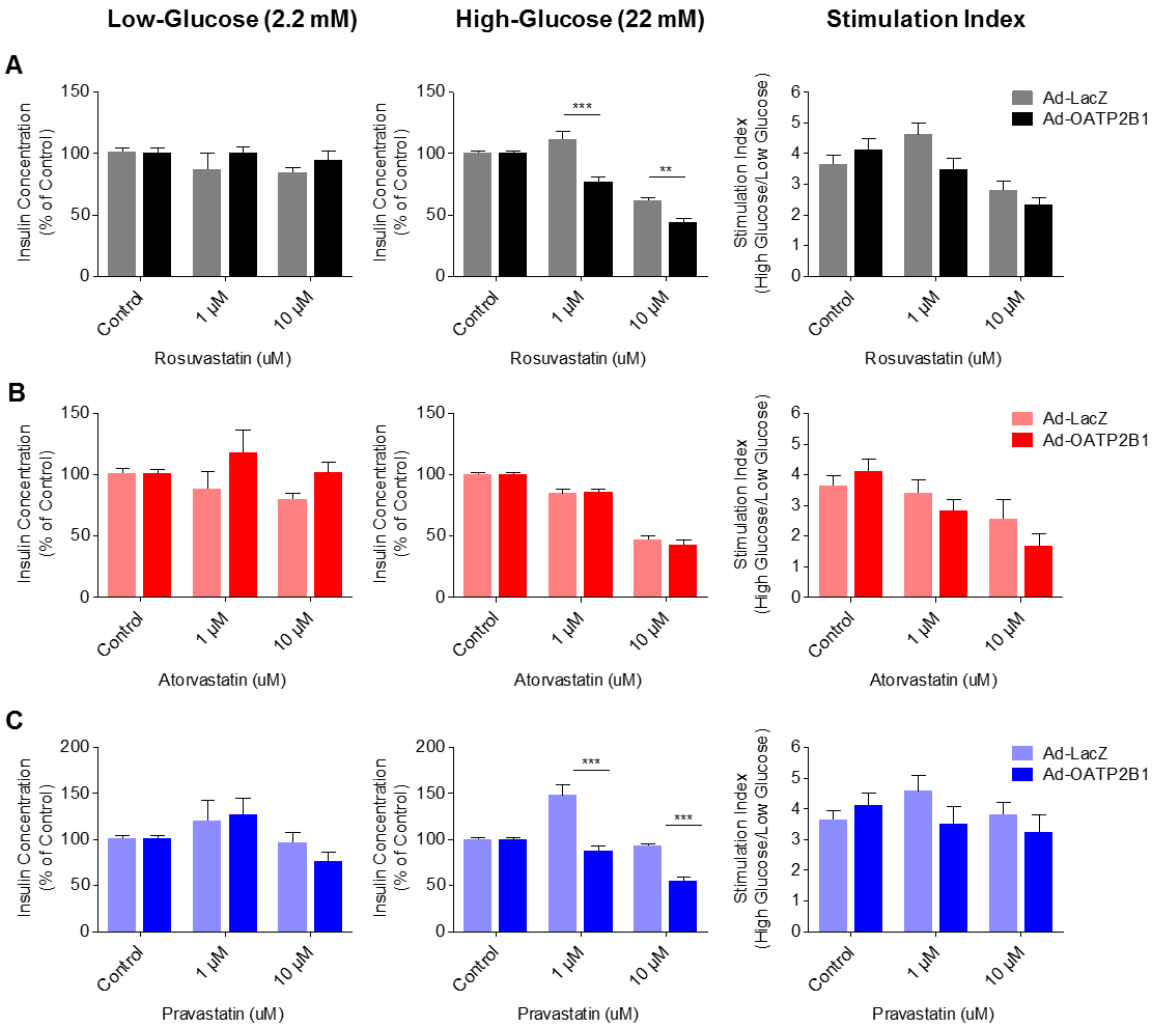

Figure 3.17. Insulin secretion in statin-treated INS-1 cells transduced with human OATP2B1 adenovirus.GSIS was assessed in INS-1 cells after treatment with **(A)** rosuvastatin, **(B)** atorvastatin, and **(C)** pravastatin after adenoviral transduction with human OATP2B1 or Ad-LacZ control. Results for low-glucose (2.2 mM) and high-glucose (22 mM) stimulation expressed as percentage of Ad-LacZ or Ad-OATP2B1 DMSO control. High glucose-stimulated insulin secretion in Ad-OATP2B1 INS-1 was significantly reduced with rosuvastatin and pravastatin (**, $P<0.01$; ***, $P<0.001$) compared to Ad-LacZ control, as determined by two-way ANOVA followed by Bonferroni post-hoc test. All results are shown as mean ± SD, n=3 (with the exception of atorvastatin 10 uM, n=2).

3.2.9 Mitochondrial function in Ad-OATP2B1 INS-1 cells treated with statins

To further evaluate the mechanism of OATP-mediated statin-induced impairment of insulin secretion, we next evaluated caspase-9 activity as a measure of mitochondrial function in rosuvastatin-treated INS-1 cells at 1 and 10 µM with or without OATP overexpression. In Ad-OATP2B1 INS-1 cells, caspase activity was significantly increased compared to Ad-LacZ control after 24-hour treatment with rosuvastatin at 1 µM and 10 µM ($P<0.01$ and $P<0.001$, respectively), with mean 1.24- and 1.48-fold differences, respectively (**Figure 3.18**).

Results for this experiment consist of a total of 9 mean values per treatment from three separate experimental days (n=3). Statistical analyses performed using two-way ANOVA followed by Bonferroni post-hoc test.

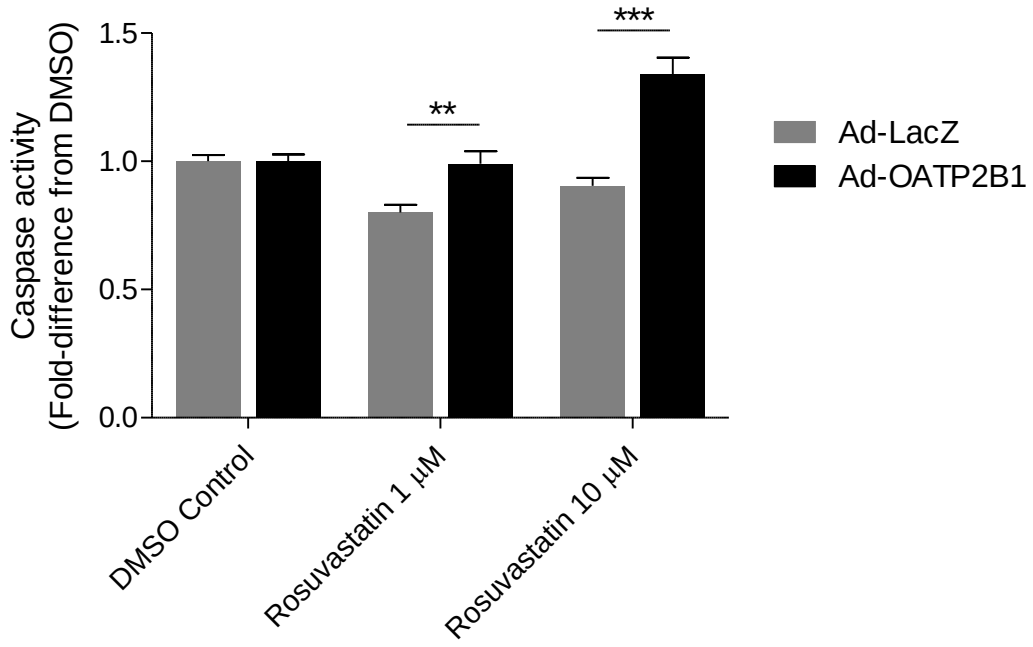

Figure 3.18. Mitochondrial function in statin-treated INS-1 cells overexpressing human OATP2B1. Caspase-9 activity used as a marker for mitochondrial function. A significant increase in caspase-9 activity was observed in rosuvastatin-treated Ad-OATP2B1 INS-1 cells compared to Ad-LacZ control (**, $P<0.01$; ***, $P<0.001$), as determined by two-way ANOVA followed by Bonferroni post-hoc test. Results shown as mean ± SD, n=3.

4 Discussion and Conclusions[1]

[1]Excerpts from this section reproduced (adapted) from: Kim M, Deacon P, Tirona RG, Kim RB, Pin CL, Meyer zu Schwabedissen HE, Wang R, and Schwarz UI (2017). Characterization of OATP1B3 and OATP2B1 transporter expression in the islet of the adult human pancreas. *Histochemistry and Cell Biology*, doi:10.1007/s00418-017-1580-6, with permission of Springer © Springer-Verlag Berlin Heidelberg 2017.

4.1 Summary of Findings

OATPs are membrane-bound uptake transporters that are recognized for their role in important physiological pathways and in the pharmacokinetics of many clinically relevant drugs. Expression and function of key members of the OATP1 and OATP2 family have been well characterized in excretory organs like the liver; however, our recent report demonstrated the presence of OATP1B3 in the islets of the human pancreas, co-localized with insulin-producing β cells (Meyer Zu Schwabedissen et al. 2014). Recent clinical and *in vitro* evidence (Cederberg et al. 2015; Zhao and Zhao 2015) have suggested cholesterol-lowering statins, many of them known OATP substrates, may disrupt insulin secretion. While the exact molecular mechanism is currently unknown, mitochondrial dysfunction and increased apoptosis of β cells (through HMG-CoA reductase inhibition) has been previously suggested, yet a role of OATP-mediated statin transport in this mechanism has not been established. We hypothesized that statin carriers of the OATP1 and OATP2 families are expressed in the β cell, and that OATPs mediate intracellular stain entry and contribute to statin-induced impairment of insulin secretion through mitochondrial dysfunction.

4.1.1 Specific Aim 1: To characterize statin carrier expression and OATP subcellular localization in human pancreatic islets

This study systematically assessed gene expression and cellular localization of important OATP1 and OATP2 family members in the human adult islet (**Figures 3.1, 3.3, 3.4, 3.7)**. Our findings confirm our previous report showing OATP1B3 expression in human islets (Meyer Zu Schwabedissen et al. 2014); however, we showed predominant co-localization of OATP1B3 with α rather than β cells (**Figures 3.3, 3.4, 3.5**). We further demonstrated substantial gene expression of two other *OATP*s in islets, *OATP2B1* and *OATP1A2*, compared to very low expression of *OATP1B1* and *OAT3* **(Figure 3.1**). We also show a distinct distribution of OATP2B1 and OATP1B3 within the islet suggesting specific roles in different endocrine cell types (**Figures 3.3, 3.4, 3.7**). In addition, abundant mRNA expression of the statin efflux transporters *BCRP* and *P-gp* was detected in islets, while *MRP2* was found at very low levels in islets (**Figure 3.2**). Overexpression of OATP1B3

was observed in islets of patients with chronic pancreatitis and pancreatic ductal adenocarcinoma, compared to tumour adjacent normal pancreatic tissue (**Figure 3.8**).

4.1.2 Specific Aim 2: To elucidate the role of OATP-mediated statin transport in pancreatic islet cell function using a murine β cell model

The rat insulinoma cell line INS-1 was used as a β cell model to evaluate statin effects on insulin secretion, as well as a direct role of OATP2B1 statin transport in mediating these effects after heterologous expression.

Using INS-1 cells, we first demonstrated expression of the rat statin carrier *Oatp1a5*, and inhibition of rosuvastatin accumulation by known OATP inhibitors rifampicin and indomethacin (**Figures 3.9**, **3.10**). Despite no relevant changes in cell viability, glucose-stimulated insulin secretion of INS-1 cells was significantly reduced with atorvastatin and rosuvastatin treatment, but not pravastatin (**Figures 3.11**, **3.12**); however, we did not demonstrate reversal in statin-induced impairment of insulin secretion with the co-administration of the OATP inhibitor rifampicin (**Figure 3.13**).

In order to study direct effects of OATP2B1 transport on statin-induced impaired insulin secretion, we transduced INS-1 cells with Ad-OATP2B1 or Ad-LacZ control. We first confirmed OATP2B1 protein expression and increased rosuvastatin accumulation in Ad-OATP2B1 transduced cells when compared with Ad-LacZ INS-1 cells (**Figures 3.14, 3.15**). No significant reduction in cell viability was observed with statin treatment at any concentration (**Figure 3.16**). Overexpression of human OATP2B1 in INS-1 cells resulted in a marked reduction in insulin secretion with high-glucose stimulation when cells were treated with 1 μM and 10 μM rosuvastatin and pravastatin, whereas no significant differences were detected between Ad-OATP2B1 and Ad-LacZ control with atorvastatin (**Figure 3.17**). Mitochondrial function was significantly impaired in Ad-OATP2B1 INS-1 treated with rosuvastatin compared to Ad-LacZ control, as demonstrated by a significant increase in caspase-9 activity (**Figure 3.18**).

4.2 Comparison and Contribution of Findings to Existing Literature

4.2.1 OATPs and other statin transporters are expressed in the endocrine pancreas

At present, OATP1B3 and OATP1B1 are widely considered liver-specific transporters (Ho et al. 2006). In comparison, OATP2B1 has been detected in many tissues throughout the human body, including liver, skeletal muscle, intestine and placenta (Kullak-Ublick et al. 2001), and OATP1A2 in the distal tubule of the kidneys, cholangiocytes, and at the blood brain barrier (Lee et al. 2005). Very few studies have examined OATP expression in the normal pancreas, let alone their cell type distribution in the islet. Our results showed high mRNA levels of *OATP1B3*, *OATP1A2* and *OATP2B1* in islet preparations of normal human adult pancreas compared to total pancreatic tissue, where *OATP2B1* islet expression even exceeded that of liver, a tissue known to harbor high transcript levels of *OATP2B1* (Kullak-Ublick et al. 2001). Previously undetected pancreatic *OATP* expression in the islets may be in part explained by the fact that endocrine tissue constitutes only about 1% to 4% of the total pancreas (Dolensek et al. 2015). Studies more frequently use preparations of total pancreas, which is most reflective of exocrine tissue making up the vast majority of pancreatic cells. In contrast, islet expression of *OATP1B1* was overall very low, a result in concordance with recent findings suggesting very limited *OATP1B1* mRNA expression in isolated normal human islets from 20 organ donors compared to liver (Kloster-Jensen et al. 2015). Gene expression of *OATP1B3* and *OATP2B1* but not *OATP1B1* has been also recently reported in normal human pancreas in a study which examined a panel of 384 samples from various cancers matched to normal controls (Pressler et al. 2011).

Importantly, here we demonstrate distinct patterns of cellular expression for OATP1B3 and OATP2B by dual immunostaining against insulin or glucagon. Whereas OATP2B1 was predominantly observed in β cells, OATP1B3 was more frequently found in α cells, suggesting differences in their functional roles within the normal endocrine pancreas. Concerning OATP1B3 distribution, these results contrast with our previous report where OATP1B3 co-localized with β cells but not α cells (Meyer Zu Schwabedissen et al. 2014). This may be explained by differences in the applied immunostaining methods.

Whereas the current study used dual immunofluorescent staining of mirrored pancreatic sections in a larger sample set, individual immunofluorescent stainings were previously performed in pancreatic sections of only 3 individuals, likely resulting in the observed discrepancy. Similarly, distinct islet expression patterns have been reported for murine Oatps closely related to human OATP1A2 when assessed with immunocytochemistry; rat Oatp1a1 largely localized to β cells, rat Oatp1a4 to α cells, and rat Oatp1a5 to both endocrine and exocrine tissues (Abe et al. 2010).

If present within the endocrine pancreas, the question emerges concerning the subcellular localization and function of these generally membrane-bound transport proteins. In case of OATP1B3, immunostaining patterns obtained with confocal microscopy appear to be more consistent with an intracellular site of action than a function at the plasma membrane. One may speculate OATPs primarily localize to the membrane of insulin- (or glucagon-) containing secretory granules of the β (or α) cells. Vesicular membrane expression in α and/or β cells has been previously reported for the vesicular nucleotide and vesicular glutamate uptake transporters (belonging to the solute carrier 17 [Slc17] phosphate transporter family), mediating ATP and glutamate uptake, respectively, into hormone-containing granules (Geisler et al. 2013; Sreedharan et al. 2010; Bai et al. 2003). As well, ATP-sensitive K_{ATP} channels have been primarily shown in the insulin-containing secretory granules of β cells, and are involved in the second-phase of insulin release (Geng et al. 2003).

The roles of OATP transporters in normal liver physiology are well established, and include bilirubin detoxification and bile acid homeostasis (Iusuf et al. 2012a); however, little is known regarding their contribution to islet cell function. These solute carriers are known to transport endogenous substrates of potential relevance to β cell survival, insulin secretion/synthesis, and glucose homeostasis such as thyroid hormones (Blanchet et al. 2012; Ianculescu et al. 2010; Mastracci and Evans-Molina 2014), sex hormone conjugates (Kullak-Ublick et al. 2001; Tiano and Mauvais-Jarvis 2012a; Tiano and Mauvais-Jarvis 2012b) and the gastrointestinal hormone cholecystokinin (Ahren et al. 2000; Kuntz et al. 2004; Linnemann and Davis 2016; Schwarz et al. 2011). Recently, a β-cell specific isoform of the hepatocyte nuclear factor-4 alpha (HNF4a), a transcription

factor belonging to the nuclear receptor superfamily, has been reported in β cells (Harries et al. 2009; Ihara et al. 2005). HNF4a, recognized as a central regulator of hepatocyte function, is essential for hepatic gene expression and lipid homeostasis (Hayhurst et al. 2001) including transcriptional regulation of the uptake carriers Oatp1a1, Oatp1a4, Oatp2b1, and sodium/taurocholate co-transporting polypeptide (Ntcp) as shown in mice lacking hepatic Hnf4a (Lu et al. 2010). Recent evidence also linked HNF4a with regulatory functions in the pancreas, most notably in islets (Harries et al. 2009). Mutations in the HNF4a gene is known to cause maturity-onset diabetes of the young (MODY1) (Byrne et al. 1995), a disorder characterized by impaired insulin secretion and progressive β cell-failure. Moreover, islets of mice with β-cell specific deficiency of Hnf4a showed impaired insulin secretion after stimulation by glucose or sulfonylurea derivatives (Miura et al. 2006). We previously identified and characterized HNF4a as a transcription factor regulating human OATP2B1 (Knauer et al. 2013), a transporter herein identified in human β cells, and showed that transient overexpression of OATP1B3 in a murine β-cell line (MIN6) enhances the insulinotropic effect of the sulfonylurea glibenclamide (Meyer Zu Schwabedissen et al. 2014), further supporting a possible role of OATPs in insulin secretion.

While we were unable to detect mRNA expression of *OAT3* in human islets, a recent study reported the presence of OAT3 in human β cells (Prentice et al. 2014). Predominantly acknowledged for its role in renal drug excretion of organic anion compounds by facilitating uptake into renal proximal tubular cells (Lin et al. 2015), this recent report now suggests an additional role of OAT3 in the development of diabetes through intracellular uptake of a diet-derived furan fatty acid metabolite into the pancreatic β cell, ultimately leading to β cell dysfunction and impaired insulin biosynthesis (Prentice et al. 2014).

Our findings also indicate high abundance of two important efflux transporters of the ABC transporter superfamily, P-gp (also MDR1 or multidrug resistance protein 1) and BCRP, in human adult islets. Known to mediate multidrug resistance, these carries mediate active removal of chemotherapeutics from cells (DeGorter et al. 2012). The presence of the P-gp in normal human islets had been previously reported (Bani et al.

1992; Kloster-Jensen et al. 2015). Bani et al. described P-gp membrane staining of endocrine islet cells as well as endothelial cells of islet capillaries (Bani et al. 1992). Recently, a much larger study utilizing isolated islets from 20 donors showed high ABCB1 gene transcript levels encoding P-gp and comparable to its hepatic expression (Kloster-Jensen et al. 2015). Immunofluorescent staining of dispersed islets supported limited co-expression with insulin- and glucagon positive islet cells (Kloster-Jensen et al. 2015). High levels of BCRP, as determined in this study, have been previously observed in human islets (Montanucci et al. 2011). Interestingly, marked expression of BCRP and MDR1 was also found in human islet-derived β precursor cells (also pancreatic stem cells) (Lechner et al. 2002; Montanucci et al. 2011), suggesting a plausible role of these transporters in β cell differentiation. The low levels of MRP2 we reported in islets are consistent with the findings of a previous study where only weak membrane staining was observed in human pancreatic islets (Sandusky et al. 2002).

4.2.2 OATP1B3 expression is upregulated in diseased pancreas

Upregulation of OATPs, particularly OATP1B3, has been previously shown in chronic pancreatitis and pancreatic cancer compared to normal or tumour-adjacent tissues (Kounnis et al. 2011; Pressler et al. 2011; Thakkar et al. 2013a; Hays et al. 2013). We observed intense OATP1B3 staining in islets of patients with chronic pancreatitis and PDAC compared to tumour-adjacent pancreatic tissue in a subset of 9 patients, supporting increased expression of this transporter in the diseased pancreas. OATP1B3 is known to facilitate cellular uptake of hormones with tumour-growth stimulating effects (sex hormones, cholecystokinin) (Konduri and Schwarz 2007; Baldwin and Shulkes 2007; Hajri and Damge 1998) and chemotherapeutics (platinum agents, anthracyclines) (Lancaster et al. 2013; Durmus et al. 2016). Given its broad substrate specificity and specific expression pattern in pancreatitis and early stages of PDAC, this carrier may play an important role in cancer progression but also enable more effective therapeutics. On the other hand, a tumour-specific variant of OATP1B3 with limited transport activity has been identified in colon and pancreatic cancer (Thakkar et al. 2013b) and while its biological relevance is still unclear, the impairment of substrate uptake may also contribute to the pathophysiology of these cancers. Extent of OATP1B3 upregulation has

shown variability within pancreatic cancer depending on the tumour type and cancer stage (Hays et al. 2013). Taken together, these findings support altered OATP expression in diseased pancreas and point toward potential differences in pancreatic OATP expression in type II diabetes, particularly statin-induced diabetes, warranting further study in assessing transporter expression in the diabetic pancreas.

4.2.3 Rosuvastatin and atorvastatin, but not pravastatin, alter glucose-stimulated insulin secretion in INS-1

This study demonstrated that rosuvastatin and atorvastatin treatment result in a significant dose-dependent reduction of insulin secretion, determined as stimulation index (SI). These results are supported by previous studies in murine β cell lines as well as human β cells showing dose-dependent reductions in glucose-stimulated insulin secretion with 24- to 48-hour statin treatments (Zhou et al. 2014; Salunkhe et al. 2016; Zhao and Zhao 2015) (**Table 1.2**). Interestingly, no significant impairment of insulin secretion was seen with pravastatin treatment. Though there is literature supporting a lack of effect of pravastatin on insulin secretion (Yada et al. 1999; Yaluri et al. 2015; Ishikawa et al. 2006), there are also conflicting reports demonstrating enhanced insulin secretion (Abe et al. 2010) and reduced insulin secretion (Zhao and Zhao 2015) with pravastatin treatment. Dose-dependence may suggest a role of HMG-CoA reductase inhibition in this mechanism (Ishikawa et al. 2006). Therefore, a lack of effect for pravastatin up to a concentration of 10 μM may be explained by differences in potency (IC_{50}: 44.1 nM) compared to rosuvastatin and atorvastatin (IC_{50}: 5.4 and 8.2 nM) (Hargreaves et al. 2005)

4.2.4 OATP inhibitor rifampicin did not improve statin-induced impairment of insulin secretion in INS-1

In this study, we assessed a potential role of OATP transport in statin effects on β cell function. We confirmed previously reported expression of rat Oatp1a5 in INS-1 cells (Abe et al. 2010) and demonstrated uptake of rosuvastatin, a known substrate of Oatp1a5 (Ho et al. 2006) that was markedly reduced via unspecific OATP inhibitors. Though we demonstrated impaired insulin secretion with rosuvastatin and atorvastatin treatment, we were unable to show a significant improvement in insulin secretion when INS-1 cells were co-treated with statins and the OATP inhibitor rifampicin. Despite rifampicin

having been well-studied as an OATP inhibitor, it has not been widely explored as a method of mitigating OATP-mediated statin effects on insulin secretion. Abe *et al.* demonstrated inhibition of pravastatin uptake by rifampicin (300 μM); however, no subsequent insulin secretion studies were performed since rifampicin treatment alone resulted in impaired insulin secretion at this high concentration (Abe et al. 2010). Lack of effect reversal may be therefore explained by insufficient inhibition of rosuvastatin uptake by rifampicin at the used concentration or direct effects of rifampicin on insulin secretion. Though no inhibition studies have been performed with rifampicin and rat Oatp1a5, potent inhibition of rat Oatp1a5 transport activity has been reported with azithromycin and clarithromycin, which belong to the same antibiotic class as rifampicin (Lan et al. 2009). Clarithromycin and rifampicin have both shown inhibition of OATP1B1 and OATP1B3 (Karlgren et al. 2012; Jacobson 2004). On the other hand, differential inhibition has been observed for rat Oatp1a1 and Oatp1a4 with rifampicin at 100 μM (Fattinger et al. 2000). Lastly, the lack of significant effect reversal in our study may also have been in part due to the variability in glucose-stimulated insulin secretion between experiments; INS-1 cells have shown batch-to-batch variability as well as changes over time and increased passage number (Hohmeier et al. 2000; Merglen et al. 2004), thus a more stable, clonal cell line highly responsive to glucose is frequently applied to overcome this limitation (Merglen et al. 2004).

4.2.5 Overexpression of human OATP2B1 in INS-1 contributes to statin-induced changes in insulin secretion

Since the role of OATPs in mediating statin effects on β cell function is largely unexplored, we overexpressed human OATP2B1 adenovirus (Ad-OATP2B1) in INS-1 cells as a model to evaluate a direct role of OATP statin transport in insulin secretion. We compared GSIS in INS-1 cells transduced with Ad-OATP2B1 to Ad-LacZ control to evaluate any change in statin effects with OATP overexpression. High glucose-stimulated insulin secretion was significantly reduced in Ad-OATP2B1 INS-1 compared to Ad-LacZ INS-1 treated with rosuvastatin and pravastatin, but not atorvastatin (**Figure 3.17**). A similar effect of Ad-OATP2B1 on insulin secretion demonstrated with rosuvastatin and pravastatin treatment is reasonable when considering substrate affinity; the OATP2B1 Michaelis constant (K_m) values are similar for rosuvastatin and pravastatin (2.4 and 2.25,

respectively) (Nozawa et al. 2004; Ho et al. 2006) (**Table 1.1**). Conversely, the same logic cannot be applied for the lack of effect observed on insulin secretion with atorvastatin in Ad-OATP2B1 INS-1 compared to Ad-LacZ control, since OATP2B1 has been reported to have a very high affinity for atorvastatin (K_m = 0.2, **Table 1.1**) (Kalliokoski and Niemi 2009). The effects may have been masked by a higher degree of INS-1 cell apoptosis for atorvastatin compared to rosuvastatin and pravastatin at the applied concentrations (Schirris et al. 2015; Sadighara et al. 2017); however, this was not investigated in our study.

Interestingly, high glucose-stimulated insulin secretion was moderately but significantly enhanced in Ad-LacZ INS-1 treated with 1 µM rosuvastatin and pravastatin. These results are not unexpected for pravastatin, which has previously been reported to enhance insulin secretion (Abe et al. 2010); however, it is slightly surprising in the context of rosuvastatin, which has more often been shown to impair insulin secretion *in vitro* (Salunkhe et al. 2016; Zhao and Zhao 2015). Though these results may be due to experimental variability, since high glucose-stimulated insulin secretion was not increased for any statins at 1 µM with statin-treated INS-1 cells (**Figure 3.12**), they may be in part explained by the mechanism described by Abe *et al.* to explain their observed insulinotropic effect of pravastatin (Abe et al. 2010). Inhibition of cholesterol synthesis by statins can also have a protective effect against lipotoxicity within the β cell, in which lipid accumulation reaches harmful levels and leads to cell death and loss of insulin secretion (Abe et al. 2010). Reduction of intracellular cholesterol in the β cell has been reported to enhance insulin secretion (Brunham et al. 2008), thus the relatively low concentration of rosuvastatin may have been more favourable for insulinotropic effects. On the contrary, though statins lower *de novo* cholesterol synthesis, upregulation of LDL receptors due to HMG-CoA reductase inhibition can elevate intracellular LDL cholesterol levels, potentially affecting β cell function via increased oxidation of LDL cholesterol resulting in inflammation, decreased mitochondrial function and β cell apoptosis (Chan et al. 2015; Sattar and Taskinen 2012).

4.2.6 OATP2B1 contributes to mitochondrial dysfunction in INS-1 cells after rosuvastatin treatment

In order to determine the underlying mechanism of OATP2B1-mediated impairment of insulin secretion by rosuvastatin, we assessed caspase-9 activity in INS-1 cells transduced with Ad-OATP2B1 and treated with statins in order to evaluate mitochondrial function. We observed a significant increase in caspase-9 activity in OATP2B1-expressing INS-1 cells from LacZ control when treated with rosuvastatin at concentrations of 1 and 10 µM. Caspase-9 activity in INS-1 cells transduced with Ad-OATP2B1 was increased about 1.24- and 1.48-fold from LacZ control with 1 µM rosuvastatin and 10 µM rosuvastatin, respectively. Similarly, Knauer *et al.* also reported a 1.5-fold increase in caspase-3/7 activity after treatment with 10 µM rosuvastatin in muscle cells transduced with Ad-OATP2B1 versus Ad-LacZ control (Knauer et al. 2010). Consequently, our results indicate that statin-induced activation of caspase-9 is mediated by OATP2B1 transport, and further suggest mitochondrial dysfunction and initiation of intrinsic apoptosis signalling as a potential mechanism of statin toxicity in the β cell. Rat pancreas mitochondrial function has recently been evaluated with a specific focus on statin treatment (Sadighara et al. 2017). Atorvastatin treatment resulted in mitochondrial swelling, increased production of reactive oxygen species (ROS), and induction mitochondrial apoptosis signalling via release of cytochrome c, a pro-apoptotic protein (Sadighara et al. 2017).

ATP concentration was not reduced in INS-1 cells expressing Ad-OATP2B1 treated for 24 hours with rosuvastatin, atorvastatin, or pravastatin at concentrations of up to 10 µM compared to Ad-LacZ control. These findings, though they appear to suggest no effect of statins on ATP, are in line with the findings of Knauer *et al.* Their study involved 48-hour statin treatment up to 100 µM in primary human skeletal muscle myoblast cells transduced with Ad-OATP2B1 (Knauer et al. 2010). No significant change in ATP level was reported after 48-hour treatment with rosuvastatin and atorvastatin at 10 µM; ATP levels were only reduced to about 80-85% of control. Thus, the lack of a significant change in ATP concentration at statin concentrations of up to 10 µM in our study is supported by literature, and suggests that viability of INS-1 cells is not compromised.

The two studies discussed above may seem contradictory in the context of our hypothesis; however, comparing the different pathways to cell death provides some support for our results. Apoptosis is a programmed and energy-dependent process consisting of activation of caspases and a complex set of events leading to cell death (Elmore 2007). Conversely, necrosis is a toxic and degradative process that is ATP-independent, over which cells have no control (Elmore 2007). Apoptosis and necrosis are not mutually exclusive events; an apoptotic process can be converted to necrosis if caspases are not readily available or if intracellular ATP is decreased (Leist et al. 1997; Lelli et al. 1998). The cytotoxic effects of statins have been shown to be largely due to induction of apoptosis (Sadighara et al. 2017; Schirris et al. 2015; Knauer et al. 2010). A study comparing mechanisms of cytotoxicity for eight different statins reported that apoptosis, and not necrosis, was the main cytotoxic mechanism for almost all statins, including rosuvastatin, atorvastatin, and pravastatin (Schirris et al. 2015). Furthermore, mitochondrial ATP production was not affected by atorvastatin, pravastatin, and rosuvastatin in their active acid forms, which were used in our study (Schirris et al. 2015; Knauer et al. 2010). Thus, the results observed in our study, unchanged ATP concentration reflecting cell viability and increased caspase-9 activity, are consistent with mitochondrial dysfunction and initiation of the apoptosis pathway, and are supported by previous findings (Schirris et al. 2015; Knauer et al. 2010).

4.3 Limitations of Study

4.3.1 Statin transporter expression data limited by sample size and methodology

A significant limitation of our gene expression data is the small sample size for human islets and other tissues. Particularly, due to limited volumes of RNA from human islets, we were only able to test between 1 and 3 islet samples for each gene of interest. Although we further validated protein expression in human islets for OATP1B3 and OATP2B1 by immunostaining, the islet mRNA expression of *OATPA2, BCRP,* and *P-gp* we observed remains exploratory up to this point due to small sample size and lack of confirmation on the protein level.

Our quantitative analysis of OATP1B3 protein expression and co-localization with endocrine markers also had a few limitations. First and foremost, although pancreatic tissue sections were labelled as normal, there may have been unknown factors for various diseases or disorders that may have further influenced co-localization analysis in these individuals. Additionally, our analyses for variability in expression were limited by the relative lack of female subjects (out of 10 patients, only 2 were female) due to the unknown sex of one individual. Additional female samples would have provided us with enough statistical power to perform the appropriate analyses for sex-related differences. Yet another limitation is that due to not knowing morphological characteristics of the complete pancreas such as pancreas volume or weight, our measurements for the endocrine and exocrine pancreas area were an estimate based on a small fraction of the pancreas.

In this study, the estimated relative β and α cell area of 4.4% and 4.6%, respectively, exceed previously reported values; endocrine islet cells typically represent less than 4% of the total pancreas volume (Dolensek et al. 2015). This may be the result of the quantitative image assessment at higher magnification, leading to a potential bias towards the islets themselves, a potential limitation of this study; however, it should be noted that similar methods for pancreatic morphometric analysis have been reported (Butler et al. 2016; Butler et al. 2003). At the level of islets, the here determined β cell to α cell area ratio of 1.34 (min-max, 0.44-3.92) is reflective of previously observed islet cell compositions for β (50-70%) and α cells (20-40%) in humans. Furthermore, our study did not detect any age or sex dependent differences in fractional β cell or α cell area; this may relate to the small sample size, another potential limitation of this study. Nevertheless, information on changes of β cell mass with age or sex are limited. A recent study in 106 lean nondiabetic subjects aged 20 to 100 years reported that the fractional β cell area to exocrine area increased with age, likely due to atrophy of exocrine tissue with advanced age, whereas the calculated β cell mass remained constant; no sex-dependent differences were observed (Saisho et al. 2013). These data suggest that mass as well as number of β cells are relatively well preserved despite increased age, supported by other research that further indicates insulin secretion may increase with age in human β cells (Arda et al. 2016).

Due to the inability to optimize conditions for immunofluorescent staining of OATP2B1 in human pancreatic tissue sections with our anti-OATP2B1 antibodies, we used immunohistochemistry to detect OATP2B1 in human pancreatic islets. We employed a consecutive staining strategy in an attempt to identify whether OATP2B1 was expressed on insulin-producing β cells or glucagon-producing α cells. We were able to see differences in staining patterns when OATP2B1 was double stained with insulin or with glucagon; as mentioned previously, OATP2B1 and insulin stains appeared to overlap more than OATP2B1 and glucagon stains. Although we are fairly confident in this association, the results would be far more convincing with dual immunofluorescent staining. Thus, immunofluorescent co-staining of OATP2B1 with insulin or glucagon in human pancreatic tissue sections and subsequent quantitative analysis should be performed to validate our conclusions that OATP2B1 is expressed primarily on β cells.

4.3.2 Use of heterogeneous INS-1 cell line

As alluded to previously, some of our results may have been affected by day-to-day experimental variability. This variability is likely due to the choice of INS-1 as our β cell model. Since its generation more than a decade ago, the INS-1 cell line has been recognized as being a more variable cell line, particularly in terms of glucose-stimulated insulin secretion (Hohmeier et al. 2000). INS-1 glucose responsiveness weakens over time and as passage number increases (Hohmeier et al. 2000), which would explain some of the discrepancies in our data as we did not use the same passage number for each experiment. In order to address these issues a more stable INS-1 cell line, INS-1E, has been created. INS-1E demonstrates improved stability compared to INS-1 and can apparently be used up to passages of 100; glucose-stimulated insulin secretion from INS-1E cells remained comparable to rat islets from passages 54-95 (Merglen et al. 2004). Thus, use of the stable INS-1E β cell line likely would have reduced our inter-experiment variability and provided more clarity in the effects of OATPs in mediating statin-induced changes in insulin secretion.

Another major limitation of using INS-1 cells is that due to their derivation from radiation-induced rat insulinoma cells (Asfari et al. 1992), they are not representative of normal β cell function in a physiological setting. For instance, the insulin content in INS-

1 cells is quite similar to tumour cells (Asfari et al. 1992), and insulin secretion only increases about 2- to 4-fold in response to glucose compared to an about 15-fold increase seen in freshly isolated primary islets (Hohmeier et al. 2000). Additionally, the INS-1 cell line has demonstrated heterogeneity – that is, it contains a mixture of glucose-responsive cells and glucose-unresponsive cells (Hohmeier et al. 2000). The use of primary islet cell culture in our experiments would be a favourable alternative as a more representative model of physiological β cell function.

4.3.3 ATP concentration as a marker of cell viability

In our study, ATP concentration was used as a marker to assess the effects of statins on INS-1 cell survival. Though it can be argued that ATP content may not be reflective of cell viability due to energy-dependent mechanisms of programmed cell death such as apoptosis and autophagy (Elmore 2007), previous *in vitro* studies have similarly measured cytotoxicity using intracellular ATP concentration following statin treatment. One study assessed the cytotoxic effects of statins on primary human skeletal muscle myoblast, measuring ATP concentration and using an MTT assay to detect formazan formation (Knauer et al. 2010). Another group examined statin-induced effects on cellular respiration and mitochondrial ATP production and reported inhibition of ATP production and impaired cell viability (Schirris et al. 2015). Furthermore, the luminescent ATP assay we used in this study has been shown to be quite sensitive with little chemical interference (Riss et al. 2004). Nonetheless, our study may have been strengthened with the use of alternative cell viability assays to supplement our findings.

4.4 Future Directions

4.4.1 Statin transporter expression in human pancreatic islets

This study has confirmed gene and protein expression of two OATP isoforms in human pancreatic islets. In addition to confirmed protein expression of OATP1B3 and OATP2B1 in human pancreatic islets, we reported gene expression of *OATP1A2, BCRP*, and *P-gp*. Due to limited sample size for islet gene expression, further studies are required in order to confirm our findings. Furthermore, confirmation of protein expression and localization for OATP1A2 and efflux transporters is required to provide

more insight regarding the interplay of transporters in statin disposition within pancreatic islets.

Another important follow-up study would be the intracellular localization of statin transporters within the β or α cells. Though OATPs are considered to be membrane-bound uptake transporters (Ho and Kim 2005; Hagenbuch and Stieger 2013), our immunostaining for OATP1B3 and OATP2B1 in human pancreatic tissue sections appeared to display more of an intracellular distribution of the protein. As described previously, this may be due to localization of OATPs to the membranes of secretory granules of islet cells. A two-step subcellular fractionation method has been previously used to investigate insulin secretory granule membranes (Brunner et al. 2007; Chen et al. 2015), and would be an effective tool in determining localization of various statin transporters including OATPs within the endocrine cells of the islets of Langerhans.

4.4.2 OATP loss-of-function studies

A more precise mechanism of confirming the role of OATPs in statin-mediated effects on insulin secretion may be knockdown or silencing of *OATP* genes. Silencing of *OATP*s in β cell models may provide more conclusive evidence of the role of OATPs in mediating statin-induced impairment of insulin secretion. We and others have reported that *Oatp1a5* is lone *Oatp* expressed in INS-1 (Abe et al. 2010); thus, *Oatp* gene silencing in this particular β cell model would be fairly straightforward. The CRISPR/Cas9 has recently been identified as an easy, efficient, and specific method of genome editing and would be a viable option for the silencing of Oatp1a5 in INS-1 cells (Sakuma et al. 2014).

Knockout mouse models have been widely used in characterizing physiological and pharmacological roles of hepatic Oatps (van de Steeg et al. 2010; Zaher et al. 2008); thus, important insights may be gained by assessing *Oatp* gene silencing in the context of the endocrine pancreas and statins. Exploratory gene expression analysis in mouse tissues showed expression of mouse *Oatp1a1*, *Oatp1a4*, *Oatp1a5*, and *Oatp1a6* in mouse islets (**Supplementary Figure 1**) and, as mentioned previously, Abe *et al.* reported mRNA expression of *Oatp1a4* and *Oatp1a5* in pancreata of db/db mice (Abe et al. 2010); thus,

an *Oatp1a*$^{-/-}$ cluster knockout mouse model may be a logical choice in assessing the role of Oatps in the endocrine pancreas.

Other preliminary data show mRNA and protein expression of mouse Oatp2b1 in wild-type mouse islets (**Supplementary Figures 2, 3**) and interestingly, preliminary metabolic studies in *Oatp2b1*$^{-/-}$ mice show significantly increased fasting blood glucose compared to wild-type mice (**Supplementary Figure 4**). Though these data are purely exploratory, they may point toward the usefulness of *Oatp2b1*$^{-/-}$ mice as a model to elucidate the relevance of Oatp2b1 in glucose homeostasis.

4.4.3 Statin-induced apoptosis in β cell models mediated by OATPs

Although our study provides more insight into the mechanism by which statins reduce insulin secretion, more investigation is required considering this very complex mechanism supported by extensive yet still inconclusive literature. We showed induction of caspase-9 activity only with rosuvastatin at two concentrations, thus it would be pertinent not only to show a wider dose response range but also to explore the effects of different statins. This would not only provide support for the hypothesis that statin-mediated reduced insulin secretion is brought on by mitochondrial dysfunction, but also provide more context for the reported discrepancy in effects depending on the type and potency of statins (Ishikawa et al. 2006; Carter et al. 2013).

Other methods have been employed to assess mitochondrial function. One study, in investigating the mechanism of statin-induced myopathy, evaluated the effects of statins on cellular respiration (Schirris et al. 2015). This study was quite comprehensive, in that it examined eight different statins and their differential impacts on cellular respiration markers in a myoblast cell line, including ATP production, basal respiratory rates, and respiration driven by and enzyme activity of each mitochondrial complex (Schirris et al. 2015). A similar approach applied in β cell models or primary islet cultures may illuminate specific mechanisms of statin-induced mitochondrial dysfunction and subsequent effects on insulin secretion.

4.4.4 Exploration of proposed mechanisms for statin-induced impairment of insulin secretion using an OATP overexpression system

As outlined previously, there are many different mechanisms that have been proposed in how statins mediate their effects on insulin secretion. To summarize, these mechanisms propose a wide variety of contributing factors including calcium signalling impairment, glucose signalling disruption, secretory granule cholesterol depletion, and electrophysiological imbalance. These studies have all been performed in various β cell models and isolated murine or human islets; however, an OATP overexpression system may further strengthen these studies by introducing a well-characterized and easily manipulated model to provide more insight into the mechanisms of statin-induced insulin secretion impairment.

4.5 Conclusions

In summary, we describe abundant expression of important solute uptake carriers of the OATP1 and OATP2 family in human adult islets, further revealing differential distribution of OATP1B3 and OATP2B1 among β and α cells. Variable co-expression of OATP1B3 with endocrine cells was observed in relation to age and pancreatic disease. Our *in vitro* findings in a murine β cell model confirm impairment of insulin secretion by rosuvastatin and atorvastatin, and support a role of OATPs in mediating statin-induced impairment of β cell function via mitochondrial dysfunction. Thus, this study has provided novel evidence of OATP expression and localization in the human endocrine pancreas and also contributed to the currently limited knowledge of the role of OATPs in statin-induced effects on insulin secretion. Since these membrane-bound carriers mediate transport of many endogenous and xenobiotic substrates of potential relevance to islet cell function, their physiological and clinical implications in pancreatic islets warrant further study.

References

Abe M, Toyohara T, Ishii A, Suzuki T, Noguchi N, Akiyama Y, Shiwaku HO, Nakagomi-Hagihara R, Zheng G, Shibata E, Souma T, Shindo T, Shima H, Takeuchi Y, Mishima E, Tanemoto M, Terasaki T, Onogawa T, Unno M, Ito S, Takasawa S, Abe T (2010) The HMG-CoA reductase inhibitor pravastatin stimulates insulin secretion through organic anion transporter polypeptides. Drug Metab Pharmacokinet 25 (3):274-282

Ahren B, Holst JJ, Efendic S (2000) Antidiabetogenic action of cholecystokinin-8 in type 2 diabetes. J Clin Endocrinol Metab 85 (3):1043-1048. doi:10.1210/jcem.85.3.6431

Anderson MS, Cote J, Liu Y, Stypinski D, Auger P, Hohnstein A, Rasmussen S, Johnson-Levonas AO, Gutstein DE (2013) Effects of Rifampin, a potent inducer of drug-metabolizing enzymes and an inhibitor of OATP1B1/3 transport, on the single dose pharmacokinetics of anacetrapib. J Clin Pharmacol 53 (7):746-752. doi:10.1002/jcph.97

Arda HE, Li L, Tsai J, Torre EA, Rosli Y, Peiris H, Spitale RC, Dai C, Gu X, Qu K, Wang P, Wang J, Grompe M, Scharfmann R, Snyder MS, Bottino R, Powers AC, Chang HY, Kim SK (2016) Age-Dependent Pancreatic Gene Regulation Reveals Mechanisms Governing Human beta Cell Function. Cell Metab 23 (5):909-920. doi:10.1016/j.cmet.2016.04.002

Asfari M, Janjic D, Meda P, Li G, Halban PA, Wollheim CB (1992) Establishment of 2-mercaptoethanol-dependent differentiated insulin-secreting cell lines. Endocrinology 130 (1):167-178. doi:10.1210/endo.130.1.1370150

Bai L, Zhang X, Ghishan FK (2003) Characterization of vesicular glutamate transporter in pancreatic alpha - and beta -cells and its regulation by glucose. Am J Physiol Gastrointest Liver Physiol 284 (5):G808-814. doi:10.1152/ajpgi.00333.2002

Baldwin GS, Shulkes A (2007) CCK receptors and cancer. Curr Top Med Chem 7 (12):1232-1238

Bani D, Brandi ML, Axiotis CA, Bani-Sacchi T (1992) Detection of P-glycoprotein on endothelial and endocrine cells of the human pancreatic islets by C 494 monoclonal antibody. Histochemistry 98 (4):207-209

Blanchet E, Bertrand C, Annicotte JS, Schlernitzauer A, Pessemesse L, Levin J, Fouret G, Feillet-Coudray C, Bonafos B, Fajas L, Cabello G, Wrutniak-Cabello C, Casas F (2012) Mitochondrial T3 receptor p43 regulates insulin secretion and glucose homeostasis. FASEB J 26 (1):40-50. doi:10.1096/fj.11-186841

Bonsu KO, Kadirvelu A, Reidpath DD (2013) Lipophilic versus hydrophilic statin therapy for heart failure: a protocol for an adjusted indirect comparison meta-analysis. Syst Rev 2:22. doi:10.1186/2046-4053-2-22

Briz O, Romero MR, Martinez-Becerra P, Macias RI, Perez MJ, Jimenez F, San Martin FG, Marin JJ (2006) OATP8/1B3-mediated cotransport of bile acids and glutathione: an export pathway for organic anions from hepatocytes? J Biol Chem 281 (41):30326-30335. doi:10.1074/jbc.M602048200

Brunham LR, Kruit JK, Verchere CB, Hayden MR (2008) Cholesterol in islet dysfunction and type 2 diabetes. J Clin Invest 118 (2):403-408. doi:10.1172/JCI33296

Brunner Y, Coute Y, Iezzi M, Foti M, Fukuda M, Hochstrasser DF, Wollheim CB, Sanchez JC (2007) Proteomics analysis of insulin secretory granules. Mol Cell Proteomics 6 (6):1007-1017. doi:10.1074/mcp.M600443-MCP200

Burg JS, Espenshade PJ (2011) Regulation of HMG-CoA reductase in mammals and yeast. Prog Lipid Res 50 (4):403-410. doi:10.1016/j.plipres.2011.07.002

Butler AE, Dhawan S, Hoang J, Cory M, Zeng K, Fritsch H, Meier JJ, Rizza RA, Butler PC (2016) beta-Cell Deficit in Obese Type 2 Diabetes, a Minor Role of beta-Cell Dedifferentiation and Degranulation. J Clin Endocrinol Metab 101 (2):523-532. doi:10.1210/jc.2015-3566

Butler AE, Janson J, Bonner-Weir S, Ritzel R, Rizza RA, Butler PC (2003) Beta-cell deficit and increased beta-cell apoptosis in humans with type 2 diabetes. Diabetes 52 (1):102-110

Byrne MM, Sturis J, Fajans SS, Ortiz FJ, Stoltz A, Stoffel M, Smith MJ, Bell GI, Halter JB, Polonsky KS (1995) Altered insulin secretory responses to glucose in subjects with a mutation in the MODY1 gene on chromosome 20. Diabetes 44 (6):699-704

Carter AA, Gomes T, Camacho X, Juurlink DN, Shah BR, Mamdani MM (2013) Risk of incident diabetes among patients treated with statins: population based study. BMJ 346:f2610. doi:10.1136/bmj.f2610

Cederberg H, Stancakova A, Yaluri N, Modi S, Kuusisto J, Laakso M (2015) Increased risk of diabetes with statin treatment is associated with impaired insulin sensitivity and insulin secretion: a 6 year follow-up study of the METSIM cohort. Diabetologia 58 (5):1109-1117. doi:10.1007/s00125-015-3528-5

Chan DC, Pang J, Watts GF (2015) Pathogenesis and management of the diabetogenic effect of statins: a role for adiponectin and coenzyme Q10? Curr Atheroscler Rep 17 (1):472. doi:10.1007/s11883-014-0472-7

Chen Y, Xia Z, Wang L, Yu Y, Liu P, Song E, Xu T (2015) An efficient two-step subcellular fractionation method for the enrichment of insulin granules from INS-1 cells. Biophys Rep 1:34-40. doi:10.1007/s41048-015-0008-x

Cheng X, Maher J, Chen C, Klaassen CD (2005) Tissue distribution and ontogeny of mouse organic anion transporting polypeptides (Oatps). Drug Metab Dispos 33 (7):1062-1073. doi:10.1124/dmd.105.003640

Choudhuri S, Cherrington NJ, Li N, Klaassen CD (2003) Constitutive expression of various xenobiotic and endobiotic transporter mRNAs in the choroid plexus of rats. Drug Metab Dispos 31 (11):1337-1345. doi:10.1124/dmd.31.11.1337

De Tata V (2014) Age-related impairment of pancreatic Beta-cell function: pathophysiological and cellular mechanisms. Front Endocrinol (Lausanne) 5:138. doi:10.3389/fendo.2014.00138

DeGorter MK, Tirona RG, Schwarz UI, Choi YH, Dresser GK, Suskin N, Myers K, Zou G, Iwuchukwu O, Wei WQ, Wilke RA, Hegele RA, Kim RB (2013) Clinical and pharmacogenetic predictors of circulating atorvastatin and rosuvastatin concentrations in routine clinical care. Circ Cardiovasc Genet 6 (4):400-408. doi:10.1161/CIRCGENETICS.113.000099

DeGorter MK, Urquhart BL, Gradhand U, Tirona RG, Kim RB (2012) Disposition of atorvastatin, rosuvastatin, and simvastatin in oatp1b2-/- mice and intraindividual variability in human subjects. J Clin Pharmacol 52 (11):1689-1697. doi:10.1177/0091270011422815

Dolensek J, Rupnik MS, Stozer A (2015) Structural similarities and differences between the human and the mouse pancreas. Islets 7 (1):e1024405. doi:10.1080/19382014.2015.1024405

Durmus S, van Hoppe S, Schinkel AH (2016) The impact of Organic Anion-Transporting Polypeptides (OATPs) on disposition and toxicity of antitumor drugs: Insights from knockout and humanized mice. Drug Resist Updat 27:72-88. doi:S1368-7646(16)30017-6 [pii]

10.1016/j.drup.2016.06.005

Elmore S (2007) Apoptosis: a review of programmed cell death. Toxicol Pathol 35 (4):495-516. doi:10.1080/01926230701320337

Fattinger K, Cattori V, Hagenbuch B, Meier PJ, Stieger B (2000) Rifamycin SV and rifampicin exhibit differential inhibition of the hepatic rat organic anion transporting polypeptides, Oatp1 and Oatp2. Hepatology 32 (1):82-86. doi:10.1053/jhep.2000.8539

Fujino H, Saito T, Ogawa S, Kojima J (2005) Transporter-mediated influx and efflux mechanisms of pitavastatin, a new inhibitor of HMG-CoA reductase. J Pharm Pharmacol 57 (10):1305-1311. doi:10.1211/jpp.57.10.0009

Gao B, Huber RD, Wenzel A, Vavricka SR, Ismair MG, Reme C, Meier PJ (2005) Localization of organic anion transporting polypeptides in the rat and human ciliary body epithelium. Exp Eye Res 80 (1):61-72. doi:10.1016/j.exer.2004.08.013

Geisler JC, Corbin KL, Li Q, Feranchak AP, Nunemaker CS, Li C (2013) Vesicular nucleotide transporter-mediated ATP release regulates insulin secretion. Endocrinology 154 (2):675-684. doi:10.1210/en.2012-1818

Geng X, Li L, Watkins S, Robbins PD, Drain P (2003) The insulin secretory granule is the major site of K(ATP) channels of the endocrine pancreas. Diabetes 52 (3):767-776

Glaeser H, Bailey DG, Dresser GK, Gregor JC, Schwarz UI, McGrath JS, Jolicoeur E, Lee W, Leake BF, Tirona RG, Kim RB (2007) Intestinal drug transporter expression and the impact of grapefruit juice in humans. Clin Pharmacol Ther 81 (3):362-370. doi:10.1038/sj.clpt.6100056

Glaeser H, Mandery K, Sticht H, Fromm MF, Konig J (2010) Relevance of conserved lysine and arginine residues in transmembrane helices for the transport activity of organic anion transporting polypeptide 1B3. Br J Pharmacol 159 (3):698-708. doi:10.1111/j.1476-5381.2009.00568.x

Goldstein JL, Brown MS (1990) Regulation of the mevalonate pathway. Nature 343 (6257):425-430. doi:10.1038/343425a0

Hagenbuch B, Meier PJ (2003) The superfamily of organic anion transporting polypeptides. Biochim Biophys Acta 1609 (1):1-18

Hagenbuch B, Meier PJ (2004) Organic anion transporting polypeptides of the OATP/ SLC21 family: phylogenetic classification as OATP/ SLCO superfamily, new nomenclature and molecular/functional properties. Pflugers Arch 447 (5):653-665. doi:10.1007/s00424-003-1168-y

Hagenbuch B, Stieger B (2013) The SLCO (former SLC21) superfamily of transporters. Mol Aspects Med 34 (2-3):396-412. doi:10.1016/j.mam.2012.10.009

Hajri A, Damge C (1998) Effects of cholecystokinin octapeptide on a pancreatic acinar carcinoma in the rat. Pharm Res 15 (11):1767-1774

Hanggi E, Grundschober AF, Leuthold S, Meier PJ, St-Pierre MV (2006) Functional analysis of the extracellular cysteine residues in the human organic anion transporting polypeptide, OATP2B1. Mol Pharmacol 70 (3):806-817. doi:10.1124/mol.105.019547

Hargreaves IP, Duncan AJ, Heales SJ, Land JM (2005) The effect of HMG-CoA reductase inhibitors on coenzyme Q10: possible biochemical/clinical implications. Drug Saf 28 (8):659-676

Harries LW, Brown JE, Gloyn AL (2009) Species-specific differences in the expression of the HNF1A, HNF1B and HNF4A genes. PLoS One 4 (11):e7855. doi:10.1371/journal.pone.0007855

Hayhurst GP, Lee YH, Lambert G, Ward JM, Gonzalez FJ (2001) Hepatocyte nuclear factor 4alpha (nuclear receptor 2A1) is essential for maintenance of hepatic gene expression and lipid homeostasis. Mol Cell Biol 21 (4):1393-1403. doi:10.1128/MCB.21.4.1393-1403.2001

Hays A, Apte U, Hagenbuch B (2013) Organic anion transporting polypeptides expressed in pancreatic cancer may serve as potential diagnostic markers and therapeutic targets for early stage adenocarcinomas. Pharm Res 30 (9):2260-2269. doi:10.1007/s11095-012-0962-7

Health Canada (2013) New statins labeling update: Risk of increased blood sugar levels and diabetes. http://healthycanadians.gc.ca/recall-alert-rappel-avis/hc-sc/2013/16949a-eng.php?_ga=2.118608781.525930.1496178051-1264272620.1496178051. Accessed May 30 2017

Hirano M, Maeda K, Matsushima S, Nozaki Y, Kusuhara H, Sugiyama Y (2005) Involvement of BCRP (ABCG2) in the biliary excretion of pitavastatin. Mol Pharmacol 68 (3):800-807. doi:10.1124/mol.105.014019

Hirano M, Maeda K, Shitara Y, Sugiyama Y (2004) Contribution of OATP2 (OATP1B1) and OATP8 (OATP1B3) to the hepatic uptake of pitavastatin in humans. J Pharmacol Exp Ther 311 (1):139-146. doi:10.1124/jpet.104.068056

Hirano M, Maeda K, Shitara Y, Sugiyama Y (2006) Drug-drug interaction between pitavastatin and various drugs via OATP1B1. Drug Metab Dispos 34 (7):1229-1236. doi:10.1124/dmd.106.009290

Hiriart M, Aguilar-Bryan L (2008) Channel regulation of glucose sensing in the pancreatic beta-cell. Am J Physiol Endocrinol Metab 295 (6):E1298-1306. doi:10.1152/ajpendo.90493.2008

Ho RH, Kim RB (2005) Transporters and drug therapy: implications for drug disposition and disease. Clin Pharmacol Ther 78 (3):260-277. doi:10.1016/j.clpt.2005.05.011

Ho RH, Tirona RG, Leake BF, Glaeser H, Lee W, Lemke CJ, Wang Y, Kim RB (2006) Drug and bile acid transporters in rosuvastatin hepatic uptake: function, expression, and pharmacogenetics. Gastroenterology 130 (6):1793-1806. doi:10.1053/j.gastro.2006.02.034

Hohmeier HE, Mulder H, Chen G, Henkel-Rieger R, Prentki M, Newgard CB (2000) Isolation of INS-1-derived cell lines with robust ATP-sensitive K+ channel-dependent and -independent glucose-stimulated insulin secretion. Diabetes 49 (3):424-430

Hou WY, Xu SF, Zhu QN, Lu YF, Cheng XG, Liu J (2014) Age- and sex-related differences of organic anion-transporting polypeptide gene expression in livers of rats. Toxicol Appl Pharmacol 280 (2):370-377. doi:10.1016/j.taap.2014.08.020

Hsiang B, Zhu Y, Wang Z, Wu Y, Sasseville V, Yang WP, Kirchgessner TG (1999) A novel human hepatic organic anion transporting polypeptide (OATP2). Identification of a liver-specific human organic anion transporting polypeptide and identification of rat and human hydroxymethylglutaryl-CoA reductase inhibitor transporters. J Biol Chem 274 (52):37161-37168

Huang L, Wang Y, Grimm S (2006) ATP-dependent transport of rosuvastatin in membrane vesicles expressing breast cancer resistance protein. Drug Metab Dispos 34 (5):738-742. doi:10.1124/dmd.105.007534

Ianculescu AG, Friesema EC, Visser TJ, Giacomini KM, Scanlan TS (2010) Transport of thyroid hormones is selectively inhibited by 3-iodothyronamine. Mol Biosyst 6 (8):1403-1410. doi:10.1039/b926588k

Ihara A, Yamagata K, Nammo T, Miura A, Yuan M, Tanaka T, Sladek FM, Matsuzawa Y, Miyagawa J, Shimomura I (2005) Functional characterization of the HNF4alpha isoform (HNF4alpha8) expressed in pancreatic beta-cells. Biochem Biophys Res Commun 329 (3):984-990. doi:10.1016/j.bbrc.2005.02.072

Ishikawa M, Okajima F, Inoue N, Motomura K, Kato T, Takahashi A, Oikawa S, Yamada N, Shimano H (2006) Distinct effects of pravastatin, atorvastatin, and simvastatin on insulin secretion from a beta-cell line, MIN6 cells. J Atheroscler Thromb 13 (6):329-335

Iusuf D, Sparidans RW, van Esch A, Hobbs M, Kenworthy KE, van de Steeg E, Wagenaar E, Beijnen JH, Schinkel AH (2012a) Organic anion-transporting polypeptides 1a/1b control the hepatic uptake of pravastatin in mice. Mol Pharm 9 (9):2497-2504. doi:10.1021/mp300108c

Iusuf D, van de Steeg E, Schinkel AH (2012b) Functions of OATP1A and 1B transporters in vivo: insights from mouse models. Trends Pharmacol Sci 33 (2):100-108. doi:10.1016/j.tips.2011.10.005

Jacobson TA (2004) Comparative pharmacokinetic interaction profiles of pravastatin, simvastatin, and atorvastatin when coadministered with cytochrome P450 inhibitors. Am J Cardiol 94 (9):1140-1146. doi:10.1016/j.amjcard.2004.07.080

Kalliokoski A, Niemi M (2009) Impact of OATP transporters on pharmacokinetics. Br J Pharmacol 158 (3):693-705. doi:10.1111/j.1476-5381.2009.00430.x

Karlgren M, Vildhede A, Norinder U, Wisniewski JR, Kimoto E, Lai Y, Haglund U, Artursson P (2012) Classification of inhibitors of hepatic organic anion transporting polypeptides (OATPs): influence of protein expression on drug-drug interactions. J Med Chem 55 (10):4740-4763. doi:10.1021/jm300212s

Kirkman MS, Briscoe VJ, Clark N, Florez H, Haas LB, Halter JB, Huang ES, Korytkowski MT, Munshi MN, Odegard PS, Pratley RE, Swift CS (2012) Diabetes in older adults. Diabetes Care 35 (12):2650-2664. doi:10.2337/dc12-1801

Kitamura S, Maeda K, Wang Y, Sugiyama Y (2008) Involvement of multiple transporters in the hepatobiliary transport of rosuvastatin. Drug Metab Dispos 36 (10):2014-2023. doi:10.1124/dmd.108.021410

Kloster-Jensen K, Vethe NT, Bremer S, Abadpour S, Korsgren O, Foss A, Bergan S, Scholz H (2015) Intracellular sirolimus concentration is reduced by tacrolimus in human pancreatic islets in vitro. Transpl Int 28 (10):1152-1161. doi:10.1111/tri.12617

Knauer MJ (2012) The Role of Drug Transporters in Statin-Induced Myopathy. Western University, Electronic Thesis and Dissertation Repository

Knauer MJ, Girdwood AJ, Kim RB, Tirona RG (2013) Transport function and transcriptional regulation of a liver-enriched human organic anion transporting polypeptide 2B1 transcriptional start site variant. Mol Pharmacol 83 (6):1218-1228. doi:10.1124/mol.112.083618

Knauer MJ, Urquhart BL, Meyer zu Schwabedissen HE, Schwarz UI, Lemke CJ, Leake BF, Kim RB, Tirona RG (2010) Human skeletal muscle drug transporters determine local exposure and toxicity of statins. Circ Res 106 (2):297-306. doi:10.1161/CIRCRESAHA.109.203596

Konduri S, Schwarz RE (2007) Estrogen receptor beta/alpha ratio predicts response of pancreatic cancer cells to estrogens and phytoestrogens. J Surg Res 140 (1):55-66. doi:10.1016/j.jss.2006.10.015

Konig J, Seithel A, Gradhand U, Fromm MF (2006) Pharmacogenomics of human OATP transporters. Naunyn Schmiedebergs Arch Pharmacol 372 (6):432-443. doi:10.1007/s00210-006-0040-y

Kopplow K, Letschert K, Konig J, Walter B, Keppler D (2005) Human hepatobiliary transport of organic anions analyzed by quadruple-transfected cells. Mol Pharmacol 68 (4):1031-1038. doi:10.1124/mol.105.014605

Kounnis V, Ioachim E, Svoboda M, Tzakos A, Sainis I, Thalhammer T, Steiner G, Briasoulis E (2011) Expression of organic anion-transporting polypeptides 1B3, 1B1, and 1A2 in human pancreatic cancer reveals a new class of potential therapeutic targets. Onco Targets Ther 4:27-32. doi:10.2147/OTT.S16706

Kowluru A, Veluthakal R (2005) Rho guanosine diphosphate-dissociation inhibitor plays a negative modulatory role in glucose-stimulated insulin secretion. Diabetes 54 (12):3523-3529

Krishnamurthy M, Li J, Fellows GF, Rosenberg L, Goodyer CG, Wang R (2011) Integrin {alpha}3, but not {beta}1, regulates islet cell survival and function via PI3K/Akt signaling pathways. Endocrinology 152 (2):424-435. doi:en.2010-0877 [pii]

10.1210/en.2010-0877

Kullak-Ublick GA, Ismair MG, Stieger B, Landmann L, Huber R, Pizzagalli F, Fattinger K, Meier PJ, Hagenbuch B (2001) Organic anion-transporting polypeptide B (OATP-B) and its functional comparison with three other OATPs of human liver. Gastroenterology 120 (2):525-533

Kuntz E, Pinget M, Damge P (2004) Cholecystokinin octapeptide: a potential growth factor for pancreatic beta cells in diabetic rats. JOP 5 (6):464-475

Lan T, Rao A, Haywood J, Davis CB, Han C, Garver E, Dawson PA (2009) Interaction of macrolide antibiotics with intestinally expressed human and rat organic anion-transporting polypeptides. Drug Metab Dispos 37 (12):2375-2382. doi:10.1124/dmd.109.028522

Lancaster CS, Sprowl JA, Walker AL, Hu S, Gibson AA, Sparreboom A (2013) Modulation of OATP1B-type transporter function alters cellular uptake and disposition of platinum chemotherapeutics. Mol Cancer Ther 12 (8):1537-1544. doi:1535-7163.MCT-12-0926 [pii]

10.1158/1535-7163.MCT-12-0926

Lau YY, Okochi H, Huang Y, Benet LZ (2006) Multiple transporters affect the disposition of atorvastatin and its two active hydroxy metabolites: application of in vitro and ex situ systems. J Pharmacol Exp Ther 316 (2):762-771. doi:10.1124/jpet.105.093088

Lazo de la Vega-Monroy ML, Fernandez-Mejia C (2011) Beta-Cell Function and Failure in Type 1 Diabetes. In: Wagner D (ed) Type 1 Diabetes - Pathogenesis, Genetics and Immunotherapy. InTech, pp 93-117. doi:10.5772/22089

Lee W, Glaeser H, Smith LH, Roberts RL, Moeckel GW, Gervasini G, Leake BF, Kim RB (2005) Polymorphisms in human organic anion-transporting polypeptide 1A2 (OATP1A2): implications for altered drug disposition and central nervous system drug entry. J Biol Chem 280 (10):9610-9617. doi:10.1074/jbc.M411092200

Leist M, Single B, Castoldi AF, Kuhnle S, Nicotera P (1997) Intracellular adenosine triphosphate (ATP) concentration: a switch in the decision between apoptosis and necrosis. J Exp Med 185 (8):1481-1486

Lelli JL, Jr., Becks LL, Dabrowska MI, Hinshaw DB (1998) ATP converts necrosis to apoptosis in oxidant-injured endothelial cells. Free Radic Biol Med 25 (6):694-702

Li DS, Yuan YH, Tu HJ, Liang QL, Dai LJ (2009) A protocol for islet isolation from mouse pancreas. Nat Protoc 4 (11):1649-1652. doi:10.1038/nprot.2009.150

Lin L, Yee SW, Kim RB, Giacomini KM (2015) SLC transporters as therapeutic targets: emerging opportunities. Nat Rev Drug Discov 14 (8):543-560. doi:10.1038/nrd4626

Link E, Parish S, Armitage J, Bowman L, Heath S, Matsuda F, Gut I, Lathrop M, Collins R (2008) SLCO1B1 variants and statin-induced myopathy--a genomewide study. N Engl J Med 359 (8):789-799. doi:10.1056/NEJMoa0801936

Linnemann AK, Davis DB (2016) Glucagon-like peptide-1 and cholecystokinin production and signaling in the pancreatic islet as an adaptive response to obesity. J Diabetes Investig 7 Suppl 1:44-49. doi:10.1111/jdi.12465

Lu H, Gonzalez FJ, Klaassen C (2010) Alterations in hepatic mRNA expression of phase II enzymes and xenobiotic transporters after targeted disruption of hepatocyte nuclear factor 4 alpha. Toxicol Sci 118 (2):380-390. doi:10.1093/toxsci/kfq280

Marcoff L, Thompson PD (2007) The role of coenzyme Q10 in statin-associated myopathy: a systematic review. J Am Coll Cardiol 49 (23):2231-2237. doi:10.1016/j.jacc.2007.02.049

Mastracci TL, Evans-Molina C (2014) Pancreatic and Islet Development and Function: The Role of Thyroid Hormone. J Endocrinol Diabetes Obes 2 (3)

Merglen A, Theander S, Rubi B, Chaffard G, Wollheim CB, Maechler P (2004) Glucose sensitivity and metabolism-secretion coupling studied during two-year continuous culture in INS-1E insulinoma cells. Endocrinology 145 (2):667-678. doi:10.1210/en.2003-1099

Meyer Zu Schwabedissen HE, Boettcher K, Steiner T, Schwarz UI, Keiser M, Kroemer HK, Siegmund W (2014) OATP1B3 is expressed in pancreatic beta-islet cells and enhances the insulinotropic effect of the sulfonylurea derivative glibenclamide. Diabetes 63 (2):775-784. doi:10.2337/db13-1005

Meyer Zu Schwabedissen HE, Ware JA, Tirona RG, Kim RB (2009) Identification, expression, and functional characterization of full-length and splice variants of murine organic anion transporting polypeptide 1b2. Mol Pharm 6 (6):1790-1797. doi:10.1021/mp900030w

Miura A, Yamagata K, Kakei M, Hatakeyama H, Takahashi N, Fukui K, Nammo T, Yoneda K, Inoue Y, Sladek FM, Magnuson MA, Kasai H, Miyagawa J, Gonzalez FJ, Shimomura I (2006) Hepatocyte nuclear factor-4alpha is essential for glucose-

stimulated insulin secretion by pancreatic beta-cells. J Biol Chem 281 (8):5246-5257. doi:10.1074/jbc.M507496200

Nakai D, Nakagomi R, Furuta Y, Tokui T, Abe T, Ikeda T, Nishimura K (2001) Human liver-specific organic anion transporter, LST-1, mediates uptake of pravastatin by human hepatocytes. J Pharmacol Exp Ther 297 (3):861-867

Navarese EP, Buffon A, Andreotti F, Kozinski M, Welton N, Fabiszak T, Caputo S, Grzesk G, Kubica A, Swiatkiewicz I, Sukiennik A, Kelm M, De Servi S, Kubica J (2013) Meta-analysis of impact of different types and doses of statins on new-onset diabetes mellitus. Am J Cardiol 111 (8):1123-1130. doi:10.1016/j.amjcard.2012.12.037

Neuvonen PJ, Backman JT, Niemi M (2008) Pharmacokinetic comparison of the potential over-the-counter statins simvastatin, lovastatin, fluvastatin and pravastatin. Clin Pharmacokinet 47 (7):463-474. doi:10.2165/00003088-200847070-00003

Neuvonen PJ, Kantola T, Kivisto KT (1998) Simvastatin but not pravastatin is very susceptible to interaction with the CYP3A4 inhibitor itraconazole. Clin Pharmacol Ther 63 (3):332-341. doi:10.1016/S0009-9236(98)90165-5

Niemi M, Arnold KA, Backman JT, Pasanen MK, Godtel-Armbrust U, Wojnowski L, Zanger UM, Neuvonen PJ, Eichelbaum M, Kivisto KT, Lang T (2006) Association of genetic polymorphism in ABCC2 with hepatic multidrug resistance-associated protein 2 expression and pravastatin pharmacokinetics. Pharmacogenet Genomics 16 (11):801-808. doi:10.1097/01.fpc.0000230422.50962.91

Niemi M, Neuvonen PJ, Hofmann U, Backman JT, Schwab M, Lutjohann D, von Bergmann K, Eichelbaum M, Kivisto KT (2005) Acute effects of pravastatin on cholesterol synthesis are associated with SLCO1B1 (encoding OATP1B1) haplotype *17. Pharmacogenet Genomics 15 (5):303-309

Niemi M, Schaeffeler E, Lang T, Fromm MF, Neuvonen M, Kyrklund C, Backman JT, Kerb R, Schwab M, Neuvonen PJ, Eichelbaum M, Kivisto KT (2004) High plasma pravastatin concentrations are associated with single nucleotide polymorphisms and haplotypes of organic anion transporting polypeptide-C (OATP-C, SLCO1B1). Pharmacogenetics 14 (7):429-440

Noe J, Portmann R, Brun ME, Funk C (2007) Substrate-dependent drug-drug interactions between gemfibrozil, fluvastatin and other organic anion-transporting peptide (OATP) substrates on OATP1B1, OATP2B1, and OATP1B3. Drug Metab Dispos 35 (8):1308-1314. doi:10.1124/dmd.106.012930

Nozawa T, Imai K, Nezu J, Tsuji A, Tamai I (2004) Functional characterization of pH-sensitive organic anion transporting polypeptide OATP-B in human. J Pharmacol Exp Ther 308 (2):438-445. doi:10.1124/jpet.103.060194

Obaidat A, Roth M, Hagenbuch B (2012) The expression and function of organic anion transporting polypeptides in normal tissues and in cancer. Annu Rev Pharmacol Toxicol 52:135-151. doi:10.1146/annurev-pharmtox-010510-100556

Orecna M, Hafko R, Bacova Z, Podskocova J, Chorvat D, Jr., Strbak V (2008) Different secretory response of pancreatic islets and insulin secreting cell lines INS-1 and INS-1E to osmotic stimuli. Physiol Res 57 (6):935-945

Pasanen MK, Neuvonen M, Neuvonen PJ, Niemi M (2006) SLCO1B1 polymorphism markedly affects the pharmacokinetics of simvastatin acid. Pharmacogenet Genomics 16 (12):873-879. doi:10.1097/01.fpc.0000230416.82349.90

Pedersen KB, Zhang P, Doumen C, Charbonnet M, Lu D, Newgard CB, Haycock JW, Lange AJ, Scott DK (2007) The promoter for the gene encoding the catalytic subunit of rat glucose-6-phosphatase contains two distinct glucose-responsive regions. Am J Physiol Endocrinol Metab 292 (3):E788-801. doi:10.1152/ajpendo.00510.2006

Preiss D, Seshasai SR, Welsh P, Murphy SA, Ho JE, Waters DD, DeMicco DA, Barter P, Cannon CP, Sabatine MS, Braunwald E, Kastelein JJ, de Lemos JA, Blazing MA, Pedersen TR, Tikkanen MJ, Sattar N, Ray KK (2011) Risk of incident diabetes with intensive-dose compared with moderate-dose statin therapy: a meta-analysis. JAMA 305 (24):2556-2564. doi:10.1001/jama.2011.860

Prentice KJ, Luu L, Allister EM, Liu Y, Jun LS, Sloop KW, Hardy AB, Wei L, Jia W, Fantus IG, Sweet DH, Sweeney G, Retnakaran R, Dai FF, Wheeler MB (2014) The furan fatty acid metabolite CMPF is elevated in diabetes and induces beta cell dysfunction. Cell Metab 19 (4):653-666. doi:10.1016/j.cmet.2014.03.008

Pressler H, Sissung TM, Venzon D, Price DK, Figg WD (2011) Expression of OATP family members in hormone-related cancers: potential markers of progression. PLoS One 6 (5):e20372. doi:10.1371/journal.pone.0020372

Quesada I, Tuduri E, Ripoll C, Nadal A (2008) Physiology of the pancreatic alpha-cell and glucagon secretion: role in glucose homeostasis and diabetes. J Endocrinol 199 (1):5-19. doi:10.1677/JOE-08-0290

Reitman ML, Chu X, Cai X, Yabut J, Venkatasubramanian R, Zajic S, Stone JA, Ding Y, Witter R, Gibson C, Roupe K, Evers R, Wagner JA, Stoch A (2011) Rifampin's acute inhibitory and chronic inductive drug interactions: experimental and model-based approaches to drug-drug interaction trial design. Clin Pharmacol Ther 89 (2):234-242. doi:10.1038/clpt.2010.271

Riss TL, Moravec RA, Niles AL, Duellman S, Benink HA, Worzella TJ, Minor L (2004) Cell Viability Assays. In: Sittampalam GS, Coussens NP, Brimacombe K et al. (eds) Assay Guidance Manual. Bethesda (MD),

Roth M, Obaidat A, Hagenbuch B (2012) OATPs, OATs and OCTs: the organic anion and cation transporters of the SLCO and SLC22A gene superfamilies. Br J Pharmacol 165 (5):1260-1287. doi:10.1111/j.1476-5381.2011.01724.x

Roy S, Sherman A, Monari-Sparks MJ, Schweiker O, Jain N, Sims E, Breda M, Byraiah GP, Belecanech RG, Coletta MD, Barrios CJ, Hunter K, Gaughan JP (2016) Association of Comorbid and Metabolic Factors with Optimal Control of Type 2 Diabetes Mellitus. N Am J Med Sci 8 (1):31-39. doi:10.4103/1947-2714.175197

Sadighara M, Amirsheardost Z, Minaiyan M, Hajhashemi V, Naserzadeh P, Salimi A, Seydi E, Pourahmad J (2017) Toxicity of Atorvastatin on Pancreas Mitochondria: A Justification for Increased Risk of Diabetes Mellitus. Basic Clin Pharmacol Toxicol 120 (2):131-137. doi:10.1111/bcpt.12656

Saisho Y, Butler AE, Manesso E, Elashoff D, Rizza RA, Butler PC (2013) beta-cell mass and turnover in humans: effects of obesity and aging. Diabetes Care 36 (1):111-117. doi:10.2337/dc12-0421

Sakuma T, Nishikawa A, Kume S, Chayama K, Yamamoto T (2014) Multiplex genome engineering in human cells using all-in-one CRISPR/Cas9 vector system. Sci Rep 4:5400. doi:10.1038/srep05400

Salunkhe VA, Elvstam O, Eliasson L, Wendt A (2016) Rosuvastatin Treatment Affects Both Basal and Glucose-Induced Insulin Secretion in INS-1 832/13 Cells. PLoS One 11 (3):e0151592. doi:10.1371/journal.pone.0151592

Sandusky GE, Mintze KS, Pratt SE, Dantzig AH (2002) Expression of multidrug resistance-associated protein 2 (MRP2) in normal human tissues and carcinomas using tissue microarrays. Histopathology 41 (1):65-74

Sattar N, Preiss D, Murray HM, Welsh P, Buckley BM, de Craen AJ, Seshasai SR, McMurray JJ, Freeman DJ, Jukema JW, Macfarlane PW, Packard CJ, Stott DJ, Westendorp RG, Shepherd J, Davis BR, Pressel SL, Marchioli R, Marfisi RM, Maggioni AP, Tavazzi L, Tognoni G, Kjekshus J, Pedersen TR, Cook TJ, Gotto AM, Clearfield MB, Downs JR, Nakamura H, Ohashi Y, Mizuno K, Ray KK, Ford I (2010) Statins and risk of incident diabetes: a collaborative meta-analysis of randomised statin trials. Lancet 375 (9716):735-742. doi:10.1016/S0140-6736(09)61965-6

Sattar N, Taskinen MR (2012) Statins are diabetogenic--myth or reality? Atheroscler Suppl 13 (1):1-10. doi:10.1016/j.atherosclerosissup.2012.06.001

Schirris TJ, Renkema GH, Ritschel T, Voermans NC, Bilos A, van Engelen BG, Brandt U, Koopman WJ, Beyrath JD, Rodenburg RJ, Willems PH, Smeitink JA, Russel FG (2015) Statin-Induced Myopathy Is Associated with Mitochondrial Complex III Inhibition. Cell Metab 22 (3):399-407. doi:10.1016/j.cmet.2015.08.002

Schmittgen TD, Livak KJ (2008) Analyzing real-time PCR data by the comparative C(T) method. Nat Protoc 3 (6):1101-1108

Schwarz UI, Meyer zu Schwabedissen HE, Tirona RG, Suzuki A, Leake BF, Mokrab Y, Mizuguchi K, Ho RH, Kim RB (2011) Identification of novel functional organic anion-transporting polypeptide 1B3 polymorphisms and assessment of substrate specificity. Pharmacogenet Genomics 21 (3):103-114. doi:10.1097/FPC.0b013e328342f5b1

Shirasaka Y, Suzuki K, Nakanishi T, Tamai I (2010) Intestinal absorption of HMG-CoA reductase inhibitor pravastatin mediated by organic anion transporting polypeptide. Pharm Res 27 (10):2141-2149. doi:10.1007/s11095-010-0216-5

Shirasaka Y, Suzuki K, Shichiri M, Nakanishi T, Tamai I (2011) Intestinal absorption of HMG-CoA reductase inhibitor pitavastatin mediated by organic anion transporting polypeptide and P-glycoprotein/multidrug resistance 1. Drug Metab Pharmacokinet 26 (2):171-179

Shitara Y, Itoh T, Sato H, Li AP, Sugiyama Y (2003) Inhibition of transporter-mediated hepatic uptake as a mechanism for drug-drug interaction between cerivastatin and cyclosporin A. J Pharmacol Exp Ther 304 (2):610-616. doi:10.1124/jpet.102.041921

Shitara Y, Sugiyama Y (2006) Pharmacokinetic and pharmacodynamic alterations of 3-hydroxy-3-methylglutaryl coenzyme A (HMG-CoA) reductase inhibitors: drug-drug interactions and interindividual differences in transporter and metabolic enzyme functions. Pharmacol Ther 112 (1):71-105. doi:10.1016/j.pharmthera.2006.03.003

Simonson SG, Raza A, Martin PD, Mitchell PD, Jarcho JA, Brown CD, Windass AS, Schneck DW (2004) Rosuvastatin pharmacokinetics in heart transplant recipients administered an antirejection regimen including cyclosporine. Clin Pharmacol Ther 76 (2):167-177. doi:10.1016/j.clpt.2004.03.010

Skarlovnik A, Janic M, Lunder M, Turk M, Sabovic M (2014) Coenzyme Q10 supplementation decreases statin-related mild-to-moderate muscle symptoms: a randomized clinical study. Med Sci Monit 20:2183-2188. doi:10.12659/MSM.890777

Sreedharan S, Shaik JH, Olszewski PK, Levine AS, Schioth HB, Fredriksson R (2010) Glutamate, aspartate and nucleotide transporters in the SLC17 family form four main phylogenetic clusters: evolution and tissue expression. BMC Genomics 11:17. doi:10.1186/1471-2164-11-17

Stanger BZ, Hebrok M (2013) Control of cell identity in pancreas development and regeneration. Gastroenterology 144 (6):1170-1179. doi:10.1053/j.gastro.2013.01.074

Stieger B, Meier PJ (2011) Pharmacogenetics of drug transporters in the enterohepatic circulation. Pharmacogenomics 12 (5):611-631. doi:10.2217/pgs.11.53

Swerdlow DI, Preiss D, Kuchenbaecker KB, Holmes MV, Engmann JE, Shah T, Sofat R, Stender S, Johnson PC, Scott RA, Leusink M, Verweij N, Sharp SJ, Guo Y, Giambartolomei C, Chung C, Peasey A, Amuzu A, Li K, Palmen J, Howard P, Cooper JA, Drenos F, Li YR, Lowe G, Gallacher J, Stewart MC, Tzoulaki I, Buxbaum SG, van der AD, Forouhi NG, Onland-Moret NC, van der Schouw YT, Schnabel RB, Hubacek JA, Kubinova R, Baceviciene M, Tamosiunas A, Pajak A, Topor-Madry R, Stepaniak U, Malyutina S, Baldassarre D, Sennblad B, Tremoli E, de Faire U, Veglia F, Ford I, Jukema JW, Westendorp RG, de Borst GJ, de Jong PA, Algra A, Spiering W, Maitland-van der Zee AH, Klungel OH, de Boer A, Doevendans PA, Eaton CB, Robinson JG, Duggan D, Consortium D, Consortium M, InterAct C, Kjekshus J, Downs JR, Gotto AM, Keech AC, Marchioli R, Tognoni G, Sever PS, Poulter NR, Waters DD, Pedersen TR, Amarenco P, Nakamura H, McMurray JJ, Lewsey JD, Chasman DI, Ridker PM, Maggioni AP, Tavazzi L, Ray KK, Seshasai SR, Manson JE, Price JF, Whincup PH, Morris RW, Lawlor DA, Smith GD, Ben-Shlomo Y, Schreiner PJ, Fornage M, Siscovick DS, Cushman M, Kumari M, Wareham NJ, Verschuren WM, Redline S, Patel SR, Whittaker JC, Hamsten A, Delaney JA, Dale C, Gaunt TR, Wong A, Kuh D, Hardy R, Kathiresan S, Castillo BA, van der Harst P, Brunner EJ, Tybjaerg-Hansen A, Marmot MG, Krauss RM, Tsai M, Coresh J, Hoogeveen RC, Psaty BM, Lange LA, Hakonarson H, Dudbridge F, Humphries SE, Talmud PJ, Kivimaki M, Timpson NJ, Langenberg C, Asselbergs FW, Voevoda M, Bobak M, Pikhart H, Wilson JG, Reiner AP, Keating BJ, Hingorani AD, Sattar N (2015) HMG-coenzyme A reductase inhibition, type 2 diabetes, and bodyweight: evidence from genetic analysis and randomised trials. Lancet 385 (9965):351-361. doi:10.1016/S0140-6736(14)61183-1

Takeda M, Noshiro R, Onozato ML, Tojo A, Hasannejad H, Huang XL, Narikawa S, Endou H (2004) Evidence for a role of human organic anion transporters in the muscular side effects of HMG-CoA reductase inhibitors. Eur J Pharmacol 483 (2-3):133-138

Thakkar N, Kim K, Jang ER, Han S, Kim D, Merchant N, Lockhart AC, Lee W (2013a) A cancer-specific variant of the SLCO1B3 gene encodes a novel human organic anion transporting polypeptide 1B3 (OATP1B3) localized mainly in the cytoplasm of colon and pancreatic cancer cells. Mol Pharm 10 (1):406-416. doi:10.1021/mp3005353

Thakkar N, Kim K, Jang ER, Han S, Kim K, Kim D, Merchant N, Lockhart AC, Lee W (2013b) A cancer-specific variant of the SLCO1B3 gene encodes a novel human organic anion transporting polypeptide 1B3 (OATP1B3) localized mainly in the cytoplasm of colon and pancreatic cancer cells. Mol Pharm 10 (1):406-416. doi:10.1021/mp3005353

Thompson PD, Clarkson P, Karas RH (2003) Statin-associated myopathy. JAMA 289 (13):1681-1690. doi:10.1001/jama.289.13.1681

Tiano J, Mauvais-Jarvis F (2012a) Selective estrogen receptor modulation in pancreatic beta-cells and the prevention of type 2 diabetes. Islets 4 (2):173-176. doi:10.4161/isl.19747

Tiano JP, Mauvais-Jarvis F (2012b) Importance of oestrogen receptors to preserve functional beta-cell mass in diabetes. Nat Rev Endocrinol 8 (6):342-351. doi:10.1038/nrendo.2011.242

Tirona RG, Leake BF, Merino G, Kim RB (2001) Polymorphisms in OATP-C: identification of multiple allelic variants associated with altered transport activity among European- and African-Americans. J Biol Chem 276 (38):35669-35675. doi:10.1074/jbc.M103792200

Tokui T, Nakai D, Nakagomi R, Yawo H, Abe T, Sugiyama Y (1999) Pravastatin, an HMG-CoA reductase inhibitor, is transported by rat organic anion transporting polypeptide, oatp2. Pharm Res 16 (6):904-908

Tsuchiya M, Hosaka M, Moriguchi T, Zhang S, Suda M, Yokota-Hashimoto H, Shinozuka K, Takeuchi T (2010) Cholesterol biosynthesis pathway intermediates and inhibitors regulate glucose-stimulated insulin secretion and secretory granule formation in pancreatic beta-cells. Endocrinology 151 (10):4705-4716. doi:10.1210/en.2010-0623

van de Steeg E, Stranecky V, Hartmannova H, Noskova L, Hrebicek M, Wagenaar E, van Esch A, de Waart DR, Oude Elferink RP, Kenworthy KE, Sticova E, al-Edreesi M, Knisely AS, Kmoch S, Jirsa M, Schinkel AH (2012) Complete OATP1B1 and OATP1B3 deficiency causes human Rotor syndrome by interrupting conjugated bilirubin reuptake into the liver. J Clin Invest 122 (2):519-528. doi:10.1172/JCI59526

van de Steeg E, Wagenaar E, van der Kruijssen CM, Burggraaff JE, de Waart DR, Elferink RP, Kenworthy KE, Schinkel AH (2010) Organic anion transporting polypeptide 1a/1b-knockout mice provide insights into hepatic handling of bilirubin, bile acids, and drugs. J Clin Invest 120 (8):2942-2952. doi:10.1172/JCI42168

VanWert AL, Gionfriddo MR, Sweet DH (2010) Organic anion transporters: discovery, pharmacology, regulation and roles in pathophysiology. Biopharm Drug Dispos 31 (1):1-71. doi:10.1002/bdd.693

Vaughan CJ, Gotto AM, Jr., Basson CT (2000) The evolving role of statins in the management of atherosclerosis. J Am Coll Cardiol 35 (1):1-10

Vaughan RA, Garcia-Smith R, Bisoffi M, Conn CA, Trujillo KA (2013) Ubiquinol rescues simvastatin-suppression of mitochondrial content, function and

metabolism: implications for statin-induced rhabdomyolysis. Eur J Pharmacol 711 (1-3):1-9. doi:10.1016/j.ejphar.2013.04.009

Volchuk A, Ron D (2010) The endoplasmic reticulum stress response in the pancreatic beta-cell. Diabetes Obes Metab 12 Suppl 2:48-57. doi:10.1111/j.1463-1326.2010.01271.x

Wang R, Li J, Yashpal N (2004) Phenotypic analysis of c-Kit expression in epithelial monolayers derived from postnatal rat pancreatic islets. J Endocrinol 182 (1):113-122

Waters DD, Ho JE, DeMicco DA, Breazna A, Arsenault BJ, Wun CC, Kastelein JJ, Colhoun H, Barter P (2011) Predictors of new-onset diabetes in patients treated with atorvastatin: results from 3 large randomized clinical trials. J Am Coll Cardiol 57 (14):1535-1545. doi:10.1016/j.jacc.2010.10.047

Williams JA (2010) Regulation of acinar cell function in the pancreas. Curr Opin Gastroenterol 26 (5):478-483. doi:10.1097/MOG.0b013e32833d11c6

Xu H, Song Y, You NC, Zhang ZF, Greenland S, Ford ES, He L, Liu S (2010) Prevalence and clustering of metabolic risk factors for type 2 diabetes among Chinese adults in Shanghai, China. BMC Public Health 10:683. doi:10.1186/1471-2458-10-683

Yada T, Nakata M, Shiraishi T, Kakei M (1999) Inhibition by simvastatin, but not pravastatin, of glucose-induced cytosolic Ca2+ signalling and insulin secretion due to blockade of L-type Ca2+ channels in rat islet beta-cells. Br J Pharmacol 126 (5):1205-1213. doi:10.1038/sj.bjp.0702397

Yaluri N, Modi S, Lopez Rodriguez M, Stancakova A, Kuusisto J, Kokkola T, Laakso M (2015) Simvastatin Impairs Insulin Secretion by Multiple Mechanisms in MIN6 Cells. PLoS One 10 (11):e0142902. doi:10.1371/journal.pone.0142902

Yin ZP (2014) In Vitro Functional Analysis Of Novel Single Nucleotide Polymorphisms In OATP1B1 And Potential Clinical Relevance. Western University, Electronic Thesis and Dissertation Repository

Zaher H, Meyer zu Schwabedissen HE, Tirona RG, Cox ML, Obert LA, Agrawal N, Palandra J, Stock JL, Kim RB, Ware JA (2008) Targeted disruption of murine organic anion-transporting polypeptide 1b2 (Oatp1b2/Slco1b2) significantly alters disposition of prototypical drug substrates pravastatin and rifampin. Mol Pharmacol 74 (2):320-329. doi:10.1124/mol.108.046458

Zhang W, Yu BN, He YJ, Fan L, Li Q, Liu ZQ, Wang A, Liu YL, Tan ZR, Fen J, Huang YF, Zhou HH (2006) Role of BCRP 421C>A polymorphism on rosuvastatin pharmacokinetics in healthy Chinese males. Clin Chim Acta 373 (1-2):99-103. doi:10.1016/j.cca.2006.05.010

Zhao W, Zhao SP (2015) Different effects of statins on induction of diabetes mellitus: an experimental study. Drug Des Devel Ther 9:6211-6223. doi:10.2147/DDDT.S87979

Zhou J, Li W, Xie Q, Hou Y, Zhan S, Yang X, Xu X, Cai J, Huang Z (2014) Effects of simvastatin on glucose metabolism in mouse MIN6 cells. J Diabetes Res 2014:376570. doi:10.1155/2014/376570

Appendices

Appendix A: Copyright Approval

SPRINGER LICENSE
TERMS AND CONDITIONS

Jun 05, 2017

This Agreement between Western University -- Michelle Kim ("You") and Springer ("Springer") consists of your license details and the terms and conditions provided by Springer and Copyright Clearance Center.

License Number	4122640698560
License date	Jun 05, 2017
Licensed Content Publisher	Springer
Licensed Content Publication	Histochemistry and Cell Biology
Licensed Content Title	Characterization of OATP1B3 and OATP2B1 transporter expression in the islet of the adult human pancreas
Licensed Content Author	Michelle Kim
Licensed Content Date	Jan 1, 2017
Type of Use	Thesis/Dissertation
Portion	Full text
Number of copies	1
Author of this Springer article	Yes and you are a contributor of the new work
Order reference number	
Title of your thesis / dissertation	The Role of OATP-Mediated Statin Transport in Pancreatic Beta Cell Function
Expected completion date	Jun 2017
Estimated size(pages)	140
Requestor Location	Michelle Kim
Billing Type	Invoice
Billing Address	
	Attn: Western University
Total	0.00 USD
Terms and Conditions	

officers, directors, employees and agents, from and against any and all claims arising out of your use of the licensed material other than as specifically authorized pursuant to this license.

No Transfer of License

This license is personal to you and may not be sublicensed, assigned, or transferred by you without Springer's written permission.

No Amendment Except in Writing

This license may not be amended except in a writing signed by both parties (or, in the case of Springer, by CCC on Springer's behalf).

Objection to Contrary Terms

Springer hereby objects to any terms contained in any purchase order, acknowledgment, check endorsement or other writing prepared by you, which terms are inconsistent with these terms and conditions or CCC's Billing and Payment terms and conditions. These terms and conditions, together with CCC's Billing and Payment terms and conditions (which are incorporated herein), comprise the entire agreement between you and Springer (and CCC) concerning this licensing transaction. In the event of any conflict between your obligations established by these terms and conditions and those established by CCC's Billing and Payment terms and conditions, these terms and conditions shall control.

Jurisdiction

All disputes that may arise in connection with this present License, or the breach thereof, shall be settled exclusively by arbitration, to be held in the Federal Republic of Germany, in accordance with German law.

Other conditions:

V 12AUG2015

Appendix B: Exploratory Evaluation of Oatp Expression in Mouse

Supplementary Materials and Methods

Statin transporter gene expression analysis in mouse pancreatic islets

Total mouse liver and pancreatic RNA were purchased from BioChain (N=1 each) and mouse pancreatic cDNA (N=2) was generously donated by Dr. Chris Pin (Children's Health Research Institute, Victoria Hospital, London, Ontario). RNA from flash-frozen mouse tissues (liver and kidney, N=3 each) were extracted with TRIzol® (Thermo-Fisher Scientific).

Islets from adult male C57BL/6 (WT) and *Oatp2b1*$^{-/-}$ (KO) mice were isolated following a modified version of a previously published protocol (Li et al. 2009). Briefly, mice were euthanized by isoflurane overdose and the abdomen cut open. The pancreas was perfused with collagenase V (1 mg/mL, C9263, Sigma-Aldrich) enzyme solution via the common bile duct then removed and placed in a tube containing enzyme solution for digestion. Once homogenous, the pancreas suspension was washed and centrifuged multiple times, resuspended, then passed through a 70 µM cell strainer. The islets, now captured on the cell strainer, were rinsed onto a cell culture dish and 10-20 islets per mouse were subsequently hand-picked for RNA extraction and gene expression analysis.

Normal adult mouse (C57BL/6) islet cDNA (N=4) was provided by Dr. Rennian Wang (Children's Health Research Institute); however, due to limited islet cDNA volumes per mouse, we could only reach 1-2 samples (N=1-2) for each gene expression analysis.

RNA samples were quantified and reverse transcribed as outlined in **Section 2.1**. Gene expression of mouse *Oatp1a1*, *Oatp1a4*, *Oatp1a5*, *Oatp1a6*, *Oatp2b1*, and *Oat3* was examined by qRT-PCR using previously published primers (**Supplemental Table 1**). Expression was normalized to mouse *Gapdh* as an internal control and fold-differences in expression determined as previously described. Runs for mouse *Oatp1a1*, *Oatp1a4*, and *Oatp1a5* were executed following a previously published method: denaturation at 94°C for 3 minutes; 35 cycles at 94°C for 45 seconds, 57°C for 1 minute, 72°C for 2 minutes; and a 72°C hold for 10 minutes (Abe et al. 2010).

Supplementary Table 1. qRT-PCR primers used to evaluate gene expression of mouse statin transporters.

Gene	*Forward (5'-3')*	*Reverse (5'-3')*	*Reference*
Oatp1a1	TTAGCTGGCATTCCGGCACCTG	CTTTAAAGTTCAGTGTGTGCGTCA	Abe et al. (2010)
Oatp1a4	AACTAGGAAGACCATTGGCCCTTTG	ATCCGAGGCATATTGGAGGTAACATG	Abe et al. (2010)
Oatp1a5	CACGCATTTTGCACAAGAATATTCGCTGGCATCCC	AAGGTTTTACTCTAAGATGATTTTGAAAGTAGCAC	Abe et al. (2010)
Oatp1a6	AACTGCACAACCAACACCAA	TCAATGGGAGCTTTGAGATG	Primer depot
Oatp1b2	TGGGCATTGGGAGTATTCTGA	CCAGGTGTATGAGTTGGACCC	Knauer (2012)
Oat3	TCTCCGAGATTCTGGACCGT	CACTTCTCAGGCTTCCCGTT	Primer depot
Oatp2b1	CTTCATCTCAGAACCATACC	ACTGGAACAGCTGCCATTG	Knauer (2012)
Gapdh	CGTCCCGTAGACAAAATGGT	TTGATGGCAACAATCTCCAC	Primer depot

Immunofluorescent staining of mouse pancreatic tissue

Pancreata from C57BL/6 mice 12-16 weeks of age were extracted and immediately fixed in 10% neutral buffered formalin solution (HT5014, Sigma-Aldrich), then embedded in paraffin and sectioned onto slides by the Molecular Pathology Facility at Robarts Research Institute (Robarts Research Institute, London, Ontario). Immunofluorescent staining of paraffin-embedded pancreatic tissue sections was performed to detect expression of mouse Oatp2b1 (anti-Oatp2b1 antibody 1:50; M-153; Santa-Cruz), insulin, and glucagon as following the previously described protocol (**Section 2.3**).

Intraperitoneal glucose tolerance test in Oatp2b1$^{-/-}$ mice

Male C57BL/6 mice (WT) and Oatp2b1$^{-/-}$ mice (KO) aged 12-16 weeks (n=6 for WT, n=6 for KO) were fasted for 16 hours with free access to water. Fasting blood glucose was measured with a OneTouch Verio Blood Glucose Meter (LifeScan Canada, Burnaby, British Columbia) and a 2 mg/g dose of glucose was administered intraperitoneally. Blood glucose was measured with the glucometer at 15, 30, 60, and 120 minutes.

Supplementary Results

Mouse pancreatic islet gene expression of statin transporters

Statin uptake transporter gene expression was assessed in mouse liver, pancreas, kidney, and islets. Mouse islets showed abundant expression of mouse statin transporters *Oatp1a1*, *Oatp1a4*, *Oatp1a5*, and *Oatp1a6* (mean C_T values: 25.5, 28.3, 26.3, 27.7) **(Supplementary Figure 1**). The respective fold-differences to liver for islet expression of these transporters were 16.0, 8.32, 384.1, and 514.4. Very low islet expression of *Oatp1b2* and *Oat3* (mean C_T values: 35.2, 34.5) was detected; *Oat3* islet expression only appears abundant when compared to the very low expression liver.

Expression of mouse *Oatp2b1* was low but detectable in wild-type mouse islets (mean C_T value: 31.5), while negligible in islets of *Oatp2b1*$^{-/-}$ mice (mean C_T value: 35.4) (**Supplementary Figure 2**).

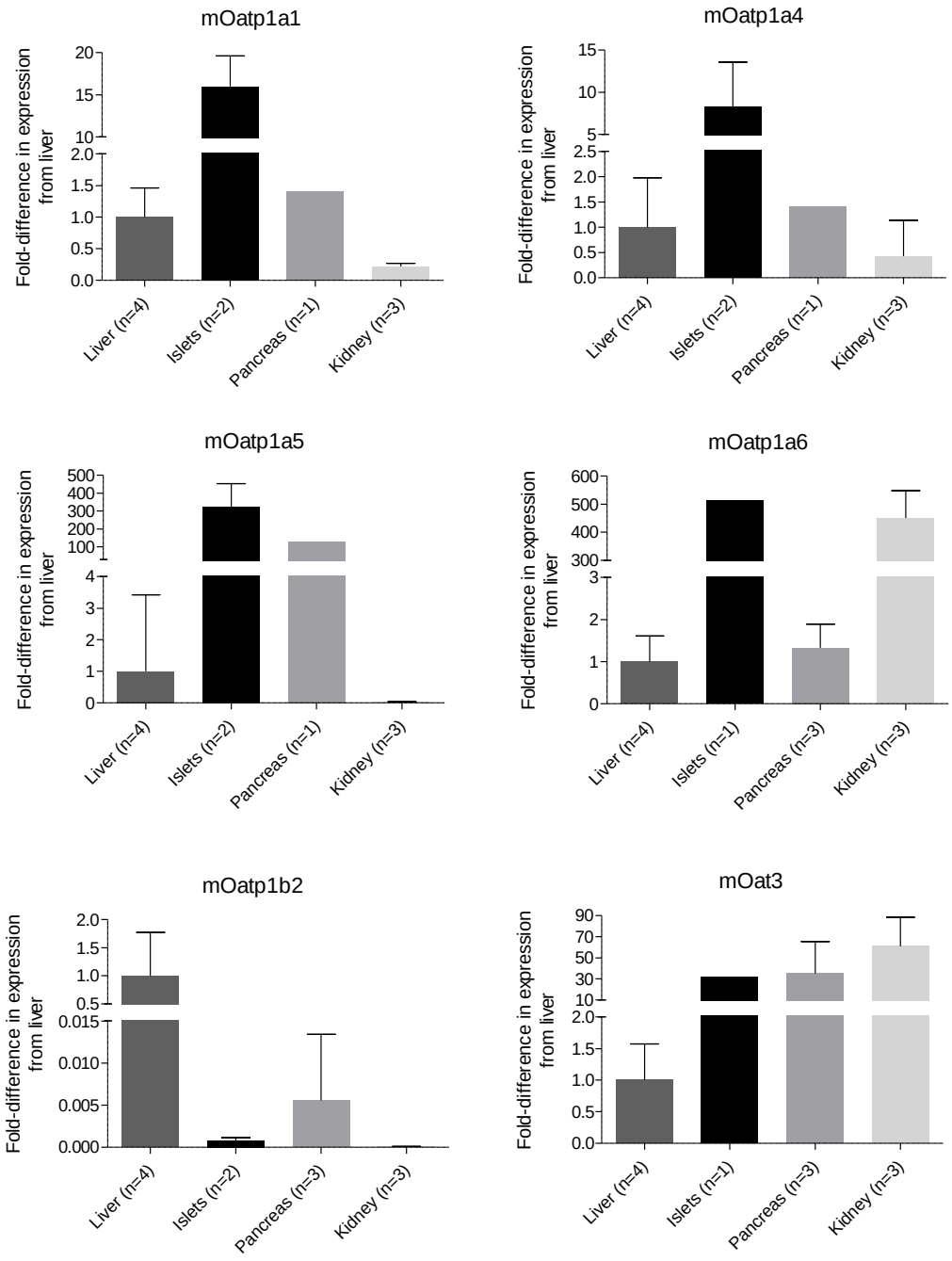

Supplementary Figure 1. Gene expression analysis of statin transporters in mouse pancreatic islets. Relative mRNA expression of statin uptake transporters in mouse tissues normalized to mouse *Gapdh* and shown as fold-difference from liver. Mouse islet cDNA and mouse pancreas cDNA (n=2) kindly provided by Dr. Rennian Wang and Dr. Chris Pin. Abundant expression of *mOatp1a1*, *mOatp1a4*, *mOatp1a5*, and *mOatp1a6* was detected in mouse islets. Results shown as mean ± SD.

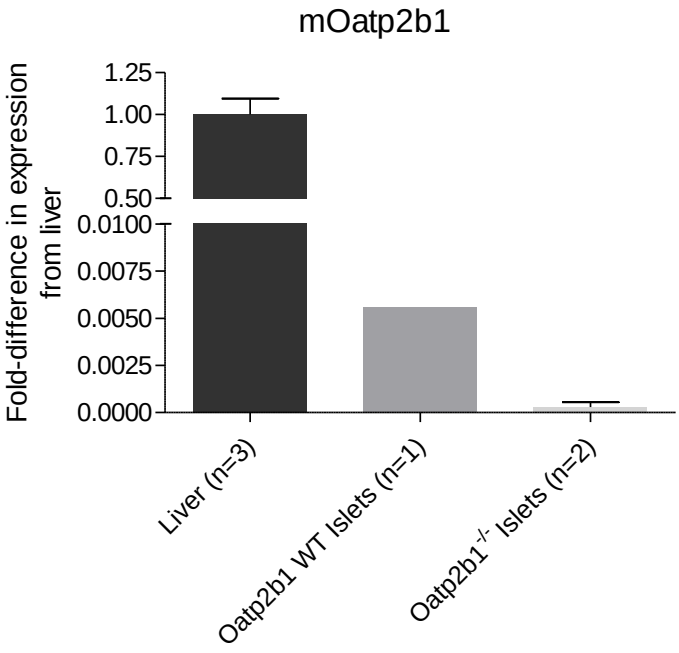

Supplementary Figure 2. Gene expression analysis of *Oatp2b1* in mouse islets.Expression of mouse *Oatp2b1* was detected in wild-type (WT) mouse islets, while expression in *Oatp2b1*$^{-/-}$ mouse islets was very low. Results shown as mean ± SD.

Protein expression of Oatp2b1 in mouse pancreatic islets

Expression of mouse Oatp2b1 protein was localized to mouse pancreatic islets. Dual immunofluorescent staining of Oatp2b1 with insulin or glucagon showed a great extent of co-localization with insulin, whereas co-localization with glucagon was less apparent (**Supplementary Figure 3**).

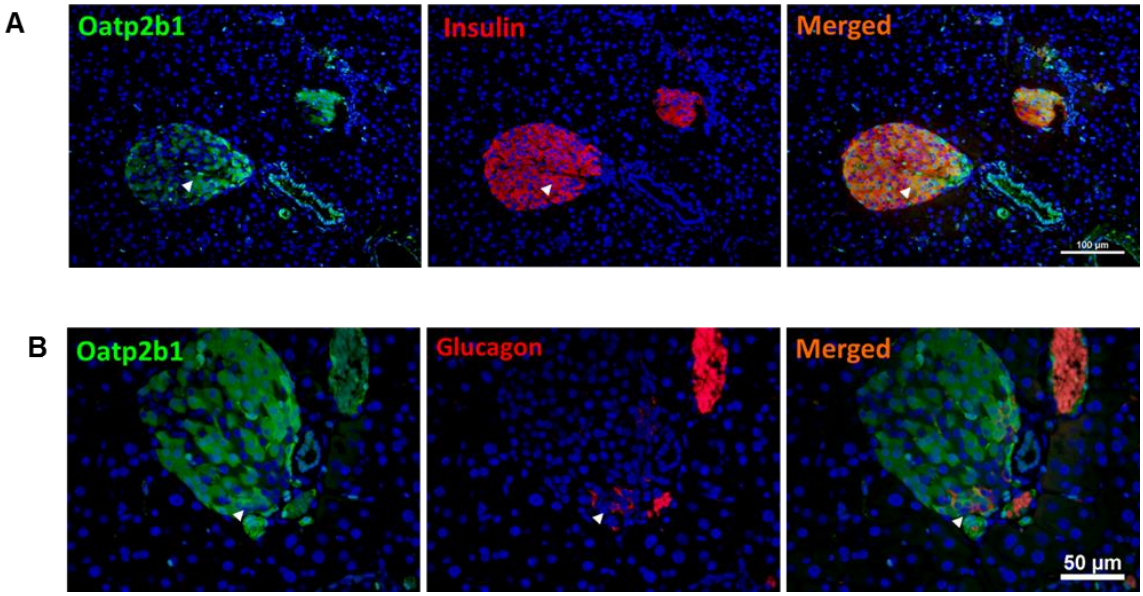

Supplementary Figure 3. Immunofluorescent staining of mouse pancreatic tissue. Immunofluorescent staining performed as previously described. **(A)** Oatp2b1 expression was detected in wild-type mouse islets with some co-localization with insulin (10x). Scale bar in 100 µm. **(B)** Some co-localization of Oatp2b1 was observed with glucagon (40x). Scale bar in 50 µm. Co-localization indicated by white arrows.

Glucose handling in Oatp2b1$^{-/-}$ mice following intraperitoneal glucose dose

Potential differences in glucose handling were evaluated in WT and *Oatp2b1*$^{-/-}$ mice following a 16 hour fast and administration of a 2 mg/g intraperitoneal glucose dose. No significant differences in blood glucose level AUC was detected between WT and *Oatp2b1*$^{-/-}$ mice for all measured timepoints. Interestingly, mean fasting blood glucose after 16 hours was significantly higher in *Oatp2b1*$^{-/-}$ mice (P=0.005) than in WT mice. Statistical analyses performed by Mann-Whitney U test (**Supplemental Figure 4**).

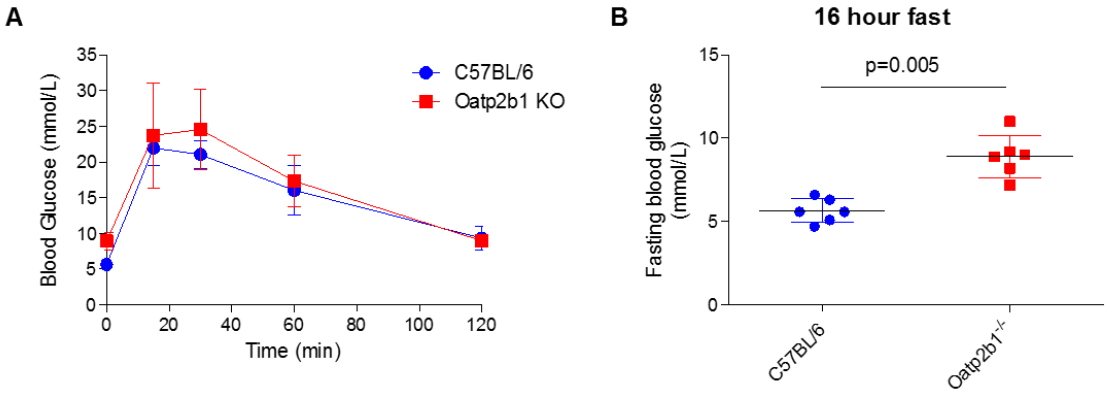

Supplementary Figure 4. Intraperitoneal glucose tolerance test in Oatp2b1$^{-/-}$ mice.(A) Blood glucose over 120 minutes following intraperitoneal administration of 2 mg/kg glucose. **(B)** Fasting blood glucose following a 16 hour fast. Blood glucose was significantly higher in Oatp2b1$^{-/-}$ mice compared to C57BL/6 mice. The fasting blood glucose of Oatp2b1 KO mice was significantly higher (P=0.005) after a 16-hour fast as determined by a Mann-Whitney U test. Results shown as mean ± SD, n=6 per group.

Appendix C: Animal Use Protocol Approval

AUP Number: 2015-080
PI Name: Schwarz, Ute
AUP Title: Role of Statin transport by OATPs in pancreatic islet cell function

Official Notification of AUS Approval: A MODIFICATION to Animal Use Protocol 2015-080 has been approved.

The holder of this Animal Use Protocol is responsible to ensure that all associated safety components (biosafety, radiation safety, general laboratory safety) comply with institutional safety standards and have received all necessary approvals. Please consult directly with your institutional safety officers.

Submitted by: Kinchlea, Will D
on behalf of the Animal Use Subcommittee

The University *of* Western Ontario
Animal Use Subcommittee / University Council on Animal Care

Curriculum Vitae

Name Michelle Sun-Mi Kim

Education

Master of Science 2014-2017
Physiology and Pharmacology
University of Western Ontario London, Ontario, Canada

Bachelor of Medical Sciences 2010-2014
Double Major in Pharmacology and Medical Sciences
University of Western Ontario London, Ontario, Canada

Awards and Scholarships

Dean's Honor List 2011, 2014
Western Scholarship of Excellence 2010

Publications and Presentations

Kim M, Deacon P, Tirona RG, Kim RB, Pin CL, Meyer zu Schwabedissen HE, Wang R, and Schwarz UI (2017) Characterization of OATP1B3 and OATP2B1 transporter expression in the islet of the adult human pancreas. *Histochem Cell Biol* doi:10.1007/s00418-017-1580-6.

Kim MS, Wang R, Schwarz UI. The role of OATP-mediated statin transport in pancreatic islet cell function. Physiology and Pharmacology Research Day, London, Ontario. November 2016. [Poster].

Kim MS, Wang R, Schwarz UI. The role of OATP-mediated statin transport in pancreatic islet cell function. Canadian Society of Pharmacology and Therapeutics 2016 Annual Meeting, Vancouver, British Columbia. September 2016. [Poster].

Kim MS, Wang R, Schwarz UI. The role of Oatp-mediated statin transport on pancreatic islet cell function. London Health Research Day, London, Ontario. March 2016. [Poster].

Kim MS, Wang R, Schwarz UI. The role of Oatp-mediated statin transport on pancreatic islet cell function. Physiology and Pharmacology Research Day, London, Ontario. November 2015. [Poster].

Kim MS, Hong K, Wang R, Schwarz UI. The role of Oatp-mediated statin uptake in altered insulin secretion in a murine beta cell model. Canadian Society of Pharmacology and Therapeutics 2015 Annual Meeting, Toronto, Ontario. June 2015. [Poster].